USER-SIDE MODELLING AND COMPARATIVE ANALYSIS OF AIRBORNE LIDAR ERRORS

PATRICK WETARNI ADDA

July 2013

TECHNICAL REPORT
NO. 285

USER-SIDE MODELLING AND COMPARATIVE ANALYSIS OF AIRBORNE LIDAR ERRORS

Patrick Wetarni Adda

Department of Geodesy and Geomatics Engineering
University of New Brunswick
P.O. Box 4400
Fredericton, N.B.
Canada
E3B 5A3

July 2013

© Patrick Wetarni Adda, 2013

PREFACE

This technical report is a reproduction of a dissertation submitted in partial fulfillment of the requirements for the degree of Doctor of Philosophy in the Department of Geodesy and Geomatics Engineering, July 2013. The research was supervised by Prof. David Coleman, and funding was provided by the New Brunswick Department of Public Safety/Emergency Measures Organization, Service New Brunswick, GEOIDE Network Canada, MITACS Elevate (co-sponsored by CARIS), and the Natural Sciences and Engineering Research Council of Canada (NSERC).

As with any copyrighted material, permission to reprint or quote extensively from this report must be received from the author. The citation to this work should appear as follows:

Adda, Patrick (2013). *User-Side Modelling and Comparative Analysis of Airborne LiDAR Errors.* Ph.D. dissertation, Department of Geodesy and Geomatics Engineering, Technical Report No. 285, University of New Brunswick, Fredericton, New Brunswick, Canada, 133 pp.

ABSTRACT

Project specifications are designed and enforced to determine whether or not delivered data met required standards. However, rapid advancements in LiDAR data capture technologies have led to major challenges for end users to validate the data and processes for fitness for use. The developed UDTEB model uses two approaches to fill this gap – 1) the deterministic approach employing CMP and SBET or their equivalent files of ALS surveys to extract the root mean square errors of points with respect to a trajectory and an estimated terrain, and 2) where these files are not available, the non-deterministic approach employing published LiDAR system performance reports to simulate flight conditions and estimate errors under defined conditions.

To validate the UDTEB model, five areas of varying topography and land cover were investigated. TIN differencing and a new method for point by point comparison of checkpoints and corresponding LiDAR points using square windows around the checkpoints were employed. When the obstructions of the checkpoints were further categorized as “clear”, “light” and “dense”, average RMSE values observed were 0.06 m, 0.05 m and 0.10 m respectively.

The UDTEB model proposes a method to equip end-users to perform error budgeting from data acquisition to the end product creation and validate the elevation accuracy of a LiDAR data at a given confidence interval. The method can be customized for a given error analysis task, allowing the user to include other error sources into the model. It can also be adopted for elevation error analysis of large datasets similar to LiDAR.

DEDICATION

To the late Mrs. Gladys Beatrice Ahiabu, (nee Tsikata). Having studied for your post-graduate degree in Nova Scotia, Canada, you challenged me in 2007 to pursue a PhD in "the country with the best educational system in the world". You followed up with continual motherly inspiration (or should I say constant heckling from a mother-in-law?) to consider Canada for my post-graduate studies. Although it was initially to call your bluff, I made an online search for "the best place to study Geomatics Engineering" and it returned the University of New Brunswick located in Canada! You won the bragging rights for this bet. And I owe my experience of an unparalleled world class education in Geomatics engineering at UNB to your challenge six years ago.

Today, although you are not physically present to see this bear fruits, I know you are smiling where you are. Mama, *Akpe ka ka ka* (translation: *thank you very much* - from the Ewe language spoken in Ghana).

ACKNOWLEDGEMENTS

- I thank the ALMIGHTY God for empowering me to complete this dissertation.
- I thank my wife, Josephine Adda and our children, Welam and Nukunu Adda for their love, sacrifices, patience and support during this study. I thank my parents, David Adda and Grace Kumah for encouraging me to achieve my goals.
- I thank my supervisor, Professor David Coleman for his patience and continuous support during this dissertation. I also thank Professors Darca Mioc, Marcelo Santos, Sue Nichols, Peter Dare, Glen Jordan, Songnian Li, James Secord, Richard Langley and Dr. Raid Al-Tahir, for their assistance in this dissertation.
- I say a very BIG thank you to Ernest McGillivray and the staff at the Department of Public Safety for data and financial support during this dissertation – Ernie, your flood design project/research provided the seed funding that brought me and my family to Canada in 2008. I thank you and the staff at DPS for giving me this great opportunity to make an impact on the lives of the people in N.B. through this research.
- David Finley's N.B. LiDAR specifications project provided the resources and support to develop the approach for creating the user's specifications part of this research. I am very grateful to you, Dave, for this opportunity to serve N.B. whiles working on the foundation for this research. Your fatherly advice is light for my professional career in Geomatics.
- I am grateful to Dr. Mark Masry and CARIS staff for their support when I did my internship in CARIS in 2012 towards understanding at firsthand how to apply

programming to solve GIS problems. I am also indebted to CARIS for co-funding my internship at CARIS through the MITACS accelerate program.

- I thank Bill Kidman of Leading Edge Geomatics (LEG) and indeed all the staff of LEG for helping me to understand how the airborne LiDAR technology performs in practice.
- I am grateful to respondents to my questioneer when the provincial users' specifications were being developed. Respondents were from government and private institutions in New Brunswick. I cannot list all the names here, but will like to let you know how much I appreciate your assistance.
- I thank my colleagues Houman Fahandezhsaadi, and Jude Kunadu-Yiadom for their assistance during the field validation surveys, and Titus Tienaah for his insights and assistance during the programming part of this research.
- The supporting staff of GGE, namely, Sylvia Whitaker, Michelle Ryan, Lorry Hunt, David Fraser, Terry Arsenault and Jay Woodyer are mentioned with gratitude, for their technical and administrative support during my studies.
- Special thanks to Ms. Wendy Wells for helping with the editing of this report.
- Lastly, but not least, I am grateful to partners who helped in various times to provide support and funding for this research. These include UNB-NSERC (funds from my supervisor, Dr. David Coleman), SNB and GEOIDE and MITACS. Please if you have not specifically mentioned here, kindly accept my apologies for the unintended omission. I do really appreciate every assistance and goodwill from all the good people of N.B. during my studies at UNB.

May the good Lord, God Almighty richly bless you all, AMEN.

Table of Contents

ABSTRACT ii
DEDICATION iii
ACKNOWLEDGEMENTS iv
Table of Contents vi
List of Tables viii
List of Figures ix
List of Abbreviations xi
CHAPTER 1. INTRODUCTION 1
1.1 PROBLEM DEFINITION 1
1.1.1 Background and Motivation 3
1.1.2 Project Area 9
1.1.3 Constraints and Challenges Encountered in this Research 10
1.2 PROPOSED APPROACH 12
1.2.1 Error Modeling and Analysis 13
1.2.2 Error Interpretation 13
1.3 MAIN CONTRIBUTION 16
1.3.1 The Total Error Model 17
1.3.2 The Software Prototype 18
1.3.3 Data Cleaning Using TPU Values 18
1.4 OUTLINE OF DISSERTATION 20
CHAPTER 2. LITERATURE REVIEW AND POSITIONING OF RESEARCH 22
2.1 INTRODUCTION 22
2.1.1 Operational Consideration for Accurate Point Cloud Acquisition 23
2.2 STATISTICAL PROCESSES AND ANALYSIS OF ERRORS 26
2.2.1 Accuracy, Error and Uncertainty/Precision 26
2.2.2 Confidence Interval 31
2.2.3 Law of Propagation of Errors 32
2.2.4 Sampling and Estimation Methods 34
2.2.5 Potential Sources and Magnitudes of Errors in LiDAR 35
2.2.6 Identifying and Removing Blunders and Errors 40
2.3 MATHEMATICAL MODELS FOR ERROR DETECTION 41
2.4 POSITIONING OF RESEARCH 45
CHAPTER 3. RESEARCH QUESTIONS OBJECTIVES AND METHODOLOGY 46
3.1 INTRODUCTION 46
3.2 RESEARCH QUESTIONS 47
3.3 RESEARCH OBJECTIVES 49
3.4 METHODOLOGY 51
3.4.1 Assumptions 52
3.4.2 Users' Requirements Definition 54
3.4.3 System Uncertainty Modeling Development 61
3.4.4 User Determined Error Modeling 73
3.4.5 Data Acquisition 84

3.4.6 Data Processing 87
3.4.7 Ground Control Quality Assurance 92
3.4.8 Point Differencing for Standard Deviation/RMSE Calculation 94
CHAPTER 4. RESEARCH RESULTS AND DISCUSSION OF RESULTS 99
4.1 ERROR CALCULATION AND FIELD VALIDATION 99
4.1.1 Point by Point Comparison 100
4.1.2 Obstruction Analysis 113
4.2 ERROR ANALYSIS OF PROJECT SPECIFIC APPLICATIONS 118
4.2.1 What are the User Requirements? 118
4.2.2 What is the Error Budget for the Flood Inundation? 119
4.2.3 Users' Requirements Compared with Vendor Delivered Specifications .. 124
CHAPTER 5. SUMMARY, CONCLUSION AND RECOMMENDATION FOR FUTURE RESEARCH 125
4.2.4 Accomplishments – Key Contributions 128
4.2.5 Limitations 130
REFERENCES 134
APPENDIX 143
APPENDIX A. UDTEB Matlab™ code 143
APPENDIX B. Matlab™ code to perform square window differencing 147
APPENDIX C. Example of point differencing between LiDAR and checkpoints 154
Curriculum Vitae

List of Tables

Table 2.1 Type I and II errors employed to accept or reject a null hypothesis 28
Table 2.2 Examples of horizontal positioning errors relating to flight altitude error at a given angular error 38
Table 2.3: Terrain Slope vs. RMS Error 39
Table 3.1 Participating stakeholders and their areas of interest relating to LiDAR 55
Table 3.2. Formats and accuracies ($RMSE_z$ at 68% confidence level) of contours required. 56
Table 3.3.Confusing specification terminology as used in the LiDAR industry supposing to describe the same characteristics. 75
Table 3.4. Error matrix for evaluating the classification accuracy of LiDAR ground points from non-ground points. 80
Table 3.5. Residuals of the NB HPN checkpoint used as Base Station in the RTK. 93
Table 3.6. Square window point difference for LiDAR and checkpoints in Wilmot Park 95
Table 3.7. Square window point difference for LiDAR and checkpoints in downtown .. 96
Table 3.8. Square window point difference for LiDAR and checkpoints in Odell Forest 97
Table 3.9. Square window point differencing results for Windsor Street 97
Table 3.10. Square window point differencing results for Avondale Ct. 98
Table 4.1 Definition of the amount of obstructions (after Martin et al. [2001]) 99
Table 4.2. Summary of the difference in elevation (m) between ground checkpoints and LiDAR points in the dense vegetation area – Odell Park used as an example. 102
Table 4.3. Comparison of errors between, UDTEB and LiDAR in built-up areas – downtown Fredericton. 105
Table 4.4. Comparing errors between Checkpoints LiDAR and UDTEB estimates in flat open terrain conditions 106
Table 4.5. Comparison of elevations in steep slope area 108
Table 4.6.Comparison of errors between, UDTEB and LiDAR with respect to Checkpoints in sparsely dense areas 111
Table 4.7. Comparing overall elevation differences in the project area 112
Table 4.8. RMSE of surveyed and field elevations in areas clear of obstructions 114
Table 4.9. RMSE analysis between surveyed and measured points in places with light obstructions 116
Table 4.10. RMSE of UDTEB compared to RMSE from field measurements in area with dense obstructions 117

List of Figures

Figure 1.1. Outline of Chapter 1 1
Figure 1.2. User requirements assessment for multiple organizations employing LiDAR 6
Figure 1.3. Point cloud data with noise with TPU values separated by range. 19
Figure 1.4. Point cloud after cleaning noise by deleting points outside TPU range 19
Figure 2.1 Outline of Chapter 2. 22
Figure 2.2. System integration in ALS surveys 23
Figure 2.3: Final accuracy factors for LiDAR data 36
Figure 2 4: Multipath in LiDAR results in spurious data points 37
Figure 2.5 (a) pitch error (b) roll error (c) heading error.. 38
Figure 2.6. Effect of slope on vertical accuracy 39
Figure 2.7. Vertical error induced by horizontal errors 39
Figure 2.8: An example of a GPS ground control network. 41
Figure 2.9 Coordinate systems and quantities of the LiDAR equation 42
Figure 3.1 Outline of Chapter 1 46
Figure 3.2 Difference between multibeam and LiDAR point clouds height realization. . 48
Figure 3.3 Relating performance standards in ALS project with varying interest in standards involving the system manufacturer, data provider and final user 51
Figure 3.4 The ideal relation of ALS performance specifications 52
Figure 3.5. Transformations between reference frames 62
Figure 3.6. Flow diagram of algorithm development for the deterministic model 69
Figure 3.7. A simplified laser scanner depicting laser range ρ, azimuth angle θ, and elevation angle ϕ 70
Figure 3.8. Defining sensor types in the non-deterministic model 72
Figure 3.9. UDTEB Model 74
Figure 3.10. Data reduction and DEM accuracy 76
Figure 3.11. Contribution of morphology in RMSE (vertical) LiDAR DEM.. 77
Figure 3.12.Project Area. Image Source: Google Inc. (C) 2012 84
Figure 3.13. Estimated trajectory used by aircraft during the survey. 84
Figure 3.14. GUI of the UDTEB showing step by step processing steps. 87
Figure 3.15. PUM options – deterministic and non-deterministic model. 87
Figure 3.16. A user interface for input of PLUM estimates. Maximum and minimum range of errors is reported in the total uncertainty report only for information purposes and advice to the user. It is not employed in this additive sense UDTEB model. 88
Figure 3.17. PRUM interface. Required: the flying height, the percentage reduction of data and the estimation of terrain morphology. 88
Figure 3.18. DIUM entry example 89
Figure 3.19. GUI of PRUM showing a user input example. GUI has three parts. The top part relates to Classification uncertainties employed in the UDTEB model. Second section records vertical references used and the third section records the datasets used. 90
Figure 3.20. GUI interface created to allow users to define LIDAR around controlled checkpoints within a rectangular window. 94

Figure 3.21. GUI showing how elevation differences between controlled checkpoints and LiDAR points are selected around a defined square window in order to compute their elevation differences. 95
Figure 4.1. Outline of Chapter 4 99
Figure 4.2. Ranges of absolute elevation differences between GNSS and LiDAR at the Odell Park Forest - units in metres. 101
Figure 4.3. Ground points of downtown Fredericton 104
Figure 4.4. A TIN created from the sampled points in open flat areas. 106
Figure 4.5. Differences in elevation compared with UDTEB errors in open flat areas.. 107
Figure 4.6. Obstruction and TIN of ground Hits. 109
Figure 4.7. Graph of RMSE of surveyed and measured points in clear obstruction. 115
Figure 4.8. RMSE between surveyed and measured points in light obstruction areas. .. 116
Figure 4.9. Proposed processing steps for the 3D flood models - from data acquisition to product creation. 119
Figure 4.10. User defined directional accuracies in metres for an envisioned flood model. 119
Figure 4.11. Summary of LUM TPUs based on system employed. All units in metres. 120
Figure 4.12. Estimating amount of slope change in area of Survey 121
Figure 4.13. PRUM user interface 122
Figure 5.1. Outline of Chapter 5. 125

List of Abbreviations

ALS	–	Airborne Laser Scanning
CI	–	Confidence Interval
CL	–	Confidence Level
DAA	–	Department of Agriculture and Aquaculture
DEM	–	Digital Elevation Model
DIUM	–	Data Integration Uncertainty Model
DNR	–	Department of Natural Resources
DOT	–	Department of Transportation
DPS	–	Department of Public Safety
DTM	–	Digital Terrain Model
ENVCan	–	Environment Canada
GPS	–	Global Positioning System
GUI	–	Graphical User Interface
IMU	–	Inertial Measurement Unit
INS	–	Inertial Navigation System
LEG	–	Leading Edge Geomatics (Limited, Fredericton, N.B.)
LiDAR	–	Light Detection and Ranging
LUM	–	LiDAR Uncertainty model
PLUM	–	Planning Uncertainty Model
POS	–	Positioning and Orientation System
PRUM	–	Processing Uncertainty Model
PUM	–	Presentation Uncertainty Model
QA/QC	–	Quality Control / Quality Assurance
QCC	–	Quality Control Checkpoint
SNB	–	Service New Brunswick
TPU	–	Total Propagated Uncertainty
TUB	–	Total Uncertainty Budget
UDTEB	–	User Determined Total Error Budget

CHAPTER 1. INTRODUCTION

CHAPTER 1.INTRODUCTION
1.1 PROBLEM DEFINITION
1.1.1 Background and Motivation
1.1.2 Project Area
1.1.3 Constraints and Challenges Encountered in this Research
1.2 PROPOSED APPROACH
1.2.1 Error Modeling and Analysis
1.2.2 Error Interpretation
1.3 MAIN CONTRIBUTION
1.3.1 The Total Error Model
1.3.2 The Software Prototype
1.3.3 Data Cleaning Using TPU Values
1.4 OUTLINE OF DISSERTATION

Figure 1.1. Outline of Chapter 1

1.1 PROBLEM DEFINITION

There are no complete and simple processes and tools to provide support for airborne LiDAR (**Li**ght **D**etection **A**nd **R**anging) users to budget errors at project inception and verify whether or not the delivered LiDAR products meet user specifications after project completion. A survey of users of LiDAR data and its derived products within New Brunswick – the project area considered for this research – showed the limitations LiDAR data custodians had in performing tasks involving LiDAR error budgeting. A further inhibition to realizing the full potential and limitations of LiDAR data and products is the difficulty to interpret the overall error and its effect on project specific applications. These abilities require expertise in LiDAR which may not be available for most LiDAR data users (or potential users). Additionally, as LiDAR systems are getting more complex, the trend now is to leave both project planning – including error

budgeting and quality control – in the hands of the vendor. Consequently, a gap exists with respect to the client being unable to independently determine whether or not a given spatial data quality is fit for use. This gap keeps widening as the systems employed for data capture become more complex.

Considering a collection of applications employing LiDAR data in the project area, this research addressed key questions as to whether manufacturers' specifications meet, surpass or fail user-demanded error budgets for specific projects. The plan of this research is to estimate the errors based on systems employed and methods used in post-processing of LiDAR data and products. If products from system specifications generally exceed user error budgets for intended projects, users may not need to worry about not meeting general requirements for accurate information derived from LiDAR data. On the other hand, system specifications may fail to meet users' intended purposes. In this case, how can *false accuracies* be identified? What will be their effects on the final information released to the public after creating applications or solutions employing a falsely specified data?

This dissertation proposes that the answer to these questions lies in the establishment of a complete system that tracks and quantifies each error source contributing to the final LiDAR data product. Some of these sources have already been identified by previous authors and are discussed in Section 2.2.5. Additional sources of error that could affect the total accuracy of a LiDAR product have been identified and discussed in Section 3.4.3. The total error (computed using methods in this research) is compared with the

initial user's requirements to determine whether or not delivered LiDAR products are fit for use.

1.1.1 Background and Motivation

In the summer of 2008, the government of New Brunswick (N.B.), Department of Public Safety (DPS), Canada, acquired LiDAR data to help study and model recurring flooding in the province. However, the technology, with a potential to greatly benefit the flood project, was new to the parties involved. There was a need to develop user capacity to benefit from the full potential of the data and know its limitations. The initial task of developing specifications to provide guidelines for departments seeking to acquire data in N.B. was carried out by Coleman and Adda [2010].

LiDAR data and its derived products have become a major source for digital spatial data acquisition used in several terrain related applications around the globe. Several authors (e.g., Hodgson and Bresnahan [2004]; Sithole and Vosselman [2003]; Hodgson et al. [2007]) report on the rapid adoption of the technology for surveys previously done using traditional photogrammetry or land surveying. El-Sheimy et al. [2005] attributes the increase in acceptance of LiDAR data as a major spatial data source to advancements in LiDAR technology.

To achieve desired accuracies, contracting companies use LiDAR equipment from different manufacturers and adopt different specifications towards LiDAR surveys. The manufacturers' specifications on horizontal and vertical accuracies are generalized for projects without regard to the terrain and specific project requirements [Ussyshkin et al., 2006]. Additionally, very few user-side methods and technologies exist to test and

analyze data and products in order to verify data quality. For those that exist, aside from the cost of acquisition and training, an in-depth knowledge of LiDAR processing may be required to use them – a skill that may not necessarily be available among the user groups in this study. In-depth processing skills can be seen to be lacking among everyday LiDAR data users in most state or provincial governments.

In New Brunswick, LiDAR products are used in various applications requiring high accuracy standards. A previous study by Coleman and Adda [2010] suggests that LiDAR data and their derived products are employed in three main areas in the province of New Brunswick, namely, emergency measures and response, environmental monitoring, and city planning (for development regulation and tourism). Furthermore, literature contributions from Desmet [1997], Chou et al. [1999], FEMA [2000], Kraus and Pfeifer [2001], Lloyd and Atkinson [2002], Lim et al. [2003], El-Sheimy et al. [2005], Hodgson et al. [2005], Fisher and Tate [2006], Lloyd and Atkinson [2006], and Liu [2008] mention these three areas as common applications that employ the use of Airborne LiDAR.

In an attempt to close the gap between user's requirements on one hand and the manufacturers' specifications on the other hand, project-specific specifications are usually described on the client side to which the vendor is expected to comply. Assuming LiDAR data standards are already over specified to meet all applications, how is this verified as satisfactory on the client side? Have clients been given false precision for their project-specific applications? If yes or no, what process can prove this on a project-specific basis?

To answer these questions, this research leveraged and extended the processes relating to the identification, quantification, and interpretation of error propagation during the process of creating airborne LiDAR products. After creating these processes, as a case study, this research analyzes the effect of uncertainties on the final information derived from flood inundation mapping. Flood inundation information is chosen for this test case because it employs the capture of both terrain and hydrographic objects. Furthermore, flood inundation maps are the basis for flood prediction and emergency response scenario simulations. The city of Fredericton considers flooding as one of its main natural disasters. Plans are made annually to predict and mitigate the effects of flooding. Spatial data plays an important role in this regard.

Estimating differences between the demand side specifications required by users for real world applications and the manufactures' specifications for ideal conditions help to resolve questions on LiDAR product errors including:

1. *"How can a user determine the amounts and effects of total propagated errors on a project-specific basis?"*
2. *"What are the causes and effects – in the possible case – when manufacturers' specifications do not meet user's specification requirements?"*
3. *"How can products from poorly specified projects be adjusted to meet more stringent user's specifications without reducing the spatial quality of the data derived products?"*

Two LiDAR projects have been undertaken prior to the inception of this research to strengthen product quality obtained in N.B. The first project, by Adda et al. [2009] and

Adda et al. [2011], was to model a flood map of downtown Fredericton using LIDAR data and water gauges. This involved the validation of elevation data from LiDAR points in downtown Fredericton by using GPS measurements. Figure 1.2 shows a graph produced after collecting and analyzing information on user requirements among participating organizations in this research. The institutions involved were the:

- Department of Public Safety (DPS);
- Department of Natural Resources (DNR);
- Department of Transportation (DOT);
- Department of Agriculture Aquaculture and Fisheries (DAA);
- Service New Brunswick (SNB);
- Environment Canada (ENVCan); and
- Cities of Fredericton, Saint John and Moncton.

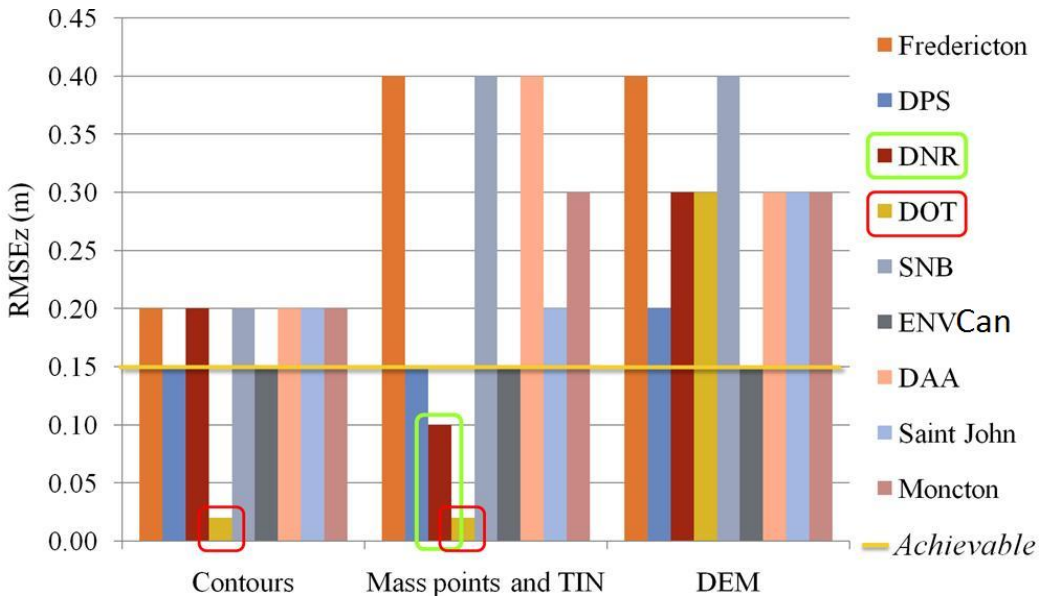

Figure 1.2. User requirements assessment for multiple organizations employing LiDAR

Figure 1.2 summarizes the data and product formats that were popular among organizations in the project area. It also reports on the vertical accuracy in terms of the RMSE in elevation (labeled as RMSEz) requirements for each institution. The achievable vertical accuracy considering the technology to be employed as of the time is also provided (yellow line). This information was used to perform a user's requirement assessments for the multiple organizations that employ LiDAR products for various applications (from Coleman and Adda [2010]).

The second project involved the design of common specifications for the capture and processing of LiDAR data in the province – keeping in mind multiple and varied user's needs as shown in Figure 1.2.

A study of Figure 1.2 shows that accuracy requirements are different among organizations. The average stated manufacturer's specification of LiDAR data acquired in the province reported a vertical accuracy of ±15 cm and horizontal accuracy of 50cm at 2-sigma. These average vendor's specifications were found to be satisfactory to seven out of nine provincial departments. Two organizations, namely DNR and the DOT, required more stringent specifications.

In both projects, it was realized that the use of LiDAR data and derived products for scenario prediction and simulations of a natural phenomenon require proof of the reliability of the information provided. The optimal way of doing this in a comprehensive manner is currently nonexistent. There have, however, been at least three different research efforts to look into the uncertainties involved in processing LiDAR [Ussyshkin et al. 2008]. However, client methods to estimate or validate error of LiDAR products for

a variety of applications are yet to be fully explored. In order to estimate possible, or even expected variations in the achievable data accuracy, the entire error budget of the LiDAR system should be considered.

Vendors of LiDAR data will design their project requirements based on the specific needs of the client [Ussyshkin et al., 2008] with typical questions like:

1. What is the coverage area?
2. How large is it?
3. What are the properties of the terrain (such as coverage, slope, and elevation above sea level)?
4. What accuracy of the point elevations is required?
5. What resolution/point spacing is anticipated?

Based on these questions, vendors are able to forecast final accuracies based on the precision of the LiDAR system. Manufacturers of LiDAR systems typically characterize LiDAR performance for the most general case of targets [Ussyshkin et al., 2008].

The challenge of translating nominal specification values to real-world achievable accuracy is left to the end-user and has long been a subject of different interpretations [Ussyshkin and Smith, 2006]. Considering the complex systems involved, the capacity of the user to perform these comparisons has been made more difficult. To solve this, a comprehensive comparison approach is required to verify whether or not vendor specifications on one hand meet user requirements on the other hand.

In summary, it is one thing to have a user's specification and another thing to be able to enforce the specification. The quest to enforce user's requirements and verify whether the delivered product met those requirements was the driving force leading to this investigation to create a User-Determined Total Error Budget (UDTEB) model. This model is created to enable everyday LiDAR users to follow a complete process to identify major error sources, quantify these errors and determine whether or not the products that contain these errors are fit for use.

1.1.2 Project Area

Fredericton and its surrounding area are considered as the project area for this research. Airborne LiDAR data and supporting data including ground control and water gauge data from the region was collected from DPS, ENVCan, SNB and Leading Edge Geomatics (LEG) Limited, Fredericton. LEG is a private survey company specializing in providing airborne LiDAR services. Field tests were performed on the data for quality assurance and control. The field exercise also allows for the collection of attributes relating to the data that may or may not be available with the data. Such attributes like terrain type, vegetative cover, building density and man-made structures on site are important factors in the final error estimation process.

The types of terrain and ground cover over LiDAR data project areas vary from place to place. The shape of the terrain and the density of features to be classified are two examples. To ensure a universality of approach, the developed error model was tested on

varying density of sensed objects and terrain conditions by considering five scenarios as follows:

1. flat even terrain– e.g., desert and fairly flat areas (a parking lots and sports fields is used to simulate this scenario);
2. undulating terrain – a well-connected representation of shallow, average; high undulating terrain;
3. vegetative areas – savannah, medium density, very dense vegetative conditions;
4. densely built up areas – (downtown Fredericton); and
5. sparsely built up areas – (outside the business areas of the city of Fredericton).

Field control using GNSS surveys were carried out at these areas to validate the UDTEB model.

1.1.3 Constraints and Challenges Encountered in this Research

During project planning, the choice of methods to meet a specified project need and the task of translating the specification error projections to real-world achievable accuracy has long been a subject of different interpretations as stated in Section 1.1. Consequently, a gap exists as a result of the contradicting interpretations between the manufacturers' stated specification and what is achievable in most project-specific applications. As this is an estimate of errors, the challenge was in providing methods for the user to employ when matching system precision estimates with real measurements to determine whether or not the spread of errors satisfies the client's requirements.

The research will not seek to refute reported system accuracies by demanding and investigating all vendor processing techniques employed and the manufacturer's instrument acquisition parameters. Understandably, manufacturers typically want to protect such information as part of their competitive advantage. Rather, this research focuses on modeling a total propagated error as a simulation of manufacturers' reported instrument precision and processes. Following that is an investigation to determine whether or not the total data or product error falls within acceptable limits of corresponding ground points. The precision of the instrument is treated as one case of measuring capability. The precision indicates that the instrument carries some amount of errors when used in ideal laboratory scenarios. The conditions under which the system is used together with the processes employed to process the data into a desired product will produce additional errors.

Finally, when products are being presented in an applied form, for instance flood modeling, certain assumptions (e.g., classifications) are made. This also carries with it some errors necessary to be considered in the total error modeling. Since the mechanical and processing capabilities of the systems and software are available, the focus will be on modeling other error sources that contribute to total data or product accuracy. The main constraint in terms of the estimated duration of this research was access to current LiDAR data with metadata to provide input into the model. The developed prototype application from the model had to wait for seven months to be tested with Fredericton data. The data were expected in the first week of November 2011 but was finally delivered in the second week of May 2012.

After data delivery, a quality control was made on the data and it was realized that the data lacked some metadata required as input into the UDTEB model. Information on system behavior during flight and the trajectory estimation used during the survey were missing in the provided metadata report. The data provider, LEG, was contacted after several attempts to extract the flight parameters from the LiDAR data. A conclusion was arrived that it was more ideal to undertake another calibration flight on June 2012 of the project area than try to "reverse engineer" the lost information.

1.2 PROPOSED APPROACH

After determining the initial user's requirements resulting in the formulation of LiDAR's specification for multiple users of the same dataset within the province, the next step is to determine a way of enforcing these specifications. Specification enforcement means having a system in place that will enable users to:

i. define requirements for projects and applications;
ii. budget or forecast the total error that will be produced from employing a system for collecting and processing the data; and
iii. determine whether or not the systems will meet set user's standards by comparing the user's requirements with delivered products.

This is the process termed *User Determined Total Error Budgeting (UDTEB).* Unlike the current LiDAR uncertainty budgeting process where all these decisions are made on the vendor's side, UDTEB seeks to enable users themselves to determine these errors and

proceed to find the errors of the points in relation to ground surveyed points measured at a higher accuracy. The process results in the removal of bias and promotes the independence of data and product accuracy verification.

1.2.1 Error Modeling and Analysis

The error modeling approach involved considering the observables in the operational functions of the LiDAR survey system. The statistical methods required for determining the accuracy and confidence intervals of the data is modeled employing a step by step approach discussed in detail in Section 3.4.

1.2.2 Error Interpretation

Questions answered with respect to this research include:

1. What limits of errors are acceptable for a particular application?
2. What are the manufacturer's documented project-specific error budgets for most LiDAR applications? Are these over-generalized, or do they cover most applications employing LiDAR products?
3. What sources of error can be identified by a user of LiDAR data?
4. How much do identified propagated errors affect the accuracies of the final deliverables?
    a. Looking at (higher accuracy) base data compared with acquired LiDAR data; and

b. Looking at airborne (high altitude and close range) LiDAR and other data forms integration.

5. How can these errors be treated? Can they be adjusted or should they be discarded?

To answer these questions, this research:

1. critically compared user-demanded accuracy specifications for Airborne LiDAR data with manufacturers' stated performance specifications (which are usually stated based on ideal conditions plus the influence or topography and ground cover) [Ussyshkin and Smith, 2006; Ussyshkin and Smith 2007; Ussyshkin et al., 2008]; and,
2. assessed the hypothesis that variations in user-demanded specifications and manufacturer's specifications - plus the influence of topography and ground cover - have significant effects in the reliability of information modeled or derived from Airborne LiDAR data.

Therefore, the hypothesis that was tested was whether *variations in user-demanded specifications and manufacturer's specification have significant effects in the confidence and quality of information modeled or derived from Airborne LiDAR data*. In this context, the term *significant* means distorting expected values by more than 25% due to errors in the data and post processing-processes. This definition of what constitute a significant distortion of expected values of spatial accuracy was derived from a previous study [Coleman and Adda, 2010], where one standard deviation (or 1-σ) represented the

worst acceptable accuracy for most applications utilizing LiDAR data in the research study area.

Confidence of information refers to the certainty that quality of information representing the spatial object met or exceeded one standard deviation of its true state or natural occurrence. The final information derived from the point cloud is of acceptable quality when the conditions defining acceptable accuracy and confidence levels are met or exceeded by the delivered spatial product. These users' requirements are stated at the beginning of the survey. Using the system precision information and ground measurements, the UDTEB model estimates the final accuracy of the survey data. After the survey has been completed, these initial requirements are also used to validate the survey and determine whether or not user's specifications have been met. Provision is made through the development of a Graphic User Interface (GUI) developed in this research to provide a platform through which this comparison can be done. Interpreting the result of this comparison is also provided by means of the GUI.

Common decisions to make involve answering the questions:

1. Have the initial user's specifications been met?
    a. If they have been met, were the vendor's quality standards over specified or is the data accuracy just right?
        i. if quality standards were over-specified, could lowering the requirement at the survey planning stage reduce over-all project time, cost and data storage problems?

ii. if the manufacturers' standards were just right for the survey, can the deliverable be considered as satisfactory?

b. If initial user specifications have not been met, can there be evidence to report to manufacturers on areas where there are deficiencies in the data?

2. Can the data be used for post processing and still meet the required final accuracy budget?
3. Based on previous points, can the data be accepted at the given accuracy and confidence to allow for closure and final payments of the survey contract?

1.3 MAIN CONTRIBUTION

This research proposed to develop and test the UDTEB model to fill the gap between manufacturer's stated uncertainties/errors and user's requirements for application-driven specifications. The method considered major contributors of errors from given airborne LiDAR data to the product processing stage. These investigations contribute to the process of quality assurance and data control of data and derived products from airborne LiDAR by providing methods and tools to fill the gap identified above. It is possible that a lack of such validation may lead to misleading public information. Very sensitive information is derived from airborne LiDAR relating to emergency prediction, environmental hazard assessment and mineral resource exploration. Misleading information will undermine the quality of these applications. Also public information on scenario simulation, environmental hazard forecasting and rescue planning missions,

derived from airborne LiDAR sources cannot be certified as accurate at a given confidence without a validation process.

This research anticipated that statistical analyses will reveal differences between the manufacturer's LiDAR specifications and real measurements. Where airborne LiDAR specifications are generally over-specified, lowering data acquisition specifications for certain terrain types may reduce cost and project processing time and still achieve desired accuracy. For instance in an flat and open terrain, specifying higher flying heights and lower points per square metres will still result in acceptable Digital Elevation Models (DEMs) as discussed in detail by Liu and Zhang [2008] where LiDAR points were reduced up to 50% but still allowed for DEM errors to ne no more than 20cm.

It was expected that the findings will enable LiDAR product users to ascertain the limits to which such systems may be pushed in terms of reliability of information derived for project-specific applications, especially emergency measures simulation and monitoring.

1.3.1 The Total Error Model

Unlike previous models that only considered the LiDAR system uncertainties (just the reported instrument precision), the UDTEB model looks into estimating other identified major contributors to error in LiDAR data. Post-processing uncertainties from created products are also considered in the model. Following that, the model combines these uncertainties to estimate the total error. Additionally, UDTEB model gives the user room to customize and add other error sources and determine the overall errors in specific

cases. Major models that are developed in this research but were not formally considered are the PLanning Uncertainty Model (PLUM), Data Integration Uncertainty Model (DIUM) and Presentation Uncertainty Model (PUM). These are discussed in detail in Chapters 3 and 4. It is important to note from this research that the total error from a LiDAR survey is not just an additive process of the various the components discussed above. Chapters 2 and 3 discuss this formulation in detail. After performing field validation surveys, identified discrepancies between the model and field values are used to further refine the proposed error model.

1.3.2 The Software Prototype

This is a further contribution beyond the stated objectives (as expatiated in Section 3.4.4). Although the model itself provides a way to design and customize the UDTEB model for a given organizations, it was necessary to provide some proof of concept. Using the error estimates in the model for the project area, a software prototype for determining whether or not specifications have been met was developed using Matlab®.

1.3.3 Data Cleaning Using TPU Values

Another contribution that evolved indirectly from this research involved the possibility of using the UDTEB model results for cleaning noise from large point cloud datasets. This has been initially explored by Adda and Hoggarth [2011] for CARIS. CARIS, in partnership with MITACS and UNB, completed a research in the summer of 2011 to

develop methods and software to calculate Total Propagated Uncertainties (TPU) of point clouds for effective visualization and analysis. A test was made on a strip of LiDAR data with points known to be falsely classified in the Fredericton area. Errors of the point clouds with respect to check points in the area were calculated. Once these errors were expressed in the same confidence interval (in terms of the ground checkpoints and the point clouds), the TPU of the final product, which in this case was a topobathymetric surface, was determined and plotted as shown in Figure 1.3. By categorizing point clouds with respect to their TPU, points with values falling outside the given elevation were separated from the point cloud as shown in Figure 1.3. Once the points were separated as shown in the red points in (lined up red points at the top of Figure 1.3), they were deleted from the dataset to create datasets with less noise as shown in Figure 1.4.

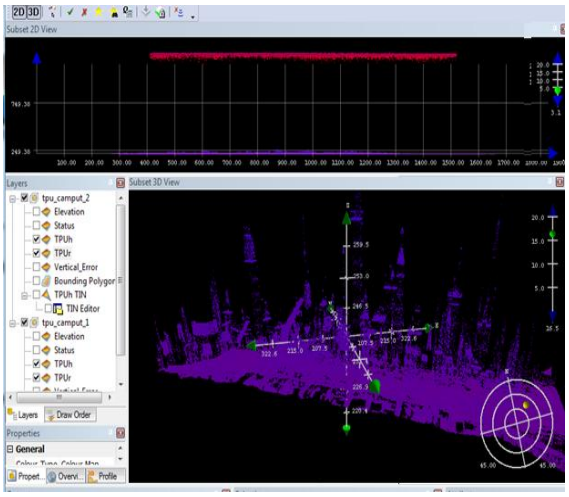

Figure 1.3. Point cloud data with noise with TPU values separated by range.

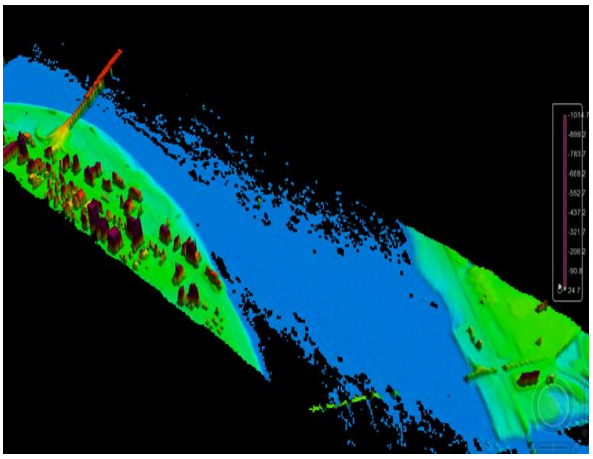

Figure 1.4. Point cloud after cleaning noise by deleting points outside TPU range

Further point processing and analysis can then proceed to create product within specifications for accuracy. For instance, in this example, all points not lying within the acceptable vertical error (±15cm) and horizontal error (±70cm) were cleared by

employing the TPU values. Further look at automating this process to perform noise cleaning would be an interesting research to undertake.

1.4 OUTLINE OF DISSERTATION

This dissertation is divided into five chapters with each chapter structured as follows:

- Chapter 1, as already discussed, provides a general overview of the research. It provides reasons for the research and main contributions expected from the work.
- Chapter 2 looks at previous literature that considered uncertainties/errors for LiDAR data and products. The key findings of importance to this research are noted, and the particular contribution of this research in the overall knowledge of LiDAR errors is presented.
- In Chapter 3 specific research questions are asked and the problem (or gap) is defined. This gap relates to the inability of most LiDAR users to determine error budgets for project specifics and verify after delivery of data whether or not the data have been provided according to specifications. The methods applied to achieve these are presented.
- Chapter 4 discusses the results of the modeling and prototype application developed in Matlab®. An analysis of the result after field tests is employed to determine whether or not the model produced realistic error budgets are made in this section. Interpretations of the error budgets and the effects on projects are discussed using flood modeling as an example.

- Conclusions on how the methods applied to solve the gap of the inability of everyday users of airborne LiDAR data to perform requisite error budgeting tasks to determine whether data is fit for a specific project is presented in Chapter 5. Recommendations for further research are also discussed.

CHAPTER 2. LITERATURE REVIEW AND POSITIONING OF RESEARCH

2.1. INTRODUCTION
- 2.1.1 Operational Consideration for Accurate Point Cloud Acquisition

2.2 STATISTICAL PROCESSES AND ANALYSIS OF ERRORS
- 2.2.1 Accuracy, Error and Uncertainty/Precision
- 2.2.2 Confidence Interval
- 2.2.3 Law of Propagation of Errors
- 2.2.4 Sampling and Estimation Methods
- 2.2.5 Potential Sources and magnitudes of errors in LiDAR
- 2.2.6 Identifying and Removing Blunders and Errors

2.3 MATHEMATICAL MODELS FOR ERROR DETECTION

2.4 POSITIONING OF RESEARCH

Figure 2.1 Outline of Chapter 2.

2.1 INTRODUCTION

This chapter discusses the efforts of authors whose previous research has bearing on this research. Most literature and efforts at determining total error budgets investigate the mechanical components of LiDAR systems, namely, the Inertial Measurement Unit (IMU), the Laser Scanning System (LSS) and the Global Positioning Systems (GPS) for ground and airborne systems [Hodgson et al., 2005; Ussyshkin et al., 2008].

Smith [2005] and Habib et al. [2005] discussed errors resulting from the post-processing of LiDAR and its products like Triangular Irregular Networks (TINs) and DEMs. These errors are not independent of each other in their contribution towards total errors [Aguilar et al., 2005; Guo et al., 2010]. The authors researched DEM interpolation errors and discuss the variations of system errors when looking at different environments and point densities.

2.1.1 Operational Consideration for Accurate Point Cloud Acquisition

Figure 2.2 shows the integration of different systems with LiDAR systems. LiDAR is an active remote sensing system that records returned signals converted to digital representations in real-time [El-Sheimy, 2005].

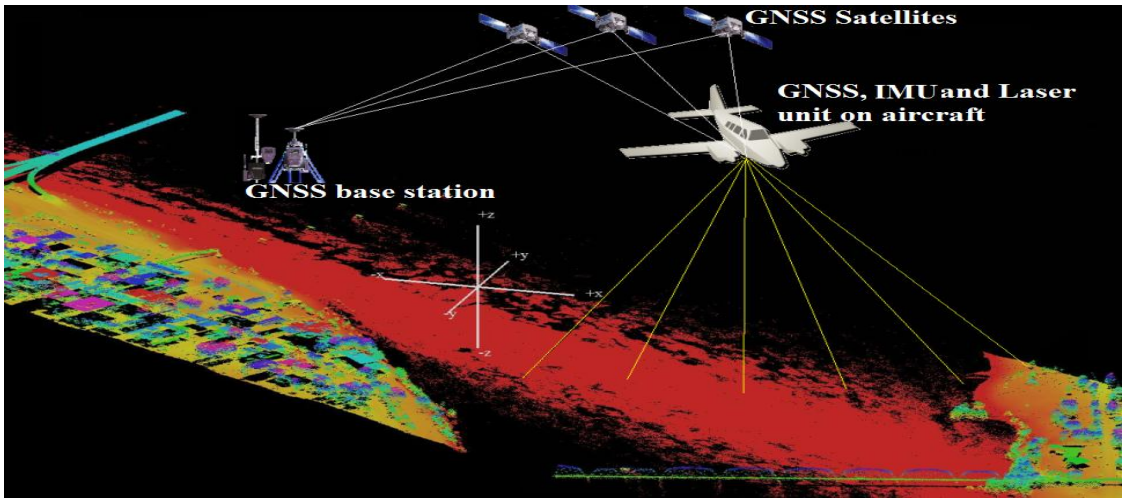

Figure 2.2. System integration in ALS surveys (from Adda and Hoggarth, 2011)

Figure 2.2 shows the major components operating in an Airborne Laser Scanning (ALS) survey. The LiDAR system consists of the integration of Inertial Measurement Unit (IMU) for orientation, remote sensing laser range finder and a scanner (Laser) for point cloud collection, and GPS for positioning. The IMU and the onboard GPS make up the Positioning and Orientation System (POS) part of the LiDAR system. These three units (i.e., the GPS, IMU and Laser) are time-synchronized in a process called *registration*, to achieve instantaneous 3D positioning. The airborne segment of airborne LiDAR systems consists of [Jie et al., 2008, pp.129-131]:

1) airborne platform;

2) LiDAR observation system; and the
3) POS, made up of GPS and IMU.

The ground segment of the airborne LiDAR system is comprised of the:

1) GPS reference stations which gather GPS data at known earth fixed positions for later computation of the airborne platform position;
2) processing hardware; and
3) software for post processing synchronization and registration.

Airborne LiDAR systems are capable of detecting multiple return signals for a single transmitted pulse [Wehr and Lohr, 1999; Charaniya et al., 2004; Reutebuch et al., 2005], but others can record up to six returns for a single pulse [Lim et al., 2003; Wagner et al., 2004]. Multiple returns occur when a laser pulse strike a target that does not completely block the path of the pulse. The remaining portion of the pulse continues on to a lower object [Reutebuch et al., 2005]. Multiple returns are particularly useful for the topographic mapping in forested areas [Sheng et al., 2003].

Spatially, LiDAR points are initially represented by latitude, longitude, and ellipsoidal height consistent with the reference ellipsoid of the GNSS ground station, ideally an Earth-Centered Earth-Fixed (ECEF) ellipsoid such as the GRS80 or the WGS84. They can be transformed to other coordinate systems. At the same time, elevations are converted from ellipsoidal heights to orthometric heights based on a national or regional height datum by using a geoid model [Webster and Dias, 2006]. Data collected by the ground stations and the onboard GPS receivers is post-processed to compute the LiDAR

positions [Wehr, 2008]. The integrated solution coming from the GPS and IMU data offers at every observation epoch:

X_{ECEF}, Y_{ECEF}, Z_{ECEF}, and the orientation parameters (roll, pitch, yaw). (*2.1)*

The position coordinates are related to the LiDAR, and the orientation angles are the rotations about the instantaneous local horizontal system.

In a second step, LiDAR and POS data have to be synchronized by the procedure of registration. After synchronization a file with the following information for each epoch is generated for further processing:

X_{ECEF}, Y_{ECEF}, Z_{ECEF} roll, pitch, yaw, scan angle, slant range and intensity. (*2.2)*

Assuming a perfect inner orientation calibration, the LiDAR geocoded laser measurement points on the ground are calculated from Eq.(2.2), once the misalignment (between IMU and LiDAR) angles in roll, pitch, and yaw are known.

After a sequence of processing steps and calibration, files containing the geocoded (also known as registered) laser measurements can be computed in chronological order:

$$X_{Laser}, Y_{Laser}, Z_{Laser,} \text{ intensity}. \quad (2.3)$$

And finally, after synchronization the laser vector for each sampled ground point can be directly transformed into an earth fixed coordinate system (e.g., WGS84) [El-Sheimy, 2005].

2.2 STATISTICAL PROCESSES AND ANALYSIS OF ERRORS

The RMSE statistic assumes that errors have a normal distribution with zero mean, and that all systematic errors have been removed. This condition is difficult to be fully satisfied, especially with LiDAR data. Some systematic errors or biases remain undetected, even after regular calibrations of LiDAR systems. However efforts are made to minimize the effects of these errors.

2.2.1 Accuracy, Error and Uncertainty/Precision

These terms seem to be similar in the field of statistics but they are indeed different and represent different characteristics of the sampled data and its relationship to the population. The following section provides an overview from Bell [1999] of what these terms represent.

2.2.1.1 Accuracy

Accuracy is a measure of spread indicating the closeness of a measurement to the true value. It is a measure of the nearness of a variation between the measured value and the true value towards zero. The validation and reporting of accuracy limits could be a mounting task in LiDAR projects. The huge size of point cloud data and the not readily available supporting information describing these files makes it more difficult to model errors per point. This is in contrast to what is practiced in the multibeam Sonar products where all position information for a given sounding is available. For instance, in multibeam echo sounding surveys, files with the ".all" file extension used by certain

systems contain all information pertaining to positioning and orientation of points. These parameters can be used to perform error analysis of the soundings. In the absence of such information on the ALS side, statistical methods have to be considered to estimate empirical measurements during the time of the survey.

2.2.1.2 Errors

An error is the cause (due to one or many factors) that results in the deviation (including *bias*) of a measurement (resulting from the use of a device and/or process) from the true value [Dare, 2013]. Error is quantified by estimating the difference between the observed or calculated value of a quantity and its true value [Oxford Dictionaries, 2012b]. When error is quantified, it represents the accuracy (i.e. the variation or *spread* between a measured value and its true value) of the measurement. Errors in measurements can be due to defects in the measuring device – and are called "*systematic errors"*. Errors can also be due to irregular changes in the measurement process, for instance unexpected changes to temperature, terrain, point density and object reflectance. These errors are known as *"random errors"*. Another reason for measurement errors are *"personal errors* or *surveyor errors"*. These errors occur when observers of a measurement adopt wrong procedures during a measurement and are technically referred to as *blunders*.

In statistics the terms "null hypothesis" and "alternative hypothesis" are used to determine if two observations have the same or inverse trends. For instance, in the case of LiDAR, we can make a null hypothesis that the population mean elevation error is equal to the hypothesized mean elevation error of ±15 cm. In mathematical terms this is written as:

H_o: $\mu = \mu_e = \pm 15$ cm.

If the results do not support the null hypothesis, we can formulate that there are three possible alternative hypotheses H_a as follows:

Case 1: H_a: $\mu \neq \mu_e$; Population mean elevation error does not agree with sampled mean elevation error – may be more or less;

Case 2: H_a: $\mu > \mu_e$; Population mean elevation error is greater than sample mean elevation error; or

Case 3: H_a: $\mu < \mu_e$; Population mean elevation error is less than sample mean elevation error.

This research employs these alternative hypothesis to disprove a two-tailed null hypothesis (H_o) that sample mean elevation errors are not equal to the population mean elevation errors (within a range of confidence).

In the quest to test H_o there are two types of errors that can be made [Kothari, 1985; Vaníček and Krakiwsky, 1986; Wang et al., 2010] as shown in Table 2.1 (from Kothari [1985], p.187] :

Table 2.1 Type I and II errors employed to accept or reject a null hypothesis

	Decision taken	
	Accept H_o	Reject H_o
H_o is true	Right decision	Type I error
Ho is false	Type II error	Right decision

1. Type I errors (also known as the α-error): Occurs when the H_o is rejected when H_o is actually true and should have been accepted.

2. Type II errors (also known as the β-error): Occurs when the H_o is accepted when H_o is actually false and should have been rejected.

2.2.1.3 Uncertainty and Error Budgeting

By definition, a measurement

> …tells us about a property of something. It might tell us how heavy an object is, or how hot, or how long it is. A measurement gives a number to that property. Measurements are always made using an instrument of some kind. Rulers, stopwatches, weighing scales, and thermometers are all measuring instruments [Bell, 1999].

The range of how well or poorly a measurement reflects reality is referred to as uncertainty. In everyday language we use the phrase "more or less" or "give or take" to express uncertainties. There is a fundamental difference between error and uncertainty (or quantified precision). While the amount of error represents the difference between a measurement and its "true" value, uncertainty refers to the spread of the precision of the measurement [Bell, 1999]. Some authors confuse the term uncertainty with error. For instance, Hunter et al. [1995] used the term "uncertainty" in relation to spatial databases to refer to differences between provided information, and the corresponding information that is directly measureable in the real world.

Uncertainty, when used in this dissertation, is defined as the validation of the amount of variation in the precision of a measurement, in the attempt of that measurement to

determine the true value of a subject. In the case of this study, the subject is a position (x,y,z) created from LiDAR points. And the true value refers to a measure that is three times more precise than the subject measurement to be validated [Chrzanowski, 1977].

The Oxford Dictionaries [2012a] define a budget as:

> "…an estimate of income and expenditure for a set period of time".

Similarly, but used in a spatial data context, error budgeting relates to the range of values estimating how accurate (within a confidence interval) a dataset can be acquired (income) and used (expenditure) for a specific engineering application within the life-cycle (set period of time) of the dataset. An error budget, as used in the project refers to two things:

- A forecast of errors – defining what is acceptable and what is not; and
- A validation that the errors are acceptable or not - with given reasons.

Uncertainty budgeting quantifies a range of values within which an error budget can be accepted as being fit for use.

For a known sample of measurement, the mean and variance are quantities than can be used to measure uncertainty and they are as calculated as follows:

$$\mu = \frac{\sum_{i}^{N} m_i}{n-1}, \qquad (2.4)$$

$$\sigma^2 = \frac{\sum_{i}^{N} (m_i - \mu)^2}{n-1}, \qquad (2.5)$$

where m_i represents the consideration of each point in the LiDAR data, μ is the mean, and σ^2 is the variance. The standard deviation can be found by finding the square root of the variance.

2.2.2 Confidence Interval

In a normal distribution (curve or table) 68.2% of values in a given sample fall between -1 and +1 σ of the population; whereas 95.4% of values fall between -2 and +2 σ. These percentages (68% or 95.4%) are referred to as Confidence Intervals (CI) and the limits (±1 and ±2) are referred to as the Expansion Factors (EF) or the better known term, critical values. Confidence intervals (different from confidence levels) define the percentage or probability that a measurement will fall within the precision or error range of the instrument. They are hypothetical in nature, drawing the information from laboratory experiments on instrument precision. However, confidence levels, refers to the probability that a measurement fall within a given accuracy observed after several empirical (real physical) measurements of the same event.

One way to be sure that a sample of LiDAR points represents the characteristics of other points is to repeat the survey hundreds of times to give us several estimates of the mean. After determining these estimates, we can then take the mean of these means and then calculate the σ.

This σ of the means is called the Standard Error (SE) or more precisely, the Standard Error of the Mean (SEM). It is surely not practical (especially in times of fiscal restraints)

to repeat experiments several times in order to obtain the Standard Error. A theoretical approach can be adopted using statistics to obtain the SE. Consider that if we had a large set of samples (n) we will have less SE. Also, we note that the smaller the σ the more confident is the value of SE. Therefore we represent the SE as follows [Kothari, 1985, pp.165-175]:

$$SE = \frac{\sigma}{\sqrt{n}} . \qquad (2.6)$$

Note that the denominator of Eq. (2.6) is √n because we have to initially calculate the "variance" and then take the square root of the variance to obtain the standard error. The confidence interval can now be determined following Eqn.(2.6) as follows *[ibid]*:

$$CI = M \pm (EF \times SE) \qquad (2.7)$$

where M represents the mean (that can be replaced by the known true value).

2.2.3 Law of Propagation of Errors

Following discussions from Vaníček and Krakiwsky [1986], the covariance law can be written as:

$$C_x = GC_lG^T , \qquad (2.8)$$

where C_l is the Covariance matrix of the observables *l,* G is the design matrix transforming *l* to the unknown parameter, *x*. Any uncertainties in *l*, will be described in the covariance matrix C_l. These uncertainties can be traced into *x* and characterized by C_x.

Following Eq.(2.8), in the special case where the unknown parameter (*x)* has only one element, and the individual elements in the vector *l* are statistically independent, a function relating *l* to *x* can be written as:

$$x = g(l) \, . \qquad (2.9)$$

Taking the partial derivatives thus expressing the variance form of Eq.(2.9) gives:

$$\sigma_x^2 = \left(\frac{\partial g}{\partial l_1}\sigma_{l_1}\right)^2 + \left(\frac{\partial g}{\partial l_2}\sigma_{l_2}\right)^2 + \left(\frac{\partial g}{\partial l_3}\sigma_{l_3}\right)^2 + \ldots + \left(\frac{\partial g}{\partial l_n}\sigma_{l_n}\right)^2 = \sum_{i=1}^{n}\left(\frac{\partial g}{\partial l_i}\sigma_{l_i}\right)^2 \, . \qquad (2.10)$$

Equation (2.10) is called the *Law of propagation of random errors* [Vaníček and Krakiwsky, 1986].

If Eq.(2.9) is linear then we can write:

$$x = Gl + w \, , \qquad (2.11)$$

where $G = [\, g_1, g_2, g_3, \ldots, g_n \,]$. And from this we can write the variance of x as:

$$\sigma_x^2 = \sum_{i=1}^{n}(g_i\sigma_{l_i})^2 \, . \qquad (2.12)$$

Let the model for *x* be statistically independent and *l* be acquired with the same accuracy, i.e., if $x = \frac{1}{n}\sum_{1}^{n} l_i$,

then:

$$\sigma_x^2 = \frac{1}{n}\sigma_l^2 \, . \qquad (2.13)$$

Again, if the function relating *x* to *l* is linear (as in Eq.(2.9)), then from Eq.(2.13), we can write:

$$\delta x = \sum_{i=1}^{n} g_i \delta l_i \ . \qquad (2.14)$$

Equation (2.14) is known as the *Law of propagation of systematic errors* [Vaníček and Krakiwsky, 1986]. The law of error propagation is applicable in both the deterministic and non-deterministic approaches to determine the standard deviations of LiDAR points in a given footprint (window). Readers will observe in Chapters 3 and 4 that error propagation has been applied in determining the contribution of errors from each of the models and their subsequent integration into one system (that is the UDTEB model). In the application stage (Section 3.4.3), error correlations between the observables, *l*, are also considered as the observables cannot be assumed to be independent.

2.2.4 Sampling and Estimation Methods

Kothari [1985, p.152] define sampling as:

> ..the selection of some part of an aggregate or totality on the basis of which judgment or inference about the aggregate or totality is made...it is the process of obtaining information about an entire population by examining only a part of it.

Sampling is necessary in validating LiDAR data as it is practically impossible to validate each LiDAR point in a survey. Estimates such as sample mean ($\bar{X}$) and sample standard deviation (σ_s) are used to estimate population parameters (φ the population mean and σ_p, the population standard deviation). Using least squares, it is possible to minimize the variations of these estimates chosen from samples of the population. To allow this to be possible, certain properties of estimations need to be considered [Kothari, 1985]. These are the property of:

1. Unbiasedness – the expected value of the estimator is equal to the parameter being estimated;
2. Efficiency – small in variance;
3. Sufficiency – use as much information available for the sampling process to represent the population; and
4. Consistency – as the sample size increases, the estimator should approach the value of the population parameter.

Applying the four estimation properties above to the UDTEB model helps the user to make more complete decisions about the data accuracy on the basis of fitness for use.

2.2.5 Potential Sources and Magnitudes of Errors in LiDAR

Although there have been considerable improvements in technology to ensure accurate production of LiDAR point clouds, there are some main sources of error of particular interest to the LiDAR industry. Ussyshkin et al. [2008] reports that due to the nature of LiDAR data collection, various operational considerations - including variations in geo-positioning data quality, ground conditions, and weather conditions - will significantly affect the achievable point accuracy in the field [Hodgson et al., 2005].

The density of the canopy cover may also affect accuracy of the Digital Terrain Model (DTM) [Witte et al., 2000]. Explicitly, the accuracy of the DEM derived from the LiDAR points may include various errors due to data interpolation and classification [Smith et al., 2005]. Although research has been done since 2000 to determine the overall accuracy that can be achieved with LiDAR and to assess achievable accuracy for various mapping

applications, the misinterpretation of the instrument accuracy specifications with the achievable accuracy of the LiDAR data is still common [Adams, 2002; Bowen, 2002; Hodgson et al., 2005]. For instance, as shown in Figures 2.3. Ussyshkin and Smith [2006] mention some important factors that affect the final operational accuracy of LiDAR data.

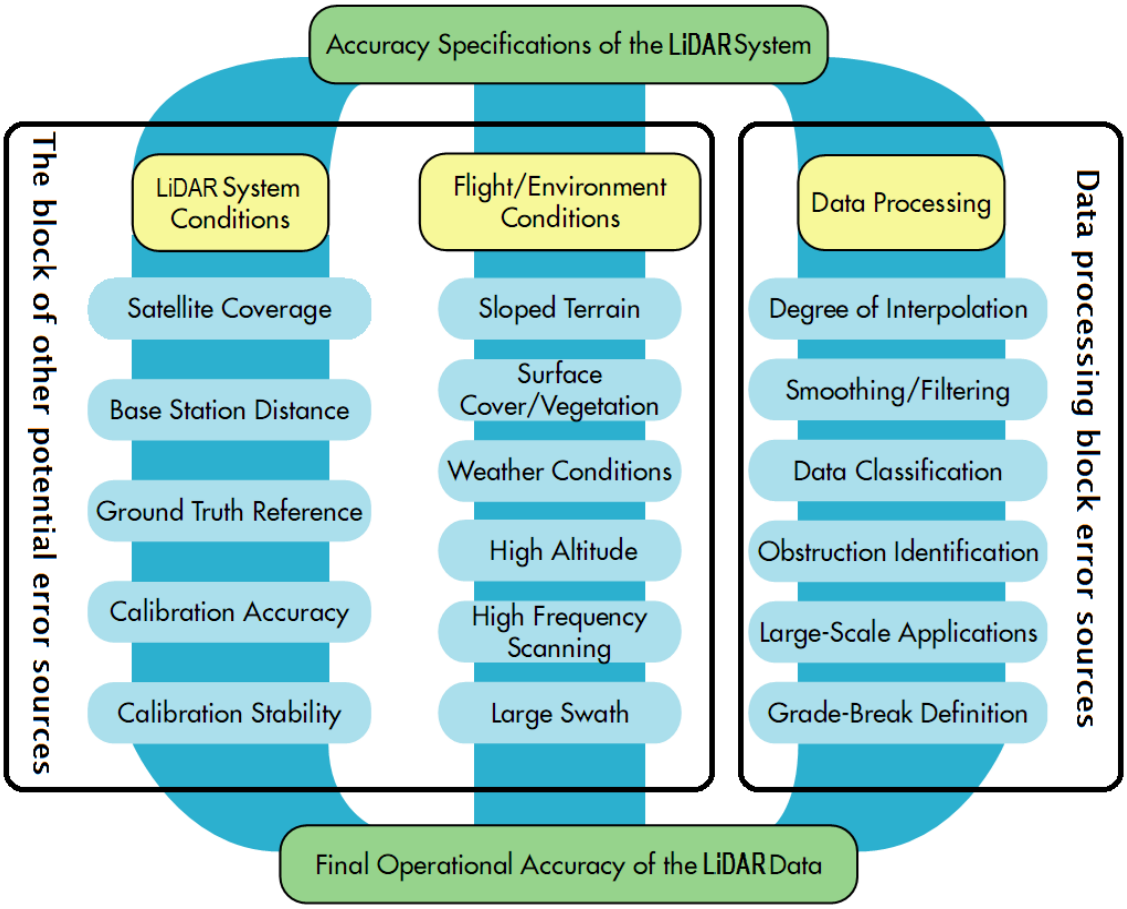

Figure 2.3: Final accuracy factors for LiDAR data (Ussyshkin and Smith [2006, p.5]

It makes sense for users to investigate the error budget associated with the data processing block as it may provide the essential pointers of error within the LiDAR survey. Processing uncertainties were considered in this research and discussed in detail in Section 3.4.4.2.

Habib et al. [2008] observed that - unlike photogrammetric techniques - the derivation of the point cloud from the LiDAR measurements is not a transparent process since the raw system measurements are not always made available to the system users. Furthermore computation of coordinate of LiDAR footprints is not based on redundant for performing an adjustment method employing redundant data.

As shown in Figure 2.4, a laser may reflect off the wall of a building thus sending the return pulse in a direction other than the source direction of the laser instrument.

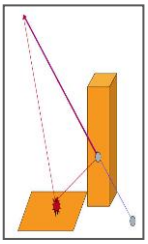

Figure 2 4: Multipath in LiDAR results in spurious data points [Lohani, 2009]

When multiple producers and collection systems are utilized to gather LiDAR data over the same project area, it is good that the data is tested separately for each producer or collection system (in terms of equipment, procedures, software) for errors and blunders [Flood, 2004].

2.2.5.1 Uncertainty in Horizontal Positioning

In terms of horizontal accuracy, the major sources of uncertainty in LiDAR data are the following [Samberg, 2005]:

1. Positioning of the carrying platform and its orientation along the trajectory
2. Errors in the electro-optical parts of the laser sensor
3. Wrong laser and INS/POS data processing

4. Careless integration and interpolation of the INS and GPS
5. Erroneous data from the reference ground GPS base stations

Roll, pitch, and heading effects on uncertainties are illustrated in Figure 2.5 (after Samberg, 2005, p.22).

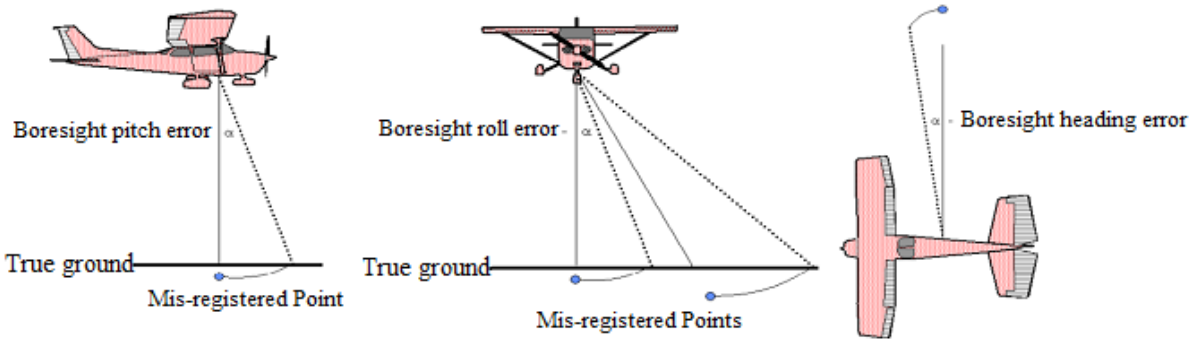

Figure 2.5 (a) pitch error (b) roll error (c) heading error. A misregistered laser observation is represented by the dotted lines

The pitch error as shown in Figure 2.5(a) results in a laser slant range to be recorded as the nadir. A roll error also causes a slant range to be incorrectly registered. The elevation differences tend to increase with a larger scan angle (Figure 2.5b). The heading error induces a skewing in each scan line (Figure 2.5c). Table 2.2 from Samberg, [2005, p.26] shows that angular error is not affected by flying at higher altitudes. However, the positioning error is worst at higher flight altitudes.

As shown in Table 2.2, differences in terrain slope have varying effects on accuracy.

Table 2.2 Examples of horizontal positioning errors relating to flight altitude error at a given angular error

Flight Altitude	**Angular Error**	**Horizontal Positioning Error**
2000 m	±0.005 °	±0.17 m
4000 m	±0.005 °	±0.35 m
6000 m	±0.005 °	±0.52 m

When the laser beam encounters sloped terrain, it results in the elongation of pulse footprints as shown in Figure 2.6. This leads to an increase in horizontal and vertical position uncertainty as further clarified in Figure 2.7 where an apparent LiDAR point and its relative vertical and horizontal errors are shown.

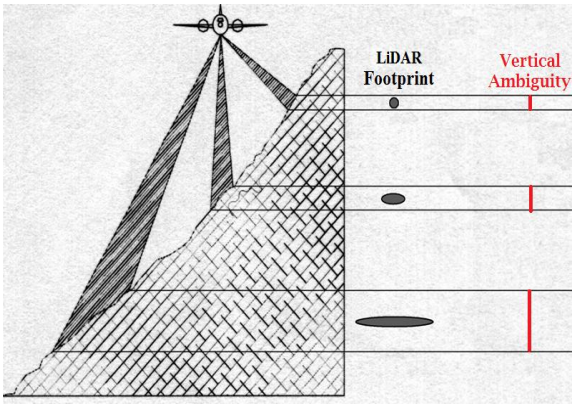

Figure 2.6. Effect of slope on vertical accuracy (from Renslow [2010, p.251,]).

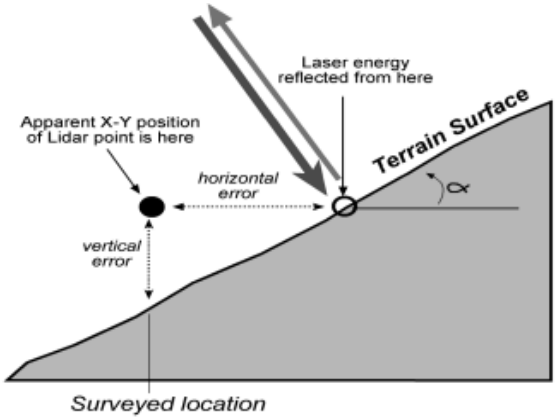

Figure 2.7. Vertical error induced by horizontal errors (Hodgson and Bresnahan, 2004, p.332

From Figure 2.7, assuming smooth even slope we can deduce the following:

$$\text{Tan } \alpha = \frac{Vertical_Error}{Horizontal_Error}, \qquad (2.15)$$

where α is the slope angle.

2.2.5.2 Uncertainty in Vertical Positioning

Hodgson et al [2005] also propose, as shown in Table 2.3, that there is an increase in overall elevation root mean square errors (RMSE) with increasing terrain slope.

Table 2.3: Terrain Slope vs. RMS Error [Hodgson et al., 2005]

Slope	0-2°	2-4°	4-6°	6-8°	8-10°
Elevation Error [cm]	±60	±65	±88	±93	±89

Uncertainties in vertical positioning as reported above are closely correlated to horizontal uncertainties. Hodgson and Bresnahan [2004] report that based on empirical measurements under ideal conditions the system error associated with the instrument's ability to report a specific location during the collection of points is generally reported to be good to the order of ±14 cm RMSE vertical. Different topography may affect the accuracy of the elevation surface [Hodgson and Bresnahan, 2004]. Dense vegetation can limit ground elevation detection – tall dense forests and even tall grass tend to cause greater elevation errors than unobstructed (short grass or barren) terrain [Flood, 2004].

2.2.6 Identifying and Removing Blunders and Errors

The identification and removal of blunders plays an important role in this process. Flood [2004] and Hodgson and Bresnahan [2004] recommend computing the magnitudes of errors using datasets higher accuracies than LiDAR. The "difference" or error for each checkpoint is computed by subtracting the surveyed elevation of the checkpoint from the LiDAR dataset elevation interpolated at the (x,y) location of the checkpoint. A positive error will mean the evaluated dataset elevation is higher than true ground in the vicinity of the checkpoint, and if the difference is a negative number, the evaluated dataset elevation is lower [Hodgson and Bresnahan, 2004].

$$\text{For checkpoint}_{[i]}, \text{ the vertical error}_{[i]} = [Z_{data[i]} - Z_{check[i]}] , \qquad (2.16)$$

where $Z_{data[i]}$ is the vertical coordinate of the i^{th} checkpoint in the dataset,

$Z_{check[i]}$ is the vertical coordinate of the i^{th} checkpoint in the independent source of higher accuracy, and

i is an integer from 1 to n; n is the number of points being checked .

Dataset to be used to verify the LiDAR data should be at least three times more accurate than the LiDAR accuracy [Flood 2004, Chrzanowski 1977]. At least three of six known control points should be fixed to control scale, orientation and position (Figure 2.8).

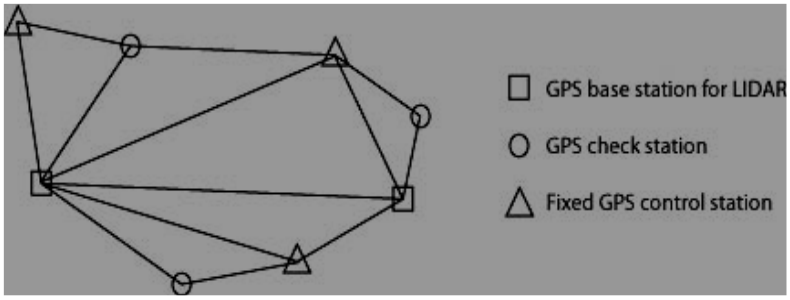

Figure 2.8: An example of a GPS ground control network (from. Samberg [2005, p30]).

The GPS base stations for the LiDAR data, the GPS check stations for the validation survey and the already known (Fixed GPS control stations) should be distributed evenly within the project area.

2.3 MATHEMATICAL MODELS FOR ERROR DETECTION

Habib et al. [2008] gives a detailed analysis of error budgets for LiDAR systems and quality control of the point cloud. The usual method of quality control by checking LiDAR data against independently surveyed points was said to be too expensive and unable to provide accurate horizontal verification of the point cloud. Since the horizontal accuracy is of inferior quality to the vertical accuracy of the LiDAR points, the authors criticized the approach proposed by Crombaghs and Bruegelmann [2000] for evaluating

overall quality by reducing discrepancies between overlapping strips. An adjustment procedure similar to photogrammetric strip adjustment proposed by Kilian et al. [1996] for improving compatibility between overlapping LiDAR strips was also flawed since the method relies on distinct points like building corners to relate overlapping LiDAR strips and surfaces. Maas [2000] method of employing least squares matching correspondence between discrete points on one LiDAR strip and TIN patches in another strip where normal distance between conjugate points were minimized was also flawed. The method proposed by Bretar et al. [2004] for improving the quality of LiDAR data using derived surfaces from photogrammetric procedures was said to have practical limitations since it required aerial imagery over the same area – which is an extra data acquisition process.

Considering these lapses, Habib et al. [2008] categorize their error sources as random errors and systematic errors. The authors then simulated system measurements (ranges, mirror angles, position and orientation) of a mapping frame, IMU body frame and the laser unit (mirror angle and range control) as shown in Figure 2.9.

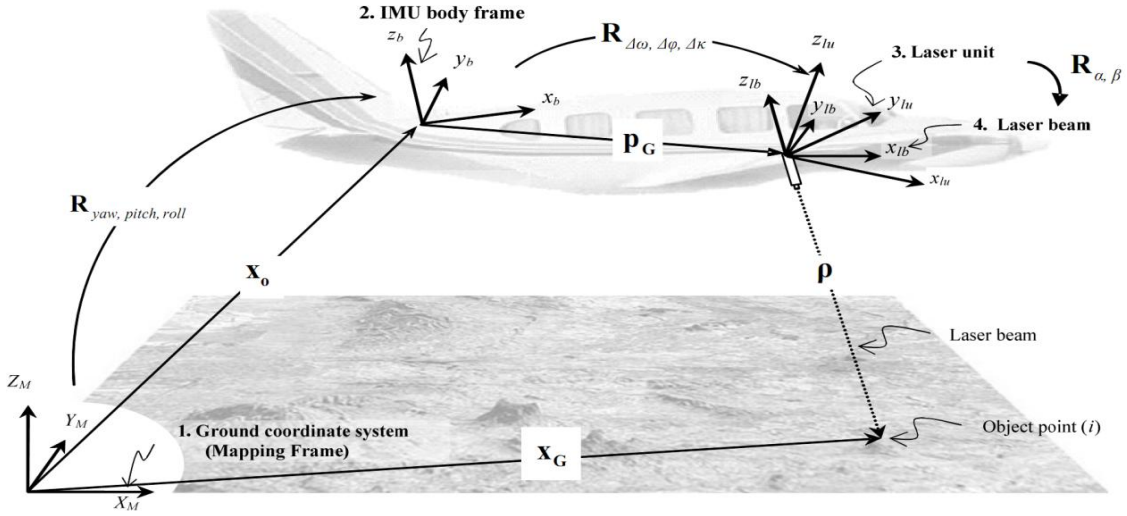

Figure 2.9 Coordinate systems and quantities of the LiDAR equation (Habib et al., [2008, p.205]).

The coordinate systems and quantities of the LiDAR equation was derived from this simulated system. Noise is added to the system measurements and the initial surface is reconstructed using the LiDAR equation:

$$\vec{X}_G = \vec{X}_0 + R_{yaw,\,pitch,\,roll}\ \vec{P}_G + R_{yaw,\,pitch,\,roll}\, R_{\Delta\omega,\,\Delta\phi,\,\Delta\kappa}\, R_{\alpha,\beta.} \begin{bmatrix} 0 \\ 0 \\ \rho \end{bmatrix}, \qquad (2.17)$$

where $\vec{X}_G$ is the position of the laser footprint; $\vec{X}_0$ is the vector between the origins of the ground and the IMU's coordinate systems; $\vec{P}_G$ is the offset between the laser unit and the IMU's coordinate systems (also known as the bore-sight offset); ρ is the laser range vector (defining the distance from the laser firing point to its footprint); $R_{yaw,\,pitch,\,roll}$ is the rotation matrix relating to the ground and the IMU coordinate systems; $R_{\Delta\omega,\,\Delta\phi,\,\Delta\kappa}$ is the rotation matrix relating the IMU and laser unit coordinate systems (angular bore-sighting); and $R_{\alpha,\beta}$ is the rotation matrix of the laser beam and laser unit coordinate systems (α and β are mirror scan angles).

In summary, it was found that in the case of random errors:

1. Position noise leads to similar noise in the derived point cloud and has the same effect independent of the system flying height and scan angle.
2. Orientation noise affects horizontal coordinates more than the vertical coordinates. The effect depends on the system's flying height and scan angle.
3. Range noise mainly affects derived vertical coordinates. The effect is independent of the system's flying height but dependent on the system's scan angle.

In the case of systematic errors, after some bias was added (instead of noise in the random error analysis above) to the simulated system, it was concluded that:

1. The discrepancies caused by the bore-sighting offset and angular biases can be modeled by shifts and a rotation across the flight direction.
2. The boresight uncertainties can be used for diagnosing the nature of the systematic errors in the system parameters.

The drawback of this system from the analysis of the author is that the modeled noise introduces bias since the difference between the modeled point clouds and the effect of the noise is actually the noise that was introduced initially. Also the simulation was tested on a fairly flat terrain which may not hold for a variable terrain. The effect, of any high-rising built-up areas was not investigated. Also missing is the effect of post-processing, data integration and interpretation uncertainties [Coleman and Adda, 2010].

Csanyi and Toth [2007] discuss the use of targets on the ground, before flying ALS surveys as a way to perform quality control. Ideally, these targets should be visible at a given LiDAR resolution and should be uniformly spread to accommodate differences in both terrain morphology and obstructions to ground. However, the targets are themselves obstructions to ground hits, and using established targets may introduce bias and may not allow for independence when a choosing checkpoints within the surveyed area.

2.4 POSITIONING OF RESEARCH

The position of this research is not to refute the processes and methods applied by manufacturers to estimate the performance of LiDAR systems. In the LiDAR market, manufacturers seek to protect their market share by limiting how many their processes and methods are available for scrutiny. The positioning of this research is to utilize previous knowledge to model LiDAR errors from the point when the delivered data is received by the user. Specifically, five important research findings were employed:

1. Habib et al., [2008] who described the error budget of LiDAR Systems and quality control of the derived point cloud. The authors looked into error simulations if original LiDAR files do not contain error information;
2. Hogdson and Bresnahan [2004] who discussed empirical assessment of DEMs derived from ALS. Also in Hogdson et al. [2005] the analysis of terrain slope error in leaf-off conditions when creating DEMs was analyzed;
3. Gonsalves [2010] who, in his PhD dissertation, discussed a comprehensive uncertainty analysis and method of geometric calibration for a circular scanning airborne LiDAR;
4. Goulden [2009] whose MSc thesis looked at the prediction of error due to terrain slope in LiDAR observations; and
5. Coleman and Adda [2010] who looked at the creation of specifications for multiple organizations looking to share LiDAR data.

By harmonizing the various research efforts mentioned above, a more comprehensive error model can be created. A field validation of the results may suggest missing error components that can be accounted for by including them in the UDTEB model.

CHAPTER 3. RESEARCH QUESTIONS OBJECTIVES AND METHODOLOGY

3.1INTRODUCTION
3.2 RESEARCH QUESTIONS
3.3 RESEARCH OBJECTIVES
3.4 METHODOLOGY
3.4.1 Assumptions
3.4.2 Users' Requirements Definition
3.4.2.1. User Needs Research
3.4.2.2. Common Needs
3.4.2.3. Differences
3.4.2.4. Main Components of Specified Minimum Requirements
3.4.3 System Uncertainty Modeling Development
3.4.3.1 Deterministic Uncertainty Modeling
3.4.3.2 Non Deterministic Uncertainty Modeling
3.4.4 User Determined Error Modeling
3.4.4.1 Planning Uncertainty Model (PLUM)
3.4.4.2 Processing Uncertainty Model (PRUM);
3.4.4.3 Data Integration Uncertainty Model (DIUM)
3.4.4.4 Presentation Uncertainty Model (PUM)
3.4.4.5 User Determined Total Error Budget Model
3.4.5 Data Acquisition
3.4.6 Data Processing
3.4.7 Ground Control Quality Assurance
3.4.8 Point differencing for Standard Deviation/RMSE Calculation

Figure 3.1 Outline of Chapter 1

3.1 INTRODUCTION

Spatial representations used in mapping attempt to model physical entities in as much detail as possible. It is currently impossible to completely replicate spatial object characteristics without distortions and generalizations of physical and geometric details. Mapping therefore respects the uncertainty principle which places limits on what we understand as a model of reality by identifying an epistemic limit beyond which it is impossible to enhance the modeling of natural phenomena. The best approach identified

by spatial scientists to dealing with uncertainties is to keep them to the minimum. This is done by designing systems and methods that would ensure results fall within a given error budget.

3.2 RESEARCH QUESTIONS

This chapter asks specific research questions relating to gaps in the LiDAR market that make it difficult for everyday users of LiDAR data to determine the quality of the dataset as fit for use or not. This gap relates to the inability of most LiDAR users to determine error budgets for project specifics and verify after data delivery whether or not the data has been provided according to specifications. These specific questions include the following:

1. How can a user determine the amount and effect of Total Propagated Errors (TPEs) on a project-specific basis?
2. What are the causes and effects when manufacturers' specifications do not meet user specification requirements for a particular application?
3. How can products produced from LiDAR data using poor specifications be adjusted to meet more stringent user specifications without compromising spatial quality of the data and derived products?

To answer these questions, literature on existing error modeling techniques were reviewed and discussed in Chapter 2. During this study, it was realized that the effects of

terrain morphology and interpolation methods – as employed in post-processing methods – on system performance have been extensively studied (Section 2.1). In order not to "re-invent the wheel", the findings of these studies were included in this model after validating these arguments by employing test data provided by the Department of Public Safety, Fredericton, and studying LiDAR systems and acquisition procedures at Leading Edge Geomatics Limited – a LiDAR and geomatics engineering firm in Fredericton.

To understand system software design, the author, through the MITACS scholarship program served as an intern in 2012 with the Software Development group at CARIS – a commercial hydrographic geographic information system software provider. Tapping into CARIS's extensive knowledge and support for processing large point cloud data, especially with respect to multibeam bathymetry, was pivotal to understanding how to deal with processing and analyzing LiDAR points since they have similar characteristics as point clouds. The main difference between multibeam and LiDAR point clouds is in the realization of the height of objects as shown in Figure 3.2.

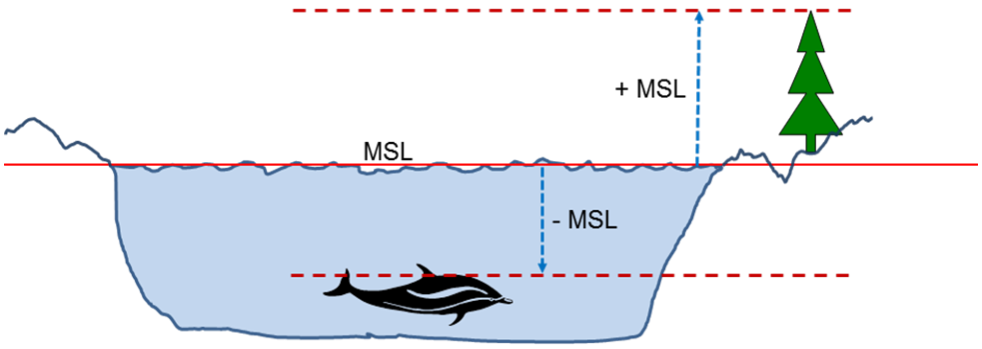

Figure 3.2 Difference between multibeam and LiDAR point clouds height realization.

In Figure 3.2, assume that a multibeam dataset of the bottom of a water body and a LiDAR dataset of neighboring terrain features share a common height reference system

e.g. Mean Sea Level (MSL). While heights of objects in the LiDAR datasets found on the terrain will be assumed to be above MSL (i.e., positive), the heights of objects in the multibeam datasets will be below MSL (i.e., negative). Following an extensive review of previous works in this area and understanding LiDAR systems and processes, a holistic approach to errors (as opposed to only considering the precision of the LiDAR systems in previous studies) was necessary towards creating a more comprehensive performance ability of the LiDAR systems. This quest for an error budget model that includes other sources of error in the LiDAR survey processes led to the objectives of this research.

3.3 RESEARCH OBJECTIVES

The purpose of this research was to:

1. critically compare user-demanded accuracy specifications for airborne LiDAR data with manufacturers' stated performance specifications (which are usually stated based on ideal conditions), and the influence of varying topography and ground cover [Ussyshkin and Smith 2006; Ussyshkin and Smith 2007; Ussyshkin et al., 2008];
2. analyze the respective influences of variations in user-demanded specifications, manufacturer's specifications, topography, and ground cover on the accuracy of information derived from Airborne LiDAR data that may be reliably modeled for project analysis and design purposes; and

3. provide a deterministic or non-deterministic method to allow users as opposed to vendors to independently quantify, validate or refute variations in user-demanded specifications and manufacturer's specifications with respect to the influence of topography and ground cover on both data and derived products within the users' error budget.

Comparing user-demanded accuracy specifications for airborne LiDAR data with manufacturers' stated performance involved matching the manufacturers' error budget specifications for Airborne LiDAR products on one hand, and user's accuracy requirements on the other end, and determining their effects on selected project-specific applications. This comparison addresses the lingering questions as to whether manufacturers' specifications meet, surpass or fail user-demanded error budgets.

In order to validate or refute claims of meeting or failing to meet user specifications, field measurements are required to compare with the accuracy specifications delivered by the vendor. Five test areas with varying topographic details are chosen to validate the model using ground truths. During LiDAR surveys, if vendor specifications generally exceed user's error budgets, there is no need to worry about not meeting general requirements for accurate information derived from LiDAR data. If the specifications fail, how can users identify *false accuracies* and what will be their effects on the resulting quality of the spatial products released to the public from creating applications employing false data quality?

3.4 METHODOLOGY

Firstly, users' specification requirements for nine public organizations are compiled. The error budgets of the users' specifications are documented. The relative accuracy of the LiDAR data provided by the vendor must fall within the error budget of the user.

LiDAR equipment manufacturers will typically report on the precision of their equipment but not the accuracy. Precision is the ability of an equipment to consistently perform a measure and produce same results [JCGM100 2008, p.35], up to a given confidence interval. In project procedures observed during this research, there were instances when manufacturer's specifications employed by a data provider met user's standards and there also instances when there were gaps between standards as shown in Figure 3.3.

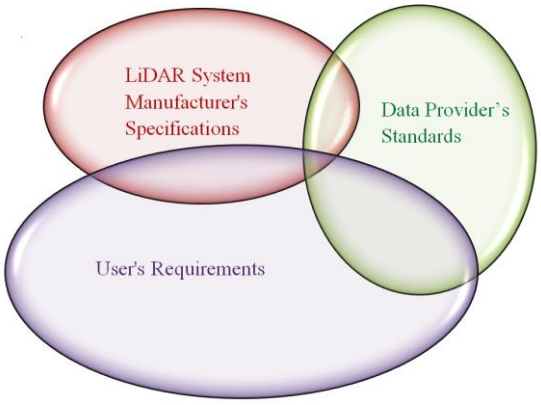

Figure 3.3 Relating performance standards in ALS project with varying interest in standards involving the system manufacturer, data provider and final user

Gaps between manufacturer's specifications and user's standards are due to the fact that it is impossible for a manufacturer to discern and design equipment to meet all user requirements. Usually, users will have to complement LiDAR systems with other equipment, methods or datasets to arrive at results that meet set standards.

If manufacturers and LiDAR systems knew all about the standards that will be required by potential data providers, and if potential data providers could envision all the requirements of potential end users as shown in Figure 3.4, then there would be no need to validate or perform quality assurance and control measurements to determine whether requirements have been met or not.

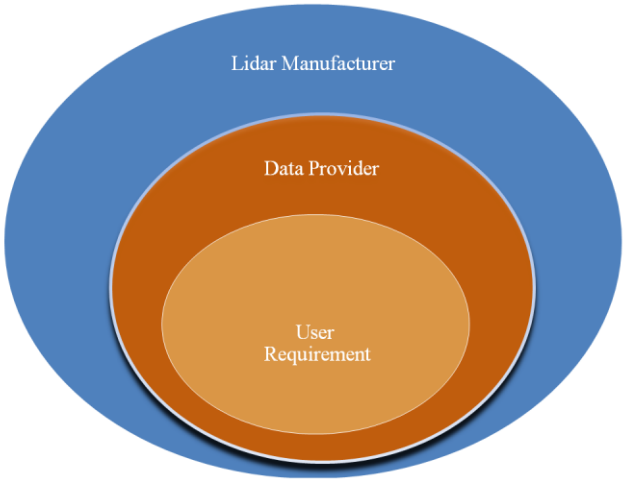

Figure 3.4 The ideal relation of ALS performance specifications

However, this is impossible in practice as LiDAR data is already used in many different applications, with new opportunities for use of the data emerging [Hans et al., 2012]. To determine if user-demanded specifications are met, these three standards are matched to through field measurements.

3.4.1 Assumptions

The definitions and distinctions between accuracy, error, uncertainties/precision, confidence intervals, confidence level and RMSE have been discussed in Section 2.2.1.

Accuracy in this dissertation refers to vertical accuracy of LiDAR as the horizontal accuracy is calculated differently – usually as a fraction of flying height. Where horizontal and radial (a combination of both the vertical and horizontal) errors are calculated, they are clearly specified.

Specifications will refer to the detailed requirements, including the quality of equipment and processes followed to achieve a requirement [Samuel and Sanders, 2007]. The quality control checkpoints (QCCs) used to validate the LiDAR and UDTEB model are assumed to be "error free". Obviously, this is not the case. Therefore a restriction for a point to be used as a controlled checkpoint is for it to have been acquired at a precision that is at least three times superior to the precision of the points it is to validate [Chrzanowski, 1977]. This has been explained in detail in Section 2.2.1.3.

All uncertainties from the various components of the LiDAR system and from post-processing and presentation procedures are considered to be measured at the same confidence interval. All component uncertainties are assumed to carry equal weights when determining the total uncertainty budget.

Finally, it is assumed significant error contributors have been accounted for in the default model. Such contributors may be:

1. a pre-existing condition in LiDAR systems before the survey;
2. acquired during the survey; and
3. included during post-processing of surveyed data

Where this is not the case, the user can customize the model to include new error factors or ignore identified factors in the default error budget.

3.4.2 Users' Requirements Definition

A user's requirement or specification as used in this research refers to the standards for data and product quality requested by the user to the vendor during LiDAR surveys. These standards are used to verify at project completion whether the vendor had satisfied the initial requirement set by the user.

A method for determining users' specifications was created during a project undertaken by the author [Coleman and Adda, 2010] as part of provincial efforts to define standards for acquiring, processing and delivering LiDAR data in New Brunswick. Initial research was conducted to review available specifications for multiple uses of LiDAR data and derived products. From this initial study, four LiDAR specifications were selected as useful references that could be used to help set standards that meet the requirements of multiple N.B. provincial organizations. These were the:

- American Society of Photogrammetry and Remote Sensing (Flood, 2004);
- United States Geological Survey (USGS). National geospatial program base LiDAR Specification Version 13 (USGS, 2010);
- Federal Emergency Measures Agency guidelines for Flood Hazard Mapping (FEMA, 2003), and

- Leading Edge Geomatics (LEG) standard specification for LiDAR data capture and processing. As of the time of this project, LEG was the only commercial LiDAR data provider in the province.

A survey was conducted through interviews with provincial users to obtain their requirements.

3.4.2.1. User Needs Research

Initial informal discussions with selected public institutions regarding the application of LiDAR data to their mandate were undertaken. Table 3.1 lists these institutions and attempts to summarize their areas of interest.

Table 3.1 Participating stakeholders and their areas of interest relating to LiDAR

Organization/Department	Area of interest relating to LiDAR
Service New Brunswick (SNB)	Provincial public administration
Department of Public Safety (DPS)	Safety advice and emergency response
Department of Natural Resources (DNR)	Protect and manage natural resources
Department of Transportation (DOT)	Safe infrastructure and travel advice
City of Fredericton (F'ton)	Information about the city
Department of Environment (ENV)	Manage land use and waste
City of Saint John (S J)	Information about the city
Department of Agriculture & Aquaculture (DAA)	Manage agriculture & aquaculture industries
Department of Wellness, Culture and Sports (WCS)	Citizen's health and well being
City of Moncton (Monc)	Information about the city
University of New Brunswick (UNB)	Research and development
NB Power	Crown Corporation – Services
JD Irving (JDI)	Private Business – Services
Leading Edge Geomatics (LEG)	Private Business – Geomatics
DataQC	Private Business – Quality Control
CARIS	Private Business – Geographic Information

The list of the nine identified institutions that acquire LiDAR data is shown in Table 3.2. It is important to note that these tables only provide the RMSE for elevations as this was what was considered in defining the error budgets for the LiDAR point clouds. LiDAR horizontal uncertainties are determined using a later approach discussed in section 2.2.5.1.

Table 3.2. Formats and accuracies ($RMSE_z$ at 68% confidence level) of contours required.

1. Contours								
	data formats used for contouring							Elevation
Institution	.DGN	NTX	.DWG	x y z	.DXF	.SHP	KML	±RMSE(m)
City of Fred'n								0.20
DPS								0.15
DNR								0.20
DOT								0.02
SNB								0.20
ENV								0.15
DAA								0.20
City of S. John								0.20
Moncton								0.20
Total	3	8	6	6	3	8	4	

RMSE: Min= 0.02 Mean=0.17 Max = 0.20

Key for Most Used	high	average	low

3.4.2.2. Common Needs

Common requirements for LiDAR data and products among participating provincial departments included the:

1. need for an inventory of available provincial LiDAR data and supporting documentation, in the form of metadata;
2. raw LiDAR point cloud, containing hydrographic features, vegetation and infrastructure (including buildings, roads and utilities);
3. filtered classified point cloud to show bare earth, vegetation, hydrographic features,

utilities and infrastructure layers;

4. intensity values, GPS and IMU data for post analysis;
5. raster DEM of bare earth surface, generated features, including contours, lines, points and polygons, 3-D models and breaklines (through a separate collection process and post processing).

3.4.2.3. Differences

Departments of Transportation and Natural Resources suggested their organizations had exceptionally high vertical accuracy requirements for all elevation data collected (±2 cm). This very high accuracy fell outside that required by other departments and by the capability of LiDAR survey technology at the time of the research.

3.4.2.4. Main Components of Specified Minimum Requirements

Minimum specifications, as indicated in this document, refer to defined basic requirements to be considered by a provincial organization when acquiring LiDAR. The purpose is to make sure that the data and processed products meet the basic data standards required by other provincial organizations. Also, compiling common standards helps to maximize the use of LiDAR and related products acquired by provincial organizations, and support easy integration of the data and products into other datasets and products already in use. This specifications document presents details of required minimum specifications to be used as a guide by provincial departments when tendering LiDAR contracts and is summarized as follows (USGS 2010; Flood 2004; FEMA 2003):

- **General responsibilities of the Vendor** - Provide the professional, technical and

material supplies necessary to complete the project as specified by the Client, and in conformity with the minimum specifications detailed in this document.

NB: Clients should define Vendor responsibilities for project specific applications.

- **General responsibilities of the Client -** Provide the logistics, quality control checks and information needed by the Vendor to understand, execute, and present the requested data and products.
- **Formats and sizes for data and products**
  - Formats for raw LiDAR data shall be *".las".* DEMs shall be in *"CARIS"* or "*.shp"* formats. Contours derived from processing the LiDAR data shall be in ESRI .shp, CARIS, or xyz formats. Mass points shall be expressed as ASCII xyz or xyzi.
  - File sizes shall not exceed one gigabyte unless otherwise specified by the contracting company.
- **Allowable time for quality assurance** - Three months after final delivery shall be allowed to complete quality assurance.
- **Rights of clients to delivered data and products**

  There could be cost savings for the client if they are willing to allow the vendor to retain some ownership rights to the raw data.

- The Client shall have unrestricted exclusive right to all data, processed products and any other supplementary information derived directly or indirectly from the LiDAR data and/or product.
- The Client shall reach an agreement with the Vendor at the beginning of the

project to discuss if sharing the raw LiDAR data will mean an extra cost.

- **Recommended payment terms** - 25% of the contract fee shall be paid upon signing the contract, 50% upon completion of flying, acquiring the data and final delivery, and the remaining 25% after quality assurance.
- **Datum and Reference systems –** LiDAR data can be collected in Spherical Coordinates (Latitude and Longitude) and shall be expressed in NAD83 (CSRS) with heights referenced to CGVD28. These reference systems are recognized as the New Brunswick's adopted reference system and in the NB Stereographic Double Projection recognized as the legal map projection for the province.

- At least three well-spaced active GPS control stations shall be occupied simultaneously during the survey. These shall be preferably located along a road, waterway or transmission line.
- The distribution of GPS ground control shall allow for no more than ±30cm (at 95% Confidence Level) GPS error contribution to vertical accuracy (LEG, 2013).

- **Horizontal and Vertical Accuracies –** Unless otherwise specified when compared to surveyed check points established for quality assurance purposes, at least 95% of all raw collected LiDAR points shall possess absolute vertical accuracy of ±30 cm RMSE in areas not obscured by vegetation;

- vertical accuracy of ±50 cm RMSE in areas obscured by ground vegetation; and
- horizontal accuracy of "±0.04" x "the flying height above ground", where units of the flying height are in metres and the resulting RMSE value is in centimetres;

- **Processing, handling and naming**

- No more than 2% of the points in any selected 1km x 1km window of the project area shall be wrongly classified or labeled.
- No raw data points are to be deleted from the swath LAS files, with the exception of extraneous data used to calibrate the flight. Voids caused by the removal of LIDAR data points on manmade structures are acceptable (FEMA, 2003).
- Data storage and naming shall be divided into three levels, namely, individual tile (1 km x 1 km window), block (containing two or more tiles) and overview (containing two or more blocks).

- **Quality Assurance (QA) –** The Vendor, Client or a contracted third party QA team shall perform checks on the processes involved in the survey process and products resulting from the process to ensure they meet or exceed the minimum standards.

- **Specifications required for metadata documentation** – Created to conform to the North American Profile of ISO19115:2003 – Geographic information – Metadata version 1.0.1[NAP, 2007].

- **Specifications required for deliverables –** Deliverables shall include the raw point cloud, classified point cloud and derived products as requested by the Client.

- **Specifications required for the acceptance or rejection of deliverables –** The Client(s) will accept results from the LiDAR project when at a minimum; the Vendor has demonstrated and performed sufficient testing to ensure that each phase of the mapping meets minimum standards as required in the previous sections of this document.

- **Projects requiring higher accuracy standards –** It is acceptable for provincial departments to acquire data at a higher accuracy than the minimum requirement.
- **Post project assistance and organizational expertise –** Where required as part of the delivery process, provide documents regarding the potential use and limitations of the delivered LiDAR products.

The minimum specifications document should have defined life cycles. Making it a living document will ensure it adapts to improvements in the positioning capabilities of LiDAR systems due to advancements in technology.

3.4.3 System Uncertainty Modeling Development

After specifications have been established, there needs to be a way to regulate the final products upon delivery to determine whether or not the specifications were met. The total uncertainty budget for a project involves specifications for both data acquisition and post processing to produce products from the point cloud. Two ways of identifying uncertainties in LiDAR systems, namely the deterministic and non-deterministic uncertainty models were employed.

3.4.3.1 Deterministic Uncertainty Modeling

Deterministic modeling of errors expects the same trend of output results with given inputs under similar conditions. These models employ user specified input to capture underlying details of complex models represented in natural systems. The inputs for such models are usually determined through “trial and error in which plausible values are postulated, the

corresponding outputs inspected, and the inputs modified until plausible outputs are obtained" [Poole and Raftery, 2000].

By modifying the Hare [2001] model for modeling uncertainties in multibeam systems, Goulden and Hopkinson [2006a] determined uncertainties that exist in LiDAR systems. The authors discussed the mathematical relations that the integration of various systems to form the LiDAR survey system plays. The error parameters and their relations have been developed from initial studies and discussed in detail in Section 2.3 of this report. In Figure 3.5 the reference frames necessary for coordinating a LiDAR point observed from an ALS system as proposed by Goulden and Hopkinson [2006b].

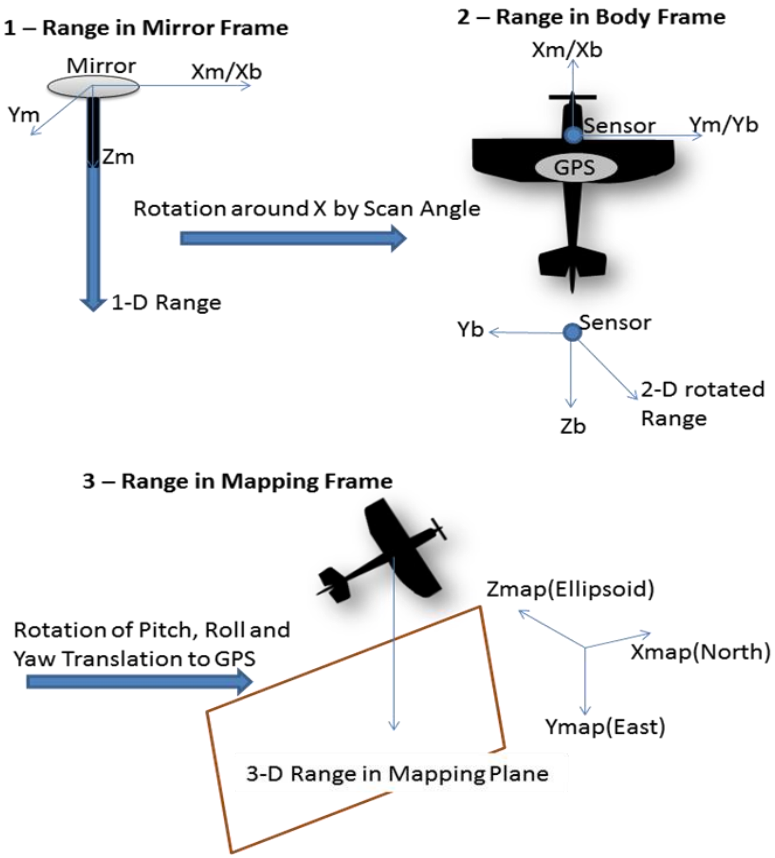

Figure 3.5. Transformations between reference frames (modified from Goulden and Hopkinson, [2006b, p.6]).

From Figure 3.5, Goulden and Hopkinson, [2006b, p.6] categorize these three reference frames as the scanning mirror frame, the aircraft body frame of the aircraft and the topocentric mapping frame.

Following these categories, Goulden and Hopkinson [2006b] derived the following relationships from Figure 3.5.

1. Going from Mirror Frame to Body Frame

   This has only a one-directional vector in the Z –axis, hence in terms of range,

$$range_m = \begin{bmatrix} 0 \\ 0 \\ range \end{bmatrix}. \qquad (3.1)$$

   Rotating Eq.(3.1) at a scan angle about the X*m* using the rotation matrix

$$R_{\substack{mirror \\ to \\ body}} = \begin{bmatrix} 1 & 0 & 0 \\ 0 & \cos\alpha & \sin\alpha \\ 0 & -\sin\alpha & \cos\alpha \end{bmatrix}, \qquad (3.2)$$

   will yield a two-dimensional (of Yb and Zb components) vector in the body frame, given as:

$$range_b = \begin{bmatrix} 0 \\ \sin(\alpha) range \\ \cos(\alpha) range \end{bmatrix}. \qquad (3.3)$$

2. Moving from Body Frame to Mapping Frame

   Employing the roll(*R*), pitch (*P*) and yaw(*Y*) rotation values from the IMU after proper flight and trajectory orientation, Latypov [2005] proposes the following relation for transforming the system from the body to the mapping frame:

$$R_{\substack{Body \\ to \\ Maping}} = \begin{bmatrix} \cos Y \cos P & \cos Y \sin P \sin R - \sin Y \cos R & \cos Y \sin P \cos R + \sin Y \sin R \\ -\sin Y \cos P & -\sin Y \sin P \sin R - \cos Y \cos R & \cos Y \sin R - \sin Y \sin P \cos R \\ \sin P & -\cos P \sin R & -\cos P \cos R \end{bmatrix}.$$

(3.4)

Assuming the eccentricity values have been applied between the GPS, IMU and the scanning mirror, the total solution from the sensor platform to the target coordinates is given as:

$$\begin{bmatrix} x \\ y \\ z \end{bmatrix}_{\substack{Target \\ MappingPlane}} = \begin{bmatrix} x \\ y \\ z \end{bmatrix}_{\substack{Mirror \\ MappingPlane}} + R_{\substack{Body \\ to \\ Mapping}} R_{\substack{Mirror \\ to \\ Body}} \begin{bmatrix} 0 \\ 0 \\ range \end{bmatrix}. \qquad (3.5)$$

Following this, the target coordinates can be deduced from the equations above from Goulden and Hopkinson [2006b, pp.7-10] as follows:

$$x_{\substack{Target \\ UTM}} = x_{\substack{Mirror \\ UTM}} + \begin{bmatrix} (\cos Y \sin P \sin R - \sin Y \cos R)(\sin \alpha) + \\ (\cos Y \sin P \cos R + \sin Y \sin R)(\cos \alpha) \end{bmatrix} Range \ , \qquad (3.6)$$

$$y_{\substack{Target \\ UTM}} = y_{\substack{Mirror \\ UTM}} + \begin{bmatrix} (-\sin Y \sin P \sin R - \cos Y \cos R)(\sin \alpha) + \\ (\cos Y \sin P \cos R - \sin Y \sin R)(\cos \alpha) \end{bmatrix} Range \ , \qquad (3.7)$$

$$z_{\substack{Target \\ UTM}} = z_{\substack{Mirror \\ UTM}} + [(-\cos P \sin R)(\sin \alpha) + (-\cos P \cos R)(\cos \alpha)] Range \ , \qquad (3.8)$$

The laws of the propagation of errors have been discussed in Section 2.2.3 from which we can determine the total errors of the final coordinates by summing the squared values of the partial derivatives of the observables, *l*, multiplied by the square of its corresponding error. The observables in this case are range, scan angle, roll, pitch, yaw and mirror coordinate giving the total uncertainty equation. Therefore, Goulden and Hopkinson, [2006b, p.11]

give an example for the X-coordinates errors (also applicable to deriving the Y and Z errors) as:

$$\sigma^2_{xT\,\mathrm{arg}\,et} = \left[\frac{\partial x_{T\,\mathrm{arg}\,et}}{\partial x_{Mirror}}\right]^2 \sigma^2_{Xmirror} + \left[\frac{\partial x_{T\,\mathrm{arg}\,et}}{\partial \alpha}\right]^2 \sigma^2_{Sangle} + \left[\frac{\partial x_{T\,\mathrm{arg}\,et}}{\partial R}\right]^2 \sigma^2_R + \left[\frac{\partial x_{T\,\mathrm{arg}\,et}}{\partial P}\right]^2 \sigma^2_P + \left[\frac{\partial x_{T\,\mathrm{arg}\,et}}{\partial Y}\right]^2 \sigma^2_Y + \left[\frac{\partial x_{T\,\mathrm{arg}\,et}}{\partial Range}\right]^2 \sigma^2_{Range} \qquad (3.9)$$

Goulden and Hopkinson [2006b] used the Optech ALTM 3100 system as a case study to determine system uncertainties. These findings are used to formulate the performance equations of the mechanical LiDAR system. In this study, it was observed that the mirror coordinate errors were associated with the GPS coordinates of the Smooth Best Estimation of Trajectory (SBET) and errors from the lever arm. The SBET is the only available RMS error source in a LiDAR file that is computed in real time. It is computed from data in the forward and backward solutions of the trajectory and is normally distributed. The errors from the lever arm are either computed from ground surveys or mathematical methods – the Kalman filtering algorithms employed in Applanix's POSPac system [Goulden and Hopkinson, 2006b, p.11]. The equivalents of SBET and lever arm error files exist in other LiDAR and post-processing systems.

We can now determine the error of a mirror coordinates *(Xm, Ym and Zm)* – for instance for *Xm*, this will be:

$$\sigma^2_{Xm} = \sigma^2_{\substack{SBET \\ Xrms}} + \sigma^2_{\substack{X \\ LeverArm}}, \qquad (3.10)$$

where σ^2_{Xm} is the total error in X coordinate; $\sigma^2_{\substack{SBET \\ Xrms}}$ is the RMS error in X from the SBET;

and $\sigma^2_{\substack{X \\ LeverArm}}$ is the Lever arm error in X.

Based on Goulden and Hopkinson [2006b. p.15] the accuracy from the angle α is assumed to be given as:

$$\sigma_\alpha^2 = [10.6'']^2 \ , \tag{3.11}$$

and the errors in roll, pitch and yaw are given as:

$$\sigma^2_{R/P/Y} = \sigma^2_{RMS_roll/pitch/yaw} \ . \tag{3.12}$$

Taking partial derivatives for errors in roll, pitch and yaw with respect to the target coordinates in Eqs. (3.6), (3.7) and (3.8), the following can be deduced and utilized in Eq.(3.9) [Goulden and Hopkinson, 2006b. p.17]:

X coordinate:

$$\left[\frac{\partial x_{Target}}{\partial R}\right] = \left[\begin{array}{l}\sin\alpha[\cos Y \sin P \cos R + \sin Y \sin R] \\ +\cos\alpha[\sin Y \cos R - \cos Y \sin P \sin R\end{array}\right] Range \ , \tag{3.13}$$

$$\left[\frac{\partial x_{Target}}{\partial P}\right] = \left[\sin\alpha[\cos Y \cos P \sin R] + \cos\alpha[\cos Y \cos P \cos R]\right] Range \ , \tag{3.14}$$

$$\left[\frac{\partial x_{Target}}{\partial Y}\right] = \left[\begin{array}{l}-\sin\alpha[\sin Y \sin P \sin R + \cos Y \cos R] \\ +\cos\alpha[\cos Y \sin R - \sin Y \sin P \sin R\end{array}\right] Range \ , \tag{3.15}$$

Y-coordinate:

$$\left[\frac{\partial y_{Target}}{\partial R}\right] = \left[\begin{array}{l}-\sin\alpha[\sin Y \sin P \cos R - \cos Y \sin R] \\ +\cos\alpha[\cos Y \cos R + \sin Y \sin P \sin R\end{array}\right] Range \ , \tag{3.16}$$

$$\left[\frac{\partial y_{Target}}{\partial P}\right] = \left[-\sin\alpha[\sin Y\cos P\sin R] + \cos\alpha[\sin Y\cos P\cos R]\right] Range \quad (3.17)$$

,

$$\left[\frac{\partial y_{Target}}{\partial Y}\right] = \begin{bmatrix} -\sin\alpha[\cos Y\sin P\sin R - \sin Y\cos R] \\ -\cos\alpha[\cos Y\sin R + \cos Y\sin P\cos R \end{bmatrix} Range \quad (3.18)$$

,

Z-coordinate:

$$\left[\frac{\partial z_{Target}}{\partial R}\right] = \left[-\sin\alpha[\cos P\cos R] + \cos\alpha[\cos P\sin R]\right] Range \quad (3.19)$$

,

$$\left[\frac{\partial z_{Target}}{\partial P}\right] = \left[\sin\alpha[\sin P\sin R] + \cos\alpha[\sin P\cos R]\right] Range \quad (3.20)$$

,

$$\left[\frac{\partial z_{Target}}{\partial Y}\right] = 0. \quad (3.21)$$

Last but not least, the range component can also be determined as follows [Goulden and Hopkinson, 2006b. p.18-19]:

For a given range, *R*, return time of a pulse, *t*, and with *c* being the speed of light we can write:

$$R = c\frac{t}{2}\ , \quad (3.22)$$

$$\sigma^2_{Range} = \left[\frac{\partial Range}{\partial t}\right]^2 \sigma_t^2\ , \quad (3.23)$$

and

$$\left[\frac{\partial Range}{\partial t}\right] = \frac{c}{2}\ . \quad (3.24)$$

Assuming that the counters have a resolution of 0.1 ns for the laser device and inputting the constant c to be equal to 299,792,458 m/s (or ~ 300,000,000 m/s), then the vertical resolution representing the minimum separation between objects along path (*Rmin)* can be calculated as [Baltsavias, 1999, p.203]:

$R_{\min} = c\frac{t_{\min}}{2}$ = 300,000,000 m/s x (0.1 x10^{-9}) s x 0.5 = 0.015 m. Therefore,

$$\sigma^2_{Range} = [1.5\text{cm}]^2 , \qquad (3.25)$$

Finally, the partial derivatives of the range that can be input in Eq.(3.9) is given as [Goulden and Hopkinson, 2006b. p.19].

$$\left\lfloor \frac{\partial x_{Target}}{\partial Range} \right\rfloor = \left\lfloor \begin{matrix} \cos Y \sin P \sin R - \sin Y \cos R][\sin \alpha] \\ + \cos Y \sin P \cos R + \sin Y \sin R][\cos \alpha] \end{matrix} \right\rfloor , \qquad (3.26)$$

$$\left\lfloor \frac{\partial y_{Target}}{\partial Range} \right\rfloor = \left\lfloor \begin{matrix} \sin Y \sin P \sin R + \cos Y \cos R][-\sin \alpha] \\ + \cos Y \sin R - \sin Y \cos R][\cos \alpha] \end{matrix} \right\rfloor , \qquad (3.27)$$

and

$$\left\lfloor \frac{\partial z_{Target}}{\partial Range} \right\rfloor = -[\cos P \sin R][\sin \alpha] + \cos P \cos R][\cos \alpha]] , \qquad (3.28)$$

These equations were implemented to estimate systematic errors in the UDTEB mode referred to as the LiDAR Uncertainty Model (LUM).

Figure 3.6 summarizes the algorithm development and step by step methods used in the deterministic approach.

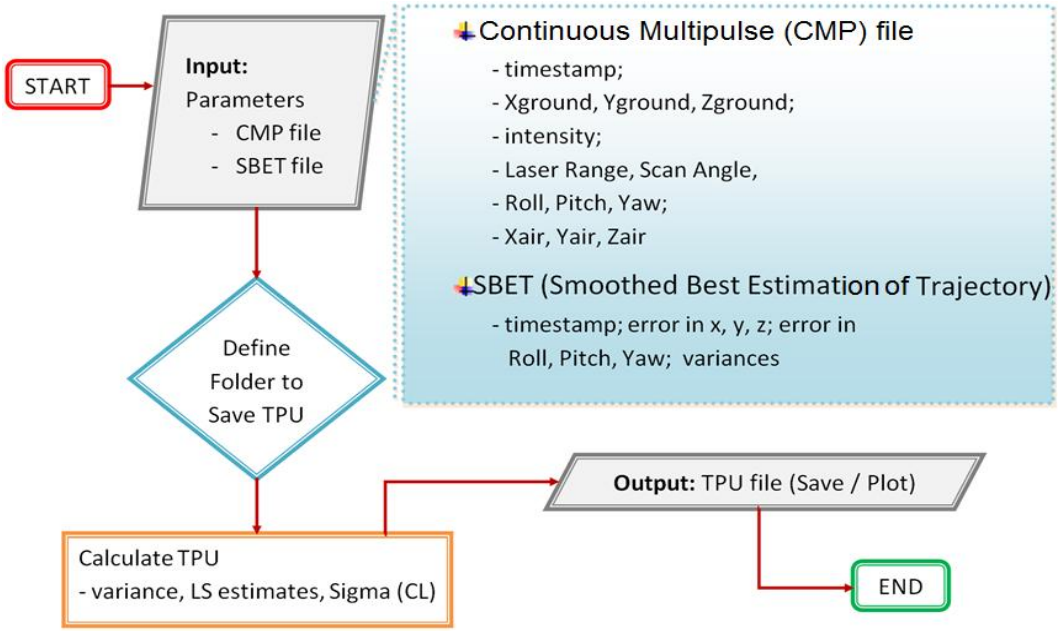

Figure 3.6. Flow diagram of algorithm development for the deterministic model

By employing the parameters in their appropriate variables provided for from Eq.(3.1) to Eq.(3.28), the TPU file containing the uncertainties (TPUx, TPUy, TPUz) of ground coordinates. can finally be computed using the steps shown in Figure 3.6.

3.4.3.2 Non Deterministic Uncertainty Modeling

The non-deterministic modeling method returns estimates of systematic errors (LUM) by estimating parameters of ALS system during the time of survey.

Gonsalves [2010, p.283-305] discussed a full wave uncertainty model for a circular laser scanner, which employed a non-deterministic approach to determine uncertainties. The primary principles adopted by Gonsalves was employed for development for the non-deterministic error modeling part of the UDTEB model.

Assume a simple scanner platform in Figure 3.7.

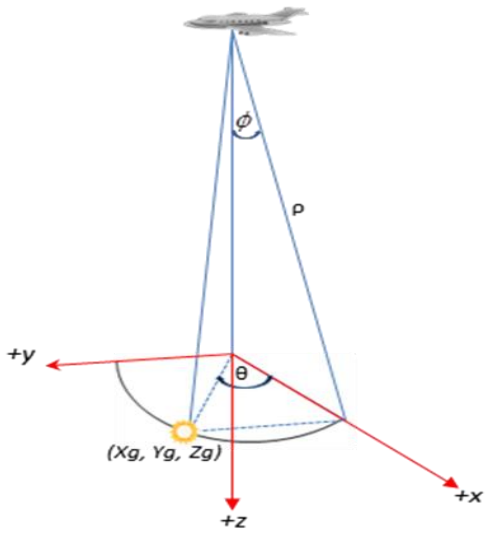

Figure 3.7. A simplified laser scanner depicting laser range ρ, azimuth angle θ, and elevation angle ϕ (modified from Gonsalves [2010, p.294])

Gonsalves [2010 p.294] discussed a simplified uncertainty propagation model and proposed parameters to employ in estimating uncertainties of a LiDAR platform. The following discussions discuss these parameters and their associated propagated uncertainties.

From Figure 3.7, given the range, the ground coordinates can be obtained by employing spherical-to-rectangular coordinate transformation as follows [Gonsalves 2010, p.294]:

$$\begin{bmatrix} x_g \\ y_g \\ z_g \end{bmatrix} = \begin{bmatrix} \rho\cos\theta\sin\phi \\ \rho\sin\theta\sin\phi \\ \rho\cos\phi \end{bmatrix} . \qquad (3.29)$$

Assuming there are no correlations between the parameters, we can deduce the following for the directional errors for *x, y and z* ground coordinates:

$$\begin{bmatrix} \sigma_{x_g}^2 \\ \sigma_{x_g}^2 \\ \sigma_{x_g}^2 \end{bmatrix} = \begin{bmatrix} \left(\frac{\partial x}{\partial \rho}\sigma_\rho\right)^2 + \left(\frac{\partial x}{\partial \theta}\sigma_\theta\right)^2 + \left(\frac{\partial x}{\partial \phi}\sigma_\phi\right)^2 \\ \left(\frac{\partial y}{\partial \rho}\sigma_\rho\right)^2 + \left(\frac{\partial y}{\partial \theta}\sigma_\theta\right)^2 + \left(\frac{\partial y}{\partial \phi}\sigma_\phi\right)^2 \\ \left(\frac{\partial z}{\partial \rho}\sigma_\rho\right)^2 + \left(\frac{\partial z}{\partial \theta}\sigma_\theta\right)^2 + \left(\frac{\partial z}{\partial \phi}\sigma_\phi\right)^2 \end{bmatrix}. \qquad (3.30)$$

Eq.(3.30) represents the errors: $\sigma_g{}^2 = \sigma_\rho{}^2 + \sigma_\theta{}^2 + \sigma_\phi{}^2$, i.e., the error in the ground coordinates as contributed by errors due to the laser range, azimuth angle and the elevation angle respectively.

However, where there are correlations, the variance, co-variance expression can be given as:

$$\begin{bmatrix} \sigma_x^2 & \sigma_{x,y} & \sigma_{x,z} \\ \sigma_{y,x} & \sigma_y^2 & \sigma_{y,z} \\ \sigma_{z,x} & \sigma_{z,y} & \sigma_z^2 \end{bmatrix} = \begin{bmatrix} \frac{\partial x}{\partial \rho} & \frac{\partial x}{\partial \theta} & \frac{\partial x}{\partial \phi} \\ \frac{\partial y}{\partial \rho} & \frac{\partial y}{\partial \theta} & \frac{\partial y}{\partial \phi} \\ \frac{\partial z}{\partial \rho} & \frac{\partial z}{\partial \theta} & \frac{\partial z}{\partial \phi} \end{bmatrix} \begin{bmatrix} \sigma_\rho^2 & \sigma_{\rho,\theta} & \sigma_{\rho,\phi} \\ \sigma_{\theta,\rho} & \sigma_\theta^2 & \sigma_{\theta,\phi} \\ \sigma_{\phi,\rho} & \sigma_{\phi,\theta} & \sigma_\phi^2 \end{bmatrix} \begin{bmatrix} \frac{\partial x}{\partial \rho} & \frac{\partial y}{\partial \rho} & \frac{\partial z}{\partial \rho} \\ \frac{\partial x}{\partial \theta} & \frac{\partial y}{\partial \theta} & \frac{\partial z}{\partial \theta} \\ \frac{\partial x}{\partial \phi} & \frac{\partial y}{\partial \phi} & \frac{\partial z}{\partial \phi} \end{bmatrix}. \qquad (3.31)$$

Eq.(3.31) is of the form $C_z = J\, C_x\, J^T$, where J, the matrix of the first-order partial derivatives of x,y,z with respect to $\rho,\ \theta,\ \phi$ (also known as the Jacobian matrix) can be written as:

$$J = \begin{bmatrix} \cos\theta\sin\phi & -\rho\sin\theta\sin\phi & \rho\cos\theta\cos\phi \\ \sin\theta\cos\phi & \rho\cos\theta\sin\phi & \rho\sin\theta\cos\phi \\ \cos\phi & 0 & -\rho\sin\phi \end{bmatrix}. \qquad (3.32)$$

As variance, covariance has been included, Eq.(3.32) now matures to the full uncertainty equation [Gonsalves 2010, p.303] for ground coordinates of the LiDAR points as follows:

$$\begin{bmatrix} \sigma_{x_g}^2 \\ \sigma_{x_g}^2 \\ \sigma_{x_g}^2 \end{bmatrix} = \begin{bmatrix} \left(\frac{\partial x}{\partial \rho}\sigma_\rho\right)^2 + \left(\frac{\partial x}{\partial \theta}\sigma_\theta\right)^2 + \left(\frac{\partial x}{\partial \phi}\sigma_\phi\right)^2 + 2\frac{\partial x}{\partial \rho}\frac{\partial x}{\partial \theta}\sigma_{\rho,\theta} + 2\frac{\partial x}{\partial \rho}\frac{\partial x}{\partial \phi}\sigma_{\rho,\phi} + 2\frac{\partial x}{\partial \theta}\frac{\partial x}{\partial \phi}\sigma_{\theta,\phi} \\ \left(\frac{\partial y}{\partial \rho}\sigma_\rho\right)^2 + \left(\frac{\partial y}{\partial \theta}\sigma_\theta\right)^2 + \left(\frac{\partial y}{\partial \phi}\sigma_\phi\right)^2 + 2\frac{\partial y}{\partial \rho}\frac{\partial y}{\partial \theta}\sigma_{\rho,\theta} + 2\frac{\partial y}{\partial \rho}\frac{\partial y}{\partial \phi}\sigma_{\rho,\phi} + 2\frac{\partial y}{\partial \theta}\frac{\partial y}{\partial \phi}\sigma_{\theta,\phi} \\ \left(\frac{\partial z}{\partial \rho}\sigma_\rho\right)^2 + \left(\frac{\partial z}{\partial \theta}\sigma_\theta\right)^2 + \left(\frac{\partial z}{\partial \phi}\sigma_\phi\right)^2 + 2\frac{\partial z}{\partial \rho}\frac{\partial z}{\partial \theta}\sigma_{\rho,\theta} + 2\frac{\partial z}{\partial \rho}\frac{\partial z}{\partial \phi}\sigma_{\rho,\phi} + 2\frac{\partial z}{\partial \theta}\frac{\partial z}{\partial \phi}\sigma_{\theta,\phi} \end{bmatrix} \quad (3.33)$$

To implement this in the proposed uncertainty model, the parameters ρ, θ, ϕ will have to be specified by the user. Four default performance precisions were obtained from a survey by *GIM International* [GIM, 2010] accessed online on February 08, 2010. In Figure 3.8, the user is asked to determine the sensor to be employed in the survey

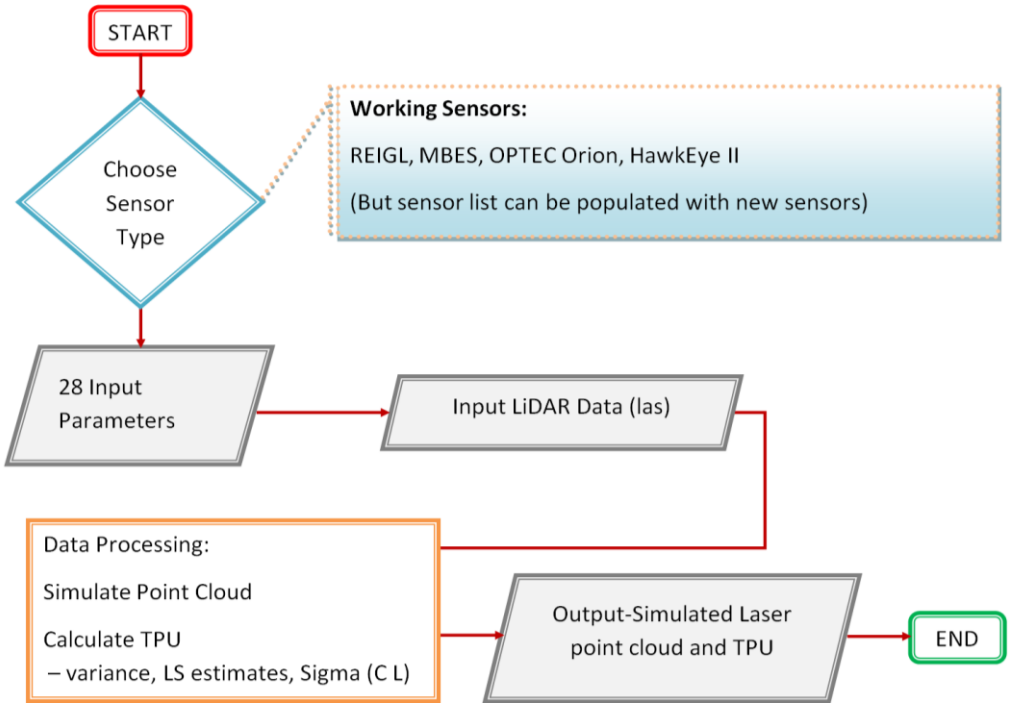

Figure 3.8. Defining sensor types in the non-deterministic model

Once a sensor is chosen, the twenty-eight parameters specific to that sensor [Gonsalves, 2010] are defined to obtain the simulated errors. After defining these 28 parameters, sample LiDAR data are simulated that is consumed by the PRUM to produce an estimate of sensor conditions at the time of survey. From these sensor conditions, new attributes of the LiDAR data in terms of horizontal and vertical coordinates are created. A modification of the simulation was made by the author to allow for the simulated data to be replaced by a sample data of the area, for instance, data from a calibration flight of the area or from previously acquired LiDAR data. Once the data and the errors are simulated, the model outputs the simulated point cloud and the associated errors. Both the deterministic and non-deterministic approach of data uncertainty modeling are necessary for cases where:

1. there are raw performance report files on a LiDAR survey. In which case we employ the deterministic approach to determine the uncertainties – or recall the uncertainties from their performance report; or
2. there are no raw error report files. In which case the user may use the non-deterministic approach to estimate these errors by employing the precision capabilities of the components of the LiDAR systems used in the survey.

3.4.4 User Determined Error Modeling

In addition to the system errors discussed in Section 3.4.2 for the case of the LUM, the UDTEB model considers other sources of uncertainty up to the point of final product delivery. These errors are random in nature and are shown in Figure 3.9.

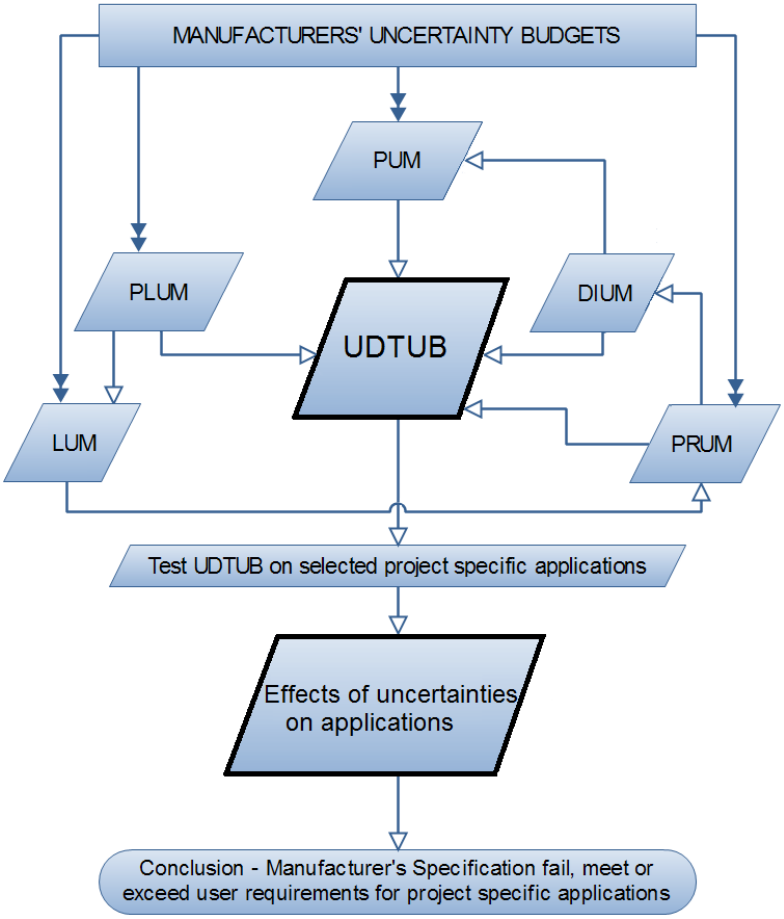

Figure 3.9. UDTEB Model

These uncertainties are divided into five parts, namely:

i. Planning uncertainty model (PLUM);

ii. LiDAR uncertainty model (LUM);

iii. Processing uncertainty model (PRUM);

iv. Presentation uncertainty model (PUM); and the

v. Data integration/interoperability uncertainty model (DIUM).

While not attempting to include all possible source of errors in product creation (which will be impossible at this point), identified major contributors to pre- and post-data errors are estimated and included in the UDTEB model.

3.4.4.1 Planning Uncertainty Model (PLUM)

The PLUM gives a general idea before flying as to whether the LiDAR data and its products will meet user standards or not. It is based on generalized uncertainty of the individual components precision integrated in the LiDAR system for the survey. This implies that PLUM will be greater or in ideal cases equal to the UDTEB.

At the initial stages of the project, the user needs to ask questions about systems precision and survey processes being applied to ensure that they will satisfy requirements. It is also important at the planning stage to consider the performance of the various systems to be employed in the survey [Nayeghandi 2007, pp.60-63]. There are other several subjective uncertainties that could influence errors in LiDAR data and products. Some of these errors (or blunders) result from the confusion of terms used in technical specifications as shown in Table 3.3 from Ussyshkin and Smith [2006].

Table 3.3.Confusing specification terminology as used in the LiDAR industry supposing to describe the same characteristics (Ussyshkin and Smith [2006, p.2]).

Characteristic	Confusing Terminology	
Laser Pulse Frequency	Pulse repetition rate	Data collection rate
Laser Beam Divergence	1/e or $1/e^2$	Full angle or Half angle
Footprint Size on the Ground from Reference Altitude	Footprint diameter, 1/e	Ground spot diameter$1/e^2$
Maximum Scan Angle	±Half-angle	Full-angle or full FOV
Scanning Rate	Scan rate	Scan cycle
Survey Altitude	Operational altitude	Slant range for max. scan angle
Vertical Accuracy	Vertical (elevation) accuracy for the max. scan angle	Vertical (elevation) accuracy versus scan angle
Horizontal (Planimetric) Accuracy	Horizontal accuracy for the max scan angle	Planimetric accuracy versus scan angle

Such confusion leads to misleading interpretation of expectations based on the operational abilities of the ALS system. As a first step solution, it is important for both the vendor and user to recognize this confusion to be clear on these terms of the contract.

3.4.4.2 Processing Uncertainty Model (PRUM)

PRUM considers common processes on the laser data employed in product creation including resampling/point reduction/filtering and DEM interpolation [Desmet 1997, Callow et al., 2007; Liu and Zhang 2008, Guo et al. 2010].

Resampling/point reduction/filtering: This modeling follows similar studies from Liu where the effects of data density on DEM accuracy was investigated for an area of 49 km^2 (Figure 3.10).

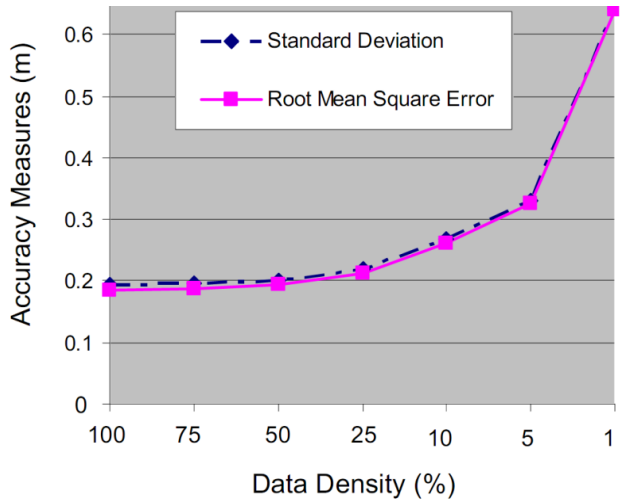

Figure 3.10. Data reduction and DEM accuracy (from, Liu and Zhang [2008, p.176])

In Liu's and Zhang's research, when the reduced datasets were used to produce corresponding DEMs with 5 m resolution, there appeared no significant difference in DEM accuracy until after more than 50% point reduction; 25% reduction produced about

1.01 *RMSE (worst case scenario based on field surveys); 10% reduction gave 1.06*RMSE, while 5% of the original point spacing yielded 1.13*RMSE. One percentage point reduction yielded an estimate of 1.45*RMSE. UDTEB generalizes errors due to data reduction by employing these RMSE values using the following inputs:

- Specify the point density (number of points per square area) of original data
- Specify the reduction percentage ($\Psi\%$) (i.e. the percentage resampling/filtering employed) and apply the corresponding error offset (Ψ). Two options exist:

a) if $0 \leq \Psi\% \leq 50$, then an error offset (or Ψ) of 0.00 is added to the model. In MATLAB™ code terms, this is written as:

If $\Psi\%$ >=0 && $\Psi\%$ <=50, Ψ = 0;

b) if $\Psi\% > 50$, then varying reduction factors are added as shown in the following syntax used in the development of the MATLAB™ code:

elseif $\Psi\%$ >50 && $\Psi\%$<=75, Ψ = 0.01;
elseif $\Psi\%$ >75 && $\Psi\%$ <=90, Ψ = 0.06;
elseif $\Psi\%$ >90 && $\Psi\%$ <=95, Ψ = 0.13;
elseif $\Psi\%$ >95 && $\Psi\%$ <=99.99, Ψ = 0.45;

INTERPOLATION and MORPHOLOGY (Δ) - Aguilar et al. [2005] investigated a theoretical empirical model for error in LiDAR-derived DEMs. After processing, the authors provided a relation between morphology and RMSE (cm) of the interpolated points as summarized in Figure 3.11.

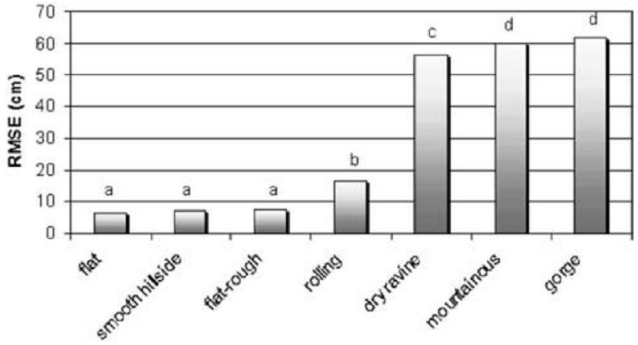

Figure 3.11. Contribution of morphology in RMSE (vertical) LiDAR DEM. From Aguilar et al., [2005], p.813. a,b,c,d are significant changes in RMSE for different terrain morphologies (with $p < 0.05$).

From this detailed research, an estimation of morphology error from interpolated DEM from LiDAR on UDTEB (given the symbol Δ) can be made by the user for a category of three significant changes as follows:

- For the planning stage where data and checkpoints are not available, estimate as:
    a. Flat: This represents surface structures that fall under the flat, smooth hillside and flat-rough morphology. In this category a slope error offset of 0 cm (i.e. no offset) is applied to the model. In this case $\Delta = 0$.
    b. Rolling: This represents average undulations in terrain morphology. An offset (or Δ) of 5 cm to 15 cm is attributed to this terrain type.
    c. Steep: This represents dry ravine, mountainous and gorge morphological types. An offset (or Δ) of between 15 cm to 60 cm is considered for this case.

However, when ground controlled checkpoints are available they are used to estimate the type of terrain and the appropriate offset based on the difference between checkpoints and the estimated terrain is applied. And finally,

$$PRUM^2 = LUM^2 + \Psi^2 + \Delta^2. \qquad (3.34)$$

3.4.4.3 Data Integration Uncertainty Model (DIUM)

The tendency is to consider errors due to data integration impossible to model as it is not possible to envision all potential datasets a user could integrate with LiDAR. However, these errors can be treated as blunders or outliers if, after the integration process, the user does not properly structure the datasets, or report accurately on the total uncertainty. In the DIUM, the contributing error per each combined dataset, *"i"* (named *"Contributing_Error$_i$"*) is given as:

$$Contributing_Error_i = \frac{\%_Coverage_i}{Total_\%Coverage} * Total_RMSE\,, \qquad (3.35)$$

where *Total RMSE* is given as:

$$Total_RMSE = \frac{\sqrt{\sum_{i=1}^{n}[Accuracy_i^2 * (\%_Coverage_i / Total_\%Coverage)]}}{n-1} \qquad (3.36)$$

where $Accuracy_i$ is the accuracy of the ith dataset, $\%_Coverage_i$ is the percentage of data covered by the ith contributing data out of the sum of all the percentages of the datasets involved in the integration process given as *Total_%Coverage*.

3.4.4.4 Presentation Uncertainty Model (PUM)

False interpretation of system performance and data leads to misleading uncertainty results. Errors (or blunders) can also affect data presentation if users do not understand the differences in elevations above different surfaces. To warn about this uncertainty, the UDTEB model requires the user to input all reference systems employed in data or datasets involved.

Classification uncertainty - Misclassification error arises when map classes (in this case the LiDAR points representing different objects) are not correctly assigned to the right objects [Carmel et al., 2001]. Table 3.4 shows an error matrix for evaluating classification results using four prominent indicators suggested by Cohen [1960] and Fenstenmaker [1994]:

1. The overall classification accuracy (Ω, which is a fraction between zero and one – one meaning points have been classified accurately by one hundred percent);
2. Type I error (B) – represent ground classes represented as non-ground;

3. Type II error (C) – refers to non-ground classes wrongly classified as ground; and
4. Kappa (κ), which is the level of agreement of the rate of occurrence of Ω.

Table 3.4. Error matrix for evaluating the classification accuracy of LiDAR ground points from non-ground points.

Compared / Reference	LiDAR Classified Points		
	Ground Point	Non-Ground Points	Summation
Ground Points	A	B	H (=A +B)
Non-ground points	C	D	I (=C+D)
	F (=A+C)	G (=B+D)	E (=F+G)

Modified from Wang et al. [2010].

Here we realize that the only useful way to obtain measurements of misclassified points is by nominal scaling [Cohen, 1960].

$$\text{Type I error} = \frac{B}{A+B} \tag{3.37}$$

Type II errors are most problematic in DEM and other LiDAR product creation. Sometimes these can go unnoticed, especially in vegetative areas where it is easy to classify tree tops as ground (Wang et al. 2010).

$$\text{Type II error} = \frac{C}{C+D} \tag{3.38}$$

.

The probability (chance of agreement rate) P_c is given as

$$P_c = \frac{F*H + G*I}{E^2} * 100 \tag{3.39}$$

,

the level of agreement of the rate of occurrence, κ (or CI), of the overall accuracy (Ω) is given by:

$$\kappa = \frac{\Omega - P_c}{1 - P_c} * 100 \tag{3.40}$$

,

and

$$\Omega = \frac{A+D}{E} \tag{3.41}$$

.

The inputs for the PUM are as follows:

1. The overall classification accuracy (*Ω);*
2. Datum/Coordination conversion applied, if applicable. Users are required to indicate if datum/coordinate transformations were applied as these can have error effects [Vaníček and Steeves, 1996]. Following that, they are required to specify each reference system (both horizontal and vertical) employed.
3. The range of values (min and max) of error limits from various datasets in the production line. The user may skip this step if only LiDAR data is under investigation; and the
4. Confidence interval – if several datasets are employed, report CI for all data.

The only factor that is estimated and used in the presentation model towards the calculation of the TPU is the error due to classification and its effects on the DEM or other product creation. However, the other errors will only be for information purposes in the final report. When Ω is calculated, the amount of error from misclassified points (Ë) is given as:

$$Ë = 1- Ω \qquad (3.42)$$

The final accuracy of UDTEB, considering Ω can be given as:

$$\text{Final Error} = \pm (TUB + Ë * TUB) \qquad (3.43)$$

Eq.(3.43) can be re-written as:

$$\text{Final Error} = TUB * (1+ Ë), \qquad (3.44)$$

and putting Eq.(3.42), into Eq.(3.44), gives the final error as:

$$\text{Final Error}= TUB * (1 +1- Ω) = TUB * (2- Ω). \qquad (3.45)$$

3.4.4.5 User Determined Total Error Budget (UDTEB) Model

The propagation of errors in the UDTEB model follows the law of the propagation of errors. Therefore the total error is not simply the addition of the errors from the LUM, PRUM, DIUM and PUM models. In Section 3.4.3, the variance and covariance (correlations) of residuals and their propagation have been discussed towards modeling the final error estimate from the model. After determining the effects of the TPU using LUM, PRUM and DIUM, the overall classification error (Ω) is determined in PUM. The final error equation reduces to form shown Eq.(3.45). From worst case scenario point of view, the planning stage errors should relate to the following computations:

$$PLUM_{Upper_Limit} \geq \sqrt{RMSE_{LUM}^2 + RMSE_{Field_Survey}^2 + RMSE_{Slope}^2 + RMSE_{PRUM}^2 + RMSE_{DIUM}^2 + RMSE_{PUM}^2} \quad (3.46)$$

where $RMSE_{LUM}$, $RMSE_{Field_Survey}$, $RMSE_{Slope}$, $RMSE_{PRUM}$, $RMSE_{DIUM}$, $RMSE_{PUM}$ are root mean square errors from the ALS system, the field control survey during the ALS survey, the average slope of the area, the PRUM, the DIUM and the PUM respectively.

From Hodgson and Bresnahan [2004], the RMSE of the LiDAR points can be written as:

$$RMSE_{LiDAR_Data}^2 = RMSE_{LUM}^2 + RMSE_{Field_Survey}^2 + RMSE_{Slope}^2. \quad (3.47)$$

Therefore,

$$PLUM_{Upper_Limit} >= \sqrt{RMSE_{LiDAR_Data}^2 + RMSE_{PRUM}^2 + RMSE_{DIUM}^2 + RMSE_{PUM}^2}\ . \quad (3.48)$$

The presence and amounts of errors due to the DIUM, given as $RMSE_{DIUM}$, creates two scenarios for the final error budget. Consider the following:

$$\text{If } RMSE_{DIUM} \leq \sqrt{RMSE_{LiDAR_Data}^2 + RMSE_{PRUM}^2}\ , \quad (3.49)$$

then, the total error,

$$UDTEB = \sqrt{RMSE_{LiDAR_Data}^2 + RMSE_{PRUM}^2 + RMSE_{PUM}^2}\ , \qquad (3.50)$$

and considering Ω as used in Eq.(3.45), the total error can also be written as:

$$UDTEB = (2 - \Omega) * \sqrt{RMSE_{LiDAR_Data}^2 + RMSE_{PRUM}^2}\ . \qquad (3.51)$$

Otherwise, if

$$RMSE_{DIUM} > \sqrt{RMSE_{LiDAR_Data}^2 + RMSE_{PRUM}^2}\ , \qquad (3.52)$$

then, the total error,

$$UDTEB = \sqrt{RMSE_{PRUM}^2 + RMSE_{DIUM}^2 + RMSE_{PUM}^2}\ , \qquad (3.53)$$

or again, from Eq.(3.45), we can write

$$UDTEB = (2 - \Omega) * \sqrt{RMSE_{DIUM}^2 + RMSE_{PRUM}^2}\ . \qquad (3.54)$$

The calculated UDTEB value can be compared with delivered data or products accuracies to determine if users' requirements have been:

1. met – i.e. the delivered data accuracy falls within the UDTEB estimates;
2. not met – i.e. the delivered data accuracy falls outside the UDTEB estimates;
3. met but over-specified – i.e. users' requirements have been met and has been exceeded by twice or more of the required user accuracy;
4. not met and underspecified – i.e. the user's requirements have not been met and the vendor's final accuracy is reported to be worse than at least twice the user's initial accuracy requirement.

3.4.5 Data Acquisition

LiDAR data were provided by the DPS and covered the province of N.B. as shown in red in Figure 3.12. The data were acquired through an ALS survey by Leading Edge Geomatics Ltd., Fredericton, in April 2011 and delivered in July 2012.

Figure 3.12. Red area shows total area covered during the LiDAR survey (obtained from Leading Edge Geomatics Ltd., Fredericton). Image Source: Google Inc. (C) 2012

The trajectory that was followed by the aircraft to collect data in the project area is as shown in Figure 3.13.

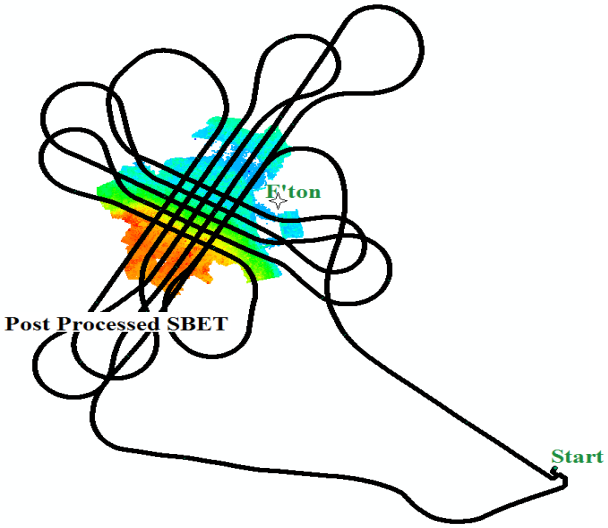

Figure 3.13. Estimated trajectory used by aircraft during the survey.

The design was to allow each swath of data observed along the trajectory to overlap 50% with adjacent trajectories in this survey. Figure 3.13 shows the swath of data covered

while following this trajectory. The system used was the Riegl Q680i, which employs a rotating multi-facet scanning mirror and a stated horizontal accuracy = 1/4,000 x altitude at 68% CI. The average flying height (for the project area) above ground was 1400 m resulting in a horizontal accuracy of approximately ±0.350 m 68% CI. Vertical positional accuracy was ±0.134 m vertical accuracy at 95% CI with an elevation RMSE of ±0.068 m [Kidman, 2012].

The initial coordinates were referenced in the planar Universal Transverse Mercator (UTM) grid coordinates system. At the request of the client, the data were also delivered in New Brunswick Double Stereographic projection on the North American Datum of 1983 of the Canadian Spatial Reference Datum (NAD83CSRS) on the GRS-1980 ellipsoid. The vertical orthometric heights were referenced using the Canadian Geodetic Vertical Datum of 1928 (CGVD28).

The software employed for post-processing the LiDAR data was 'Virtual Geomatics – VG4E^{TM}'. Three classes were identified in the dataset:

1. Ground (classified as 2);
2. Low Vegetation (classified as 3); and
3. High Vegetation (classified as 5).

GNSS data were initially obtained using Topcon's Hiper® Light+. The projection of the equipment was set to: UTM East, North -Zone_19N: 72W to 66W and Datum: NAD83 (CSRS 98). In this first instance of measuring ground checkpoints, Real Time Kinematic (RTK) was envisioned to be used. However, due to an observed defect in the radio link of

the survey instrument, Post Processing Kinematic (PPK) process was used. At post-processing, a restriction was set to only accept values that were precise to less than or equal to ±0.05 m at 95 % confidence interval. All other values that do not conform to this restriction were to be flagged and removed. During analysis, the PPK method did not achieve the required results as there was GNSS error in the checkpoints resulting in over a metre difference in some of the observed values. This instrument error was missed in this survey because the PPK method does not allow for the observer to determine whether or not there was an acceptable vertical or horizontal fix (at a given precision) when the checkpoint is being observed [LEG, 2013]. The experience from this survey indicates the effect of the *surveyor's blunders* in validating LiDAR elevation errors.

A second field survey was made February, 2013 to correct this instrument error. Two instruments were employed in this Survey. For the areas where GNSS RTK observation were possible (i.e. Windsor Street, Avondale Court, Wilmot Park and Odell Park in Fredericton), the TopCon Her Ga GNSS receiver (with Serial # 457-004213) employing a Getac controller in which the TopSurv 8 software was installed was employed. The receiver was set to *Rover* mode and by employing Topcon's TopNET live RTK reference stations as the *Base* [TopNET live, 2012], checkpoints were observed at these four areas. The accuracy of the field elevations was achieved to less than the required 5cm at 95% CI. When the RTK observations were attempted for downtown Fredericton, it was not possible to obtain a fixed point (only floating points could be observed). Therefore, a Total Station survey was adopted. The instrument employed in this case was the Nikon NPL 332. Temporary benchmarks were established and coordinated by traversing using

GNSS (RTK method) from HPN points in the area. These HPN stations were checked using RTK surveys for accuracy by observing them as a rover while occupying the HPN control monument *941007* located at the Department of Forestry building in Fredericton.

3.4.6 Data Processing

After extracting the bare earth points from the dataset, the UDTEB was used to estimate the total propagated uncertainties of simulated or observed LiDAR points by following the step by step employing an interactive Graphic User Interface (GUI) (Figure 3.14).

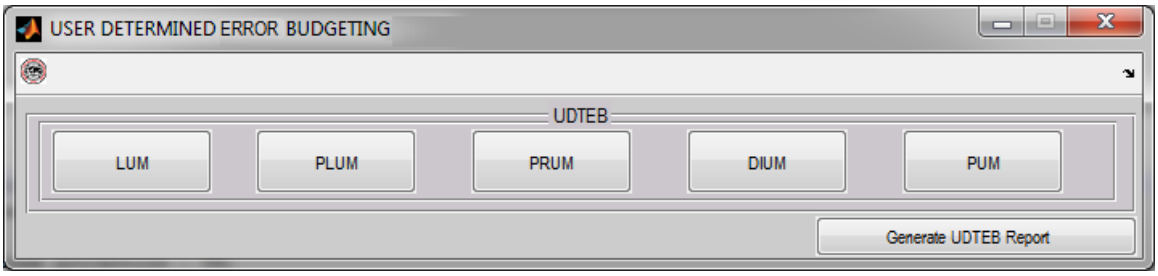

Figure 3.14. GUI of the UDTEB showing step by step processing steps.

The GUI was developed based on the equations described in Section 3.4.7. The user begins by estimating the errors of the LiDAR system (LUM) as shown in Figure 3.15.

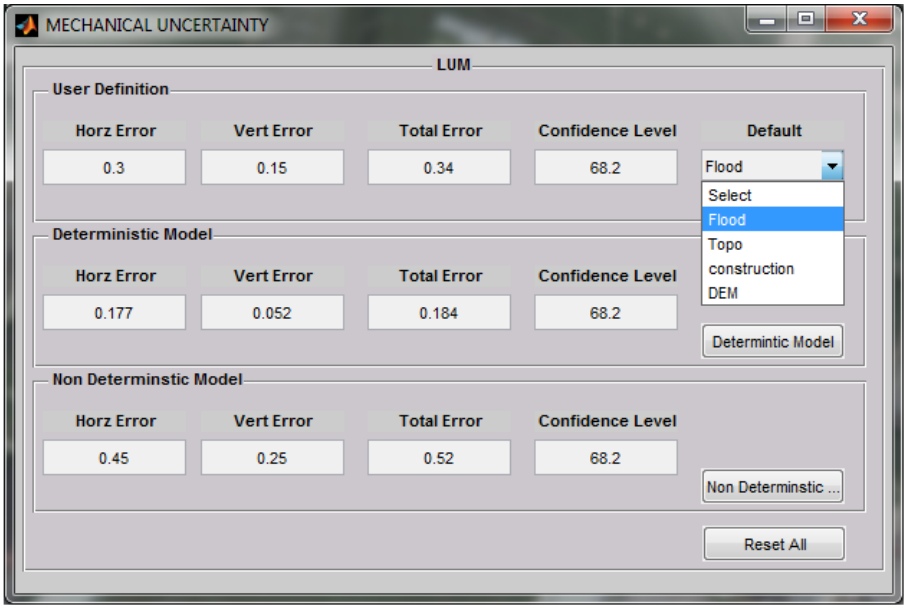

Figure 3.15. PUM options – deterministic and non-deterministic model.

The LUM allows for the estimation of uncertainties in the LiDAR system as discussed in Section 3.4.3. Once engaged, the user is given the chance to first specify their requirement under the "User Definition" section and proceed to determine the PLUM as shown in Figure 3.16.

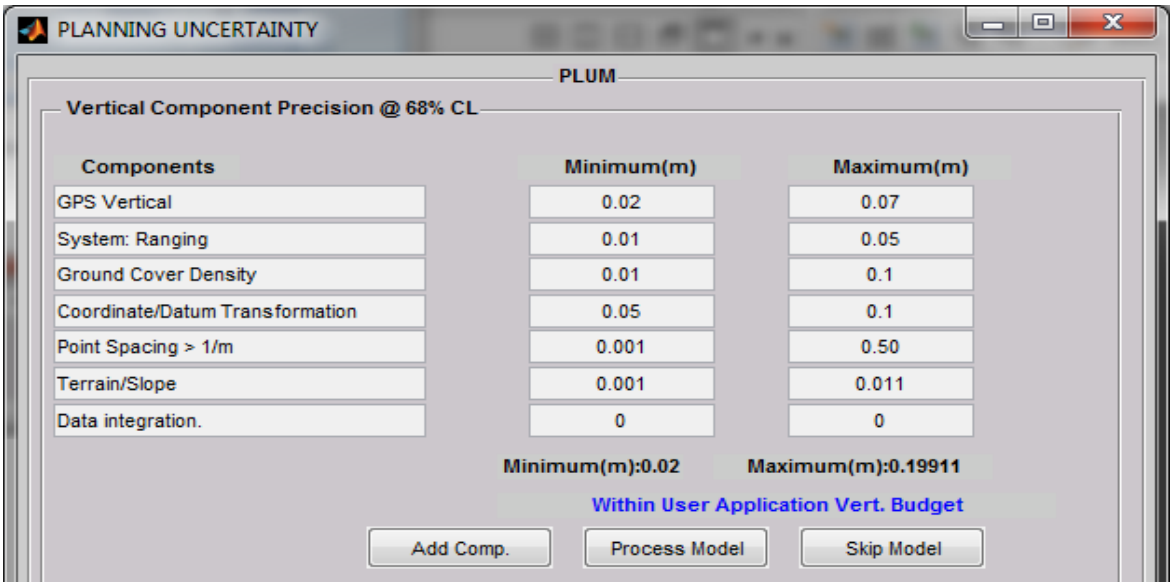

Figure 3.16. A user interface for input of PLUM estimates. Maximum and minimum range of errors is reported in the total uncertainty report only for information purposes.

When the PRUM model is calculated, the user determines the uncertainties due to processing by using the PRUM interface as shown in Figure 3.17.

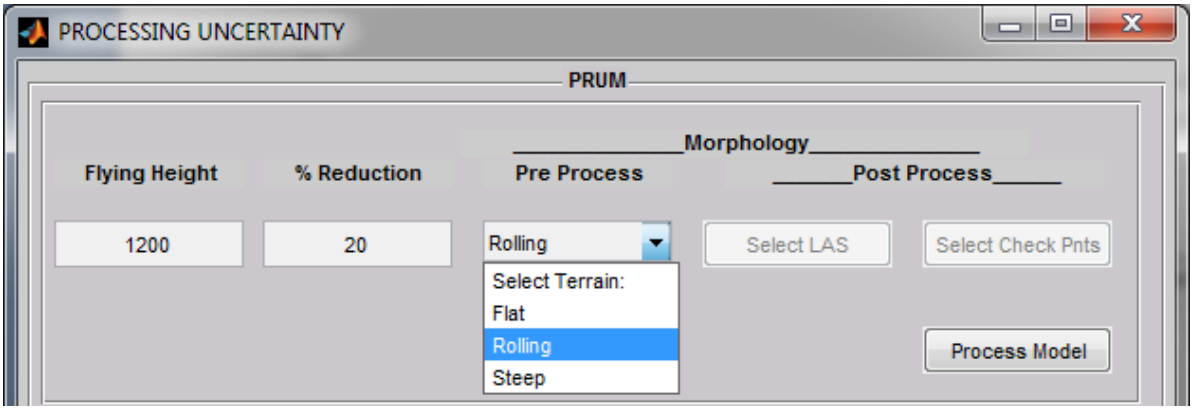

Figure 3.17. PRUM interface. Required: the flying height, the percentage reduction of data and the estimation of terrain morphology.

In the case of simulated LiDAR data obtained from the non-deterministic model, the “Pre Process” approach is employed. In this method the average flying height, the reduction percentage of the data if it has been re-sampled and “average terrain type” are interactively selected by the user. Where a sample LiDAR data is used with known controlled checkpoints within the project area, the “Post Process” is used.

The next entry involves an optional uncertainty processing interface for the contributions of errors from data integration if any. The DIUM interface is shown in Figure 3.18.

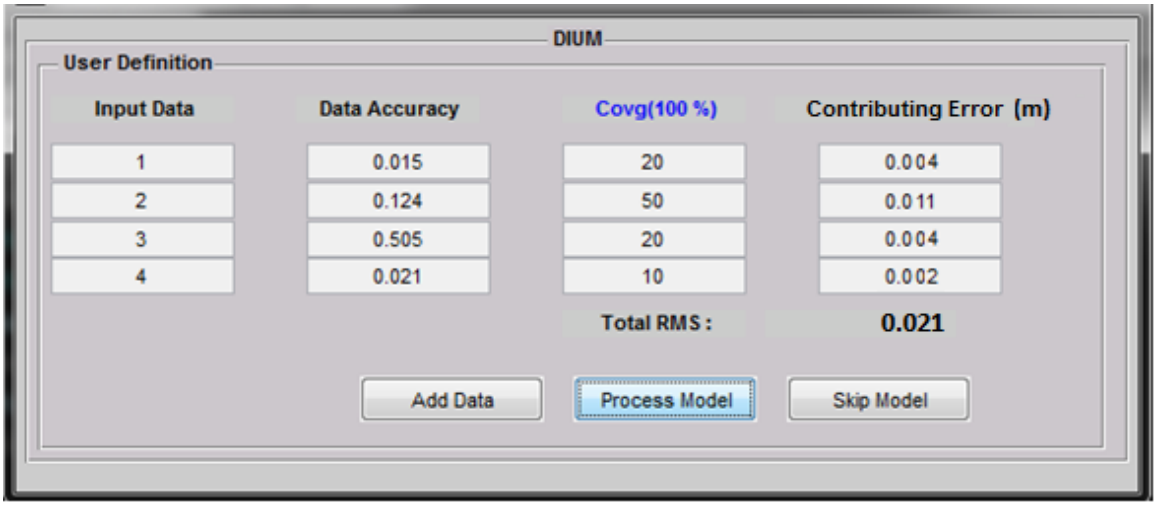

Figure 3.18. DIUM entry example

These uncertainties are only estimated when several datasets are to be integrated towards meeting the final accuracies of a LiDAR product as discussed in Section 3.4.4.3. Figure 3.19 depicts the GUI that was developed to provide the user with a simple interface to enter classification accuracies estimated from the LiDAR data. The vertical reference systems employed is required to be entered. Entering the extra information on the of coordinates system help identify coordinate system conflicts. In the case where there are several datasets were integrated employing various coordinate systems, for each

coordinate system employed, the user is required to state the name and accuracy of each of the datasets.

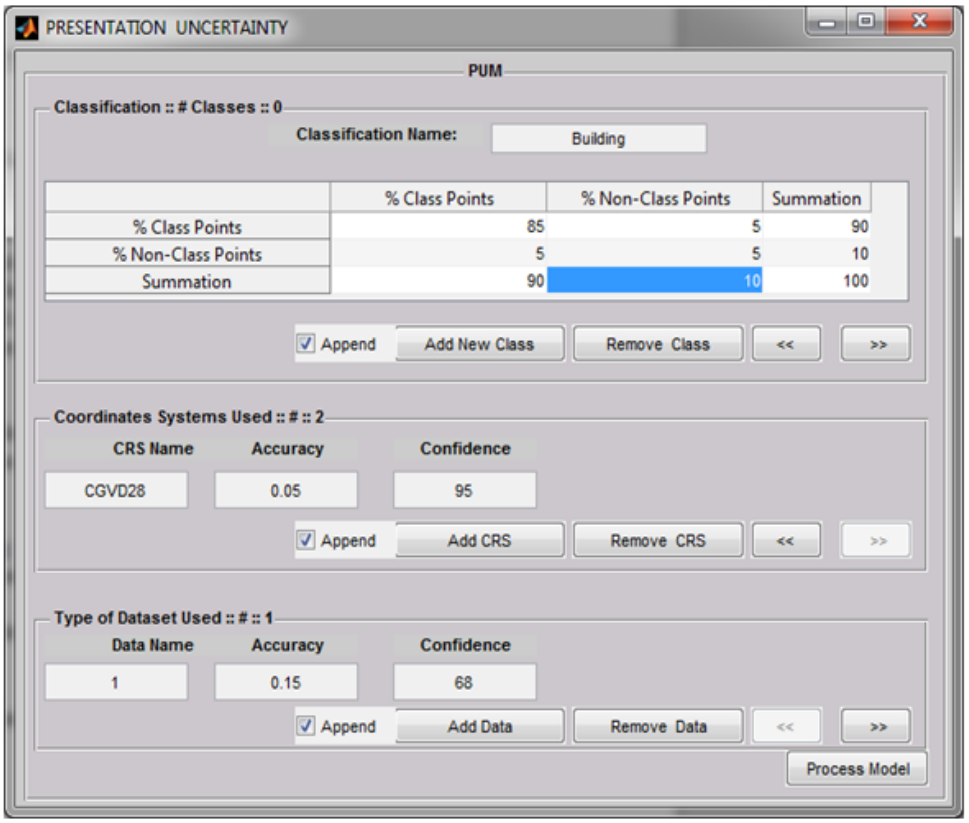

Figure 3.19. GUI of PRUM showing a user input example. GUI has three parts. The top part relates to Classification uncertainties employed in the UDTEB model. Second section records vertical references used and the third section records the datasets used.

A sample of the report is as shown below:

UDTEB REPORT
==========

Error Budget Summary (±m)

Vertical accuracy (Z)	CI% (vertical)
0.718	68.2

Horizontal Accuracy	CI% (Horizontal)
0.86	68.2

Radial Accuracy	CI% (Radial)
1.120	68.2

User Accuracy Requirement (±m) U(v) U(h) U(r) U(CL)

	0.15	0.3	0.34	68.2

Estimated LiDAR Accuracy	E(v)	E(h)	E(CL)
	0.07	0.95	0.22

Reference System	Name	Accuracy	Conf. Interval (%)
	HTV2	0.200	68
	CGVD	0.150	95

Error Budgeting:

Will user specification for the project in mind using the systems defined be met?

Vertical: User Vertical Accuracy Requirements not met

Quality Control Vertical: User Vertical Requirements Under Specified

Horizontal: User Horizontal Accuracy Requirements Not Met

Quality Control Horizontal: User Horizontal Requirements Under Specified

Planning Uncertainty (±m) Vertical Precision of components (without correlated Errors)

Sum Min Error	Sum Max Error	Range
0.01	0.4	0.4

LiDAR Uncertainty Deterministic / Non Deterministic

Same Values, See "Estimated LiDAR Accuracy"

Processing Uncertainty (±m)

Reduction? Yes

%Point Reduction 0.5

Reduction Factor 0

Uncertainty due to Interpolation and Morphology :0.142

Consideration for PRUM at planning stage

Terrain Type	Slope Error Offset
Rolling	0.142

Consideration for Post Processing

Number of LiDAR points = 2530416

Number of Check points = 122

Standard deviation of Check points = ±0.002

Estimated PRU 0.142

Data Integration Uncertainty (±m)

Number of data sets used : 2

Data	Accuracy	%Coverage Area	Combined Accuracy
las	0.12	30	0.239
shp	0.20	50	0.398

Total RMSE for Combine data: 0.6373

Presentation Uncertainty (±m)

Class Accuracy

Class	Type I Error	Type II Error	%Agreement Rate	(%Agreement Level)	Ω
Building	0.06	0.134	86.01	92.71	
Ground	0.02	0.000	94.12	100	0.900

3.4.7 Ground Control Quality Assurance

With respect to empirical validation of large point clouds, the patch validation process for LiDAR data employed over the years by Merrett Survey Partnership in UK and US [Merrett, 2008] was adopted for the field validation process. The patch method employs conventional land surveys over a test area to validate LiDAR coordinates. In this method it is assumed that the conventional survey methods were of higher accuracy than the LiDAR data [Flood, 2004 and Chrzanowski 1977]. The method was modified to cover varying terrain morphologies ground cover of five randomly selected areas for testing for positional accuracy of the LiDAR data. A total of 157 controlled checkpoints were used to verify the LiDAR points on the project area. From Aguilar and Mills [2008, p.163] a minimum of 60 controlled and an average of 100 such checkpoints is required to obtain 95% confidence level in LiDAR elevation control. The number of points actually used was chosen such that it met or surpassed this average number of checkpoints the authors recommended. The project summarized morphology and land cover characteristics of features by dividing it into five categories.

The five areas had the following properties to help reduce bias and incorporate morphological differences within the project area into the final error calculation:

1. High obstruction: Built-up area of downtown Fredericton;
2. Flat-open terrain: Tennis court at Wilmotpark
3. Dense forest: Odell Park, Fredericton
4. Steep slope terrain : Windsor Street with a slope angle of 5 degrees from the highest point to the lowest point; and
5. Low obstruction – Avondale Court region in Fredericton used as example.

The varying topography also helps ascertain the contribution of morphology on LiDAR elevation accuracy in the project area as discussed in Section 2.2.5. Firstly, during field reconnaissance, SNB's HPN N.B. Survey Control Network monument 941007 was identified within the project area. The provincial controls had an A1 classification which means the monuments were obtained using GPS surveys within a distance of 100 to 500 km within the Canadian Base network (CBN). CBN monuments provide up to centimetre-level accuracy with respect to the Canadian Active Control System (CACS) which consist of a network of unmanned GPS tracking stations known as the Active Control Points (ACPs). The ACPs continuously measure carrier phase and pseudo-range values for all satellites at their location. These are processed on a daily basis [SNB, 2002]. Their residuals fell within the error budget expected of the controlled checkpoints as shown in Table 3.5.

Table 3.5. Residuals of the NB HPN checkpoint used as Base Station in the RTK.

NB Control Name	Directional Differences (linear units in metres)				Class
	Easting	Northing	Vector (E & N)	Elevation	
941007	0.005	0.001	0.005	0.02	A1

3.4.8 Point Differencing for Standard Deviation/RMSE Calculation

It is important to compare the LiDAR points within a given window with controlled checkpoint stations in order to determine the RMSE in LiDAR elevations with respect to the corresponding checkpoint. A method to determine this window was developed by the author. This method intentionally deviates from the industry practice of using a radius approach to compare LiDAR points and ground controlled checkpoints. A square search window was designed and applied to calculate the difference because -- whether the user is considering points, lines, polygon, DEM/TIN or area differencing -- it will not only involve points or vector objects but will in most cases involve raster objects. These raster objects are defined by pixels and are in square shapes when depicting the terrain morphology. It therefore makes sense to use a window that better estimates the area of coverage when analyzing feature differences. Furthermore, to allow for choosing different resolutions, the square window method allows the user to choose a window that corresponds to the resolution of the LiDAR product to be created when calculating the differences between the observed LiDAR and the ground controlled checkpoints. Figure 3.20 shows the interface that is opened after controlled checkpoints and surrounding LiDAR points are loaded.

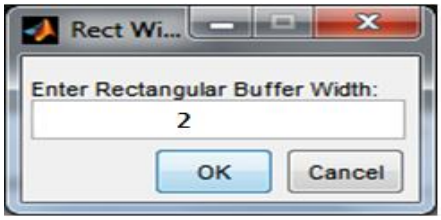

Figure 3.20. GUI interface created to allow users to define LIDAR around controlled checkpoints within a rectangular window. The value of the rectangular buffer width depends on the resolution of the LiDAR. The value"2" entered as above, makes a bounding box of 2 by 2 m around the controlled checkpoint.

The same approach can be applied even if differencing is based on point spacing, the point density or point per square metre. Once this rectangular buffer width is entered, each of the LiDAR points that fall inside the window is compared with the elevation of points at the controlled checkpoint stations. The user calculates the difference using the GUI provided in Figure 3.21.

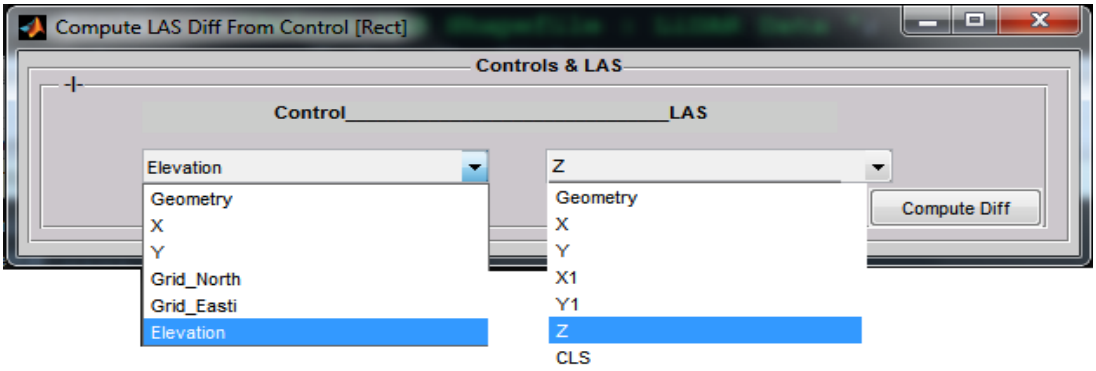

Figure 3.21. GUI showing how elevation differences between controlled checkpoints and LiDAR points are selected around a defined square window in order to compute their elevation differences.

Table 3.6 shows the differences in elevation between LiDAR points within a square window around a corresponding GNSS controlled checkpoints in Wilmot Park, Fredericton, NB. At least one LiDAR point was observed within a 2 by 2 m window around the 7 ground controlled checkpoints at the Wilmot Park tennis field area.

Table 3.6. Square window point difference for LiDAR and checkpoints in Wilmot Park

Tennis	**Elevation Diff.= LiDAR – Checkpoint**			**Absolute Elevation Difference**		
Error	TIN	1 m^2 window	4 m^2 window	TIN	1 m^2 window	4 m^2 window
Max	0.18	0.22	0.22	0.31	0.22	0.37
Average	0.03	0.11	0.04	0.12	0.11	0.15
Min	-0.31	0.01	-0.37	0.01	0.01	0.01
#Points	NA	6/7	7/7	NA	6/7	7/7

Where #Point= $\frac{\text{Number of CCPs with LiDAR points within a square window}}{\text{Number of CCPs surveyed in the area}}$

Not Applicable (NA) is entered for the case of the TIN as the checkpoints are interpolated from the TIN surface.

There are obstructions due to tree cover around the tennis field and also due to the wire fencing around the tennis court. The project investigates the effects of these errors and is discussed in detail in Chapter 4. APPENDIX C gives some example of results obtained for downtown Fredericton. In order to determine the accuracy of the LiDAR points with respect to GNSS points in built-up areas, downtown Fredericton was chosen for the controlled survey. The GNSS measurements were measured around areas in downtown which included the Bank of Montreal (BMO) offices on Kings Street and other high structures. Table 3.7 shows the point differencing between the controlled checkpoints and the LiDAR elevations in downtown Fredericton. 20 out of 23 surveyed ground controlled checkpoints had at least one LiDAR point within a 4 m^2 window around the checkpoints in downtown Fredericton.

Table 3.7. Square window point difference for LiDAR and checkpoints in downtown

Downtown	**Elevation Diff.= LiDAR – Checkpoint**			**Absolute Elevation Difference**		
Error	TIN	1 m^2 window	4 m^2 window	TIN	1 m^2 window	4 m^2 window
Max	0.34	0.34	0.37	0.34	0.34	0.37
Average	0.13	0.14	0.14	0.13	0.14	0.14
Min	0.07	0.05	0.05	0.07	0.05	0.05
#Points	NA	14/23	20/23	NA	14/23	20/23

The Odell Park areas used to study the errors of LiDAR derived elevations in high vegetation of forested areas (Table 3.8). LiDAR elevations in this area were observed to be generally lower than the QCCs. The reason was that under leave-off conditions (which was when the LiDAR flight was made) the LiDAR points really hit ground unlike in the other instances when it could have been hitting low grass and returning it as ground.

Table 3.8. Square window difference for LiDAR and checkpoints in Odell Forest

Odell	**Elevation Diff.= LiDAR – Checkpoint**			**Absolute Elevation Difference**		
Error	TIN	1 m^2 window	4 m^2 window	TIN	1 m^2 window	4 m^2 window
Max	0.08	0.07	0.16	0.54	0.12	0.16
Average	-0.04	-0.04	-0.02	0.06	0.05	0.05
Min	-0.54	-0.12	-0.15	0.01	0.00	0.00
#Points	NA	16/32	25/32	NA	16/32	25/32

The next step was to determine the elevation difference between the controlled checkpoints and areas with steep slope. Table 3.9 shows how controlled checkpoints distributed in the project area are used to determine elevation differences due to steep slopes.

The Windsor Street in Fredericton UNB campus was used for this test with a slope angle of 5 degrees between highest checkpoint (200) and lowest checkpoint (227).

Table 3.9. Square window point differencing results for Windsor Street

Windsor	**Elevation Diff.= LiDAR – Checkpoint**			**Absolute Elevation Difference**		
Error	TIN	1m^2 window	4m^2 window	TIN	1m^2 window	4m^2 window
Max	0.11	0.12	0.18	0.11	0.12	0.18
Average	0.03	0.02	0.03	0.03	0.04	0.06
Min	-0.03	-0.07	-0.10	0.00	0.00	0.00
#Points	NA	29/29	29/29	NA	29/29	29/29

All 29 of the ground controlled checkpoints in this area had LiDAR data within the 2m^2 window applied around each checkpoint.

The Avondale Court area in Fredericton was used to investigate the case for areas with sparse obstructions to ground cover as shown in Table 3.10.

Table 3.10. Square window point differencing results for Avondale Ct.

Av_Ct.	**Elevation Diff.= LiDAR – Checkpoint**			**Absolute Elevation Difference**		
Error	TIN	$1m^2$ window	$4m^2$ window	TIN	$1m^2$ window	$4m^2$ window
Max	0.19	0.18	0.27	0.25	0.18	0.27
Average	0.06	0.06	0.07	0.08	0.07	0.08
Min	-0.25	-0.04	-0.06	0.01	0.01	0.00
#Points	NA	31/51	51/51	NA	31/51	51/51

As there was less ground cover obstructions here, more successful ground hits than at the built up or forested areas were expected. All 51 ground controlled checkpoints had at least one LiDAR point within a $2m^2$ window around the checkpoints.

Finally, by employing a proposed square window method by the author, point differencing between controlled checkpoints and LiDAR elevations lying within the square window is used to validate ground points. There are observed differences between interpolated the corresponding height of the LiDAR points for their respective checkpoints when using the TIN method as in LAStools and the authors square window method.

The tables containing the results of all the differences discussed above for the sampled project areas are provided in Chapter 4. A more detailed discussion of these results is discussed in this chapter. A comparison of errors measured between the LiDAR and ground points versus the errors estimated by the UDTEB model is presented in Chapter 4 as well.

CHAPTER 4. RESEARCH RESULTS AND DISCUSSION OF RESULTS

4. RESEARCH RESULTS AND DISCUSSION OF RESULTS
4.1 ERROR CALCULATION AND FIELD VALIDATION
4.1.1 Point by Point Comparison
4.1.2 Obstruction Analysis
4.2 ERROR ANALYSIS OF PROJECT SPECIFIC APPLICATIONS
4.2.1 What are the User Requirements?
4.2.2 What is the Error Budget for the Flood Inundation?
4.2.3 Users' Requirements Compared with Vendor Delivered Specifications

Figure 4.1. Outline of Chapter 4

4.1 ERROR CALCULATION AND FIELD VALIDATION

In order to determine the differences between the users' defined errors based on set requirements and the vendor-delivered data or product error reports, the ground controlled checkpoints and bare earth LiDAR points were recorded in Section 3.4.7. The attributes that contribute to these results include:

1. GNSS coordinates of the ground controlled checkpoints used;
2. slope, aspect at each ground checkpoint;
3. an estimate of the amount of obstruction at the checkpoint point as "dense", "medium" or "light" after Martin et al [2001, p.7] as shown in Table 4.1.

   Table 4.1 Definition of the amount of obstructions (after Martin et al. [2001])

Point Obstruction (%)	Description
0-32	Light
33-65	Medium
66 - 100	Dense

4. elevation RMSE for the ground checkpoint, LiDAR and UDTEB estimates; and
5. confidence interval of the measurements, which was set to 95%.

4.1.1 Point by Point Comparison

With respect to empirical validation of the LiDAR points, the patch validation process (discovered from personal communications with Merrett Survey Partnership UK) was employed. The method uses conventional land surveys in a defined test area to validate LiDAR coordinates. This was modified to cover varying terrain morphologies and ground cover for five randomly selected test areas. The procedure is referred to as *checkpatching* in this research. The Checkpatching process adopted for the project area was as follows:

1. The elevations at checkpoints in the five study areas were recorded;
2. A TIN is created for each of the study area from clipped LiDAR ground points.
3. The ground controlled checkpoints are included on the TIN.
4. The checkpoints are used to derive their corresponding LiDAR elevations from the TIN.
5. The difference between the checkpoint elevations and their corresponding LiDAR elevations are determined (named *ElvDiff*) and used to calculate the RMSE for the study area.
6. Differences between the field-observed errors and UDTEB estimated errors were determined (called *ComDiff*)
7. Finally, RMSE are calculated from *ElvDiff* and the RMSE calculated from the UDTEB modeled errors (*Err_U*) is now compared for each study area.

Another method to investigate this difference was explored using the square window point differencing approach developed by the author and presented in APPENDIX C.

4.1.1.1 Forested Areas - Odell Park Fredericton

After filtering out all points and leaving only ground points from the LiDAR data, the remaining bare earth points were used to simulate the floor of the forest in Odell Park, Fredericton as shown in Figure 4.2.

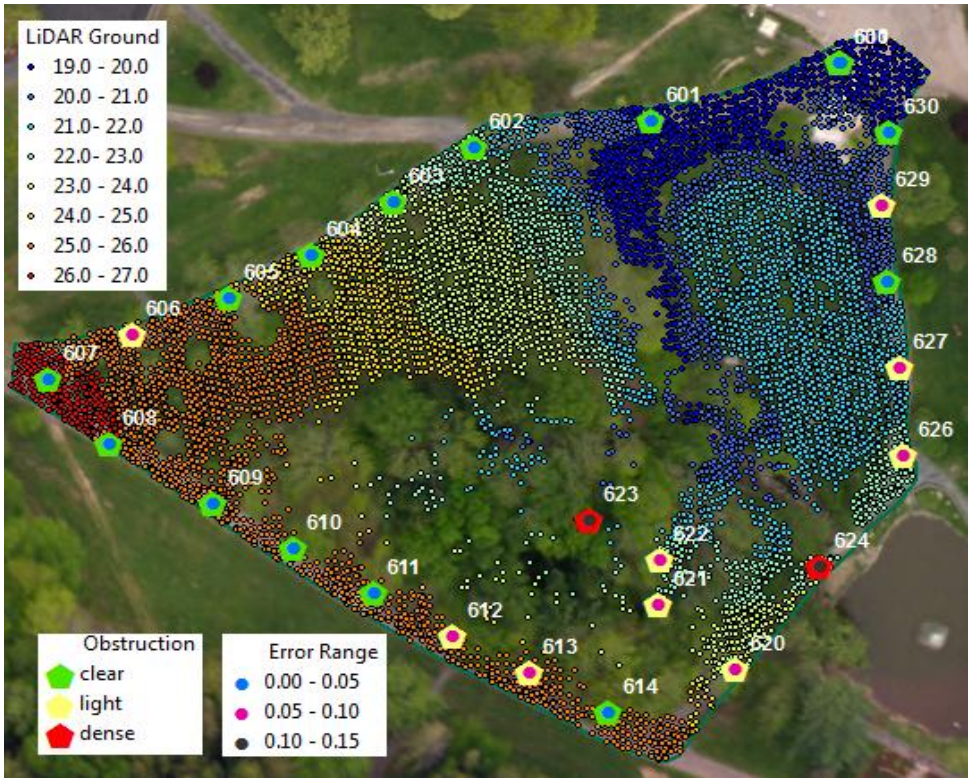

Figure 4.2. Ranges of absolute elevation differences between GNSS and LiDAR at the Odell Park Forest - units in metres.

It can be observed from Figure 4.2 that the areas of thick vegetation had the least ground hits. This had effects on elevation and horizontal accuracy and was investigated by applying the developed square window differencing method discussed in Section 3.4. Large differences between the LiDAR-derived elevations and surveyed elevations of the checkpoints 623 and 624 were due to obstructions caused by vegetation affecting both the GNSS readings and the readings of the LiDAR point clouds. Table 4.2 summarizes the

differences in elevations between the LiDAR and ground checkpoints on one hand (named *Elvdiff*), and the UDTEB estimates on the other hand.

Table 4.2. Summary of the difference in elevation (m) between ground checkpoints and LiDAR points in the dense vegetation area – Odell Park used as an example.

Ground(m)				**LiDAR**	**Lelv - Celv**	**Obstn.**	**Abs Elv Diff**	**UDTUB error**	**Err_U - elvdiff**	**Abs Com Diff**
QCC	Easting	Northing	Celv	Lelv	ElvDiff			Err_U	ComDiff	
600	681071.63	5091959.17	19.61	19.62	0.02	clear	0.02	0.05	0.03	0.03
601	681040.55	5091947.9	19.9	19.88	-0.01	clear	0.01	0.07	0.08	0.08
602	681011.28	5091942.25	22.22	22.2	-0.02	clear	0.02	0.09	0.11	0.11
603	680998.19	5091931.98	23.49	23.45	-0.04	clear	0.04	0.02	0.06	0.06
604	680984.77	5091921.81	24.49	24.5	0.01	clear	0.01	0.11	0.10	0.10
605	680971.28	5091913.61	25.12	25.11	-0.01	clear	0.01	0.08	0.09	0.09
606	680955.3	5091906.67	25.66	25.6	-0.06	light	0.06	0.09	0.15	0.15
607	680941.73	5091898.26	26.12	26.11	-0.01	clear	0.01	0.06	0.07	0.07
608	680952.09	5091886.98	26.02	25.99	-0.04	clear	0.04	0.15	0.19	0.19
609	680969.83	5091876.84	25.78	25.79	0.01	clear	0.01	0.08	0.07	0.07
610	680983.26	5091869.16	25.59	25.58	-0.01	clear	0.01	0.06	0.07	0.07
611	680996.96	5091861.65	25.32	25.34	0.02	clear	0.02	0.02	0.00	0.00
612	681010.42	5091854.12	25.25	25.31	0.06	light	0.06	0.13	0.07	0.07
613	681023.33	5091848.08	25.31	25.25	-0.06	light	0.06	0.09	0.15	0.15
614	681036.75	5091841.23	25.4	25.43	0.03	clear	0.03	0.08	0.05	0.05
620	681057.65	5091849.67	23.73	23.67	-0.06	light	0.06	0.09	0.15	0.15
621	681044.59	5091860.97	23.11	23.17	0.07	light	0.07	0.09	0.02	0.02
622	681044.43	5091868.83	22.3	22.38	0.08	light	0.08	0.01	-0.07	0.07
623	681032.39	5091875.61	21.65	21.52	-0.13	dense	0.13	0.07	0.20	0.20
624	681071.1	5091868.46	22.96	22.84	-0.12	dense	0.12	0.09	0.21	0.21
626	681084.52	5091889.07	22.48	22.4	-0.08	light	0.08	0.06	0.14	0.14
627	681083.18	5091904.87	21.67	21.61	-0.06	light	0.06	0.11	0.17	0.17
628	681080.77	5091920.29	20.9	20.85	-0.05	clear	0.05	0.15	0.20	0.20
629	681079.36	5091933.89	20.48	20.4	-0.07	light	0.07	0.13	0.20	0.20
630	681080.3	5091946.93	20.03	19.98	-0.04	clear	0.04	0.15	0.19	0.19
631	681071.6	5091959.13	19.61	19.63	0.02	clear	0.02	0.11	0.09	0.09
					RMSE		***0.06***	***0.10***		
							Diff	***0.04***		

***Celv =Checkpoint elevation and Lelv = elevation of corresponding LiDAR point.*

From Table 4.2, it can be noted that there are differences between the LiDAR elevations and the elevations of the surveyed checkpoints. Also, ideally, the UDTEB values and the elevations difference should be similar. However, due to surveyor errors, systematic errors not accounted for, and obstructions to actual ground hits due to vegetation cover, there are differences between of Elvdiff and UDTEB errors, *Err_U*. Points with negative

difference indicate places where the checkpoint elevations were higher than the LiDAR elevations. Large UDTEB errors are observed at some clear areas (e.g. checkpoints 604, 608, 612, 628). These points are located at the islands of the SBET and their high errors are due to the interpolation of their TPU values in the LUM model. Similarly, points at the peripherals of the trajectory show high estimated UDTEB errors. Obstructions in this area affect the GNSS measurements as well. This could be a hint of blunders in the measurements. As can be noted from Table 4.2, most of the elevation differences (elvdiff) are negative, but in varying magnitudes. The small and varying magnitudes rule out systematic bias in the LiDAR elevation values but give an indication that due to the vegetative obstructions and snow cover on the ground during the GNSS survey, the QCC measurements did not observe the same level of ground as was observed by the LiDAR sensor. However *ComDiff*, which is the difference between the elevation errors obtained through the field validation surveys and the UDTEB modeled errors, was no more than 21cm.

4.1.1.2 Built-up Areas – Downtown Fredericton

Figure 4.3 shows the ground points for downtown Fredericton considered for the analysis of errors in built-up areas. The QCCs on this area could not be observed using RTK as it was not possible to obtain a fix when occupying the QCCs. A conventional total station survey was employed to obtain the QCCs. The high buildings in the area contribute to errors as they obstruct the path of the laser sensor at a given scan angle along the trajectory as discussed in Section 3.4. The multi-storey buildings were obstructions that limited successful LiDAR ground hits in this particular area.

Figure 4.3. Ground points of downtown Fredericton

However, there were spaces between the buildings that allowed the laser sensor to return successful ground hits in parts of this area. Elevations of the area varied from 8.38 m to 9.42 m (orthometric heights). Assuming there are no systematic errors from the measurements obtained from the GNSS and the LiDAR system, then the residual errors not accounted for this area due to multipath will be equal to the difference in RMSE between UDTEB and *elvdiff*. Clearly, point 103 stands out as the point with the highest elevation difference. In this case, the LiDAR elevation values indicate that multipath errors were affecting the GNSS and the LiDAR measurements resulting in erroneous ground hits. Numerical results of the interpolation process to determine the LiDAR elevation for corresponding Checkpoints is given in Table 4.3.

Table 4.3. Comparison of errors between, UDTEB and LiDAR in built-up areas – downtown Fredericton.

Ground				LiDAR	Lelv-Celv	Obstn.	Abs Elv Diff	UDTUB error	Err_U - elvdiff	Abs Com Diff
Point	Easting	Northing	Celv	Lelv	ElvDiff			Err_U	Com Diff	
100	682843.67	5092437.61	9.22	9.29	0.07	light	0.07	0.15	0.08	0.08
101	682825.81	5092450.41	9.25	9.33	0.08	light	0.08	0.16	0.08	0.08
102	682868.46	5092427.17	8.97	9.04	0.07	light	0.07	0.16	0.09	0.09
103	682819.98	5092420.29	9.01	9.35	0.34	dense	0.34	0.15	-0.19	0.19
104	682884.75	5092413.70	9.16	9.26	0.10	light	0.10	0.14	0.04	0.04
105	682853.57	5092472.68	9.42	9.51	0.09	light	0.09	0.16	0.07	0.07
106	682861.59	5092485.84	9.23	9.32	0.09	light	0.09	0.17	0.08	0.08
107	682819.34	5092409.92	9.22	9.32	0.10	dense	0.10	0.14	0.04	0.04
108	682824.08	5092416.57	9.23	9.33	0.10	dense	0.10	0.15	0.05	0.05
109	682808.38	5092393.39	8.81	8.94	0.13	dense	0.13	0.14	0.01	0.01
110	682825.45	5092383.52	8.98	9.09	0.11	dense	0.11	0.15	0.04	0.04
111	682834.87	5092377.71	9.01	9.10	0.09	light	0.09	0.15	0.06	0.06
112	682839.58	5092375.43	8.99	9.18	0.19	dense	0.19	0.17	-0.02	0.02
113	682786.24	5092519.08	8.58	8.71	0.13	dense	0.13	0.12	-0.01	0.01
115	682776.67	5092502.31	8.68	8.84	0.16	dense	0.16	0.17	0.01	0.01
117	682763.90	5092478.77	8.67	8.85	0.18	dense	0.18	0.15	-0.03	0.03
118	682749.83	5092454.52	8.55	8.72	0.17	dense	0.17	0.15	-0.02	0.02
119	682741.84	5092434.57	8.38	8.54	0.16	dense	0.16	0.15	-0.01	0.01
120	682769.59	5092414.61	8.59	8.74	0.15	dense	0.15	0.14	-0.01	0.01
121	682787.24	5092404.91	8.68	8.83	0.15	dense	0.15	0.14	-0.01	0.01
122	682802.78	5092396.81	8.81	8.93	0.12	dense	0.12	0.17	0.05	0.05
					RMSE		***0.15***	***0.16***	***0.06***	
							Diff	***0.01***		

A further investigation of point 103 showed that it was located close to a tall building occupied by the National Bank and the AVIS car rental company. The tall buildings caused obstruction to GNSS and LiDAR measurements for the area.

4.1.1.3 Open Flat Areas – Tennis courts at the Wilmot Park, Fredericton

To study areas with flat open terrain types the tennis fields at the Wilmot Park was employed. GNSS controlled checkpoints were observed and the TIN of the LiDAR ground points was created as shown in Figure 4.4. The corresponding differences are as shown in Table 4.4 where it can be observed that the difference in RMSE between the modeled error and measured error was 0.07 m but was as low as 0.03 m in clear areas.

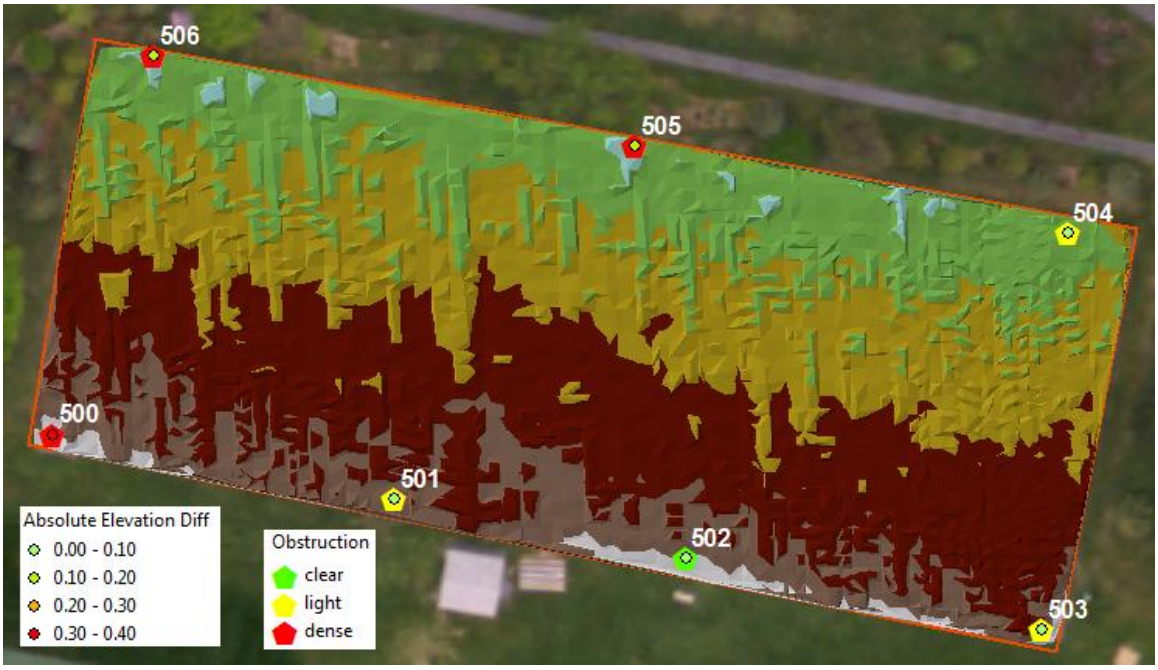

Figure 4.4. A TIN created from the sampled points in open flat areas.

In this test area, the principal limitations to the model due to ground cover and slope at clear checkpoints are negligible. This is confirmed in Table 4.4 where the clear point, 502 recorded a difference on 0.03m between the corresponding LiDAR-derived and surveyed checkpoint elevation.

Table 4.4. Comparing errors between Checkpoints LiDAR and UDTEB estimates in flat open terrain conditions

Ground				**LiDAR**	**Lelv-Celv**	**Obstn.**	**Abs Elv Diff**	**UDTUB error**	**Err_U - elvdiff**	**Abs Com Diff**
Point	Easting	Northing	Celv	Lelv	elvdiff			Err_U	ComDiff	
500	681460.46	5092646.74	9.91	9.60	-0.31	dense	0.31	0.06	0.37	0.37
501	681493.75	5092641.52	9.60	9.69	0.09	light	0.09	0.13	0.04	0.04
502	681522.11	5092636.70	9.59	9.58	-0.01	clear	0.01	0.02	0.03	0.03
503	681556.88	5092630.94	9.53	9.62	0.09	light	0.09	0.14	0.05	0.05
504	681558.13	5092669.28	9.91	9.97	0.06	light	0.06	0.12	0.06	0.06
505	681516.03	5092676.41	9.81	9.94	0.13	dense	0.13	0.09	-0.04	0.04
506	681469.11	5092683.69	9.87	10.05	0.18	dense	0.18	0.03	-0.15	0.15
					RMSE		***0.17***	***0.10***		
							Diff	***-0.07***		

In places where there are light obstructions for the flat open areas, i.e. checkpoints 501, 503, 504 the elevation difference between the LiDAR elevations and the QCCs where under 10 cm. Figure 4.5 gives a graph of the errors with respect to the open flat areas.

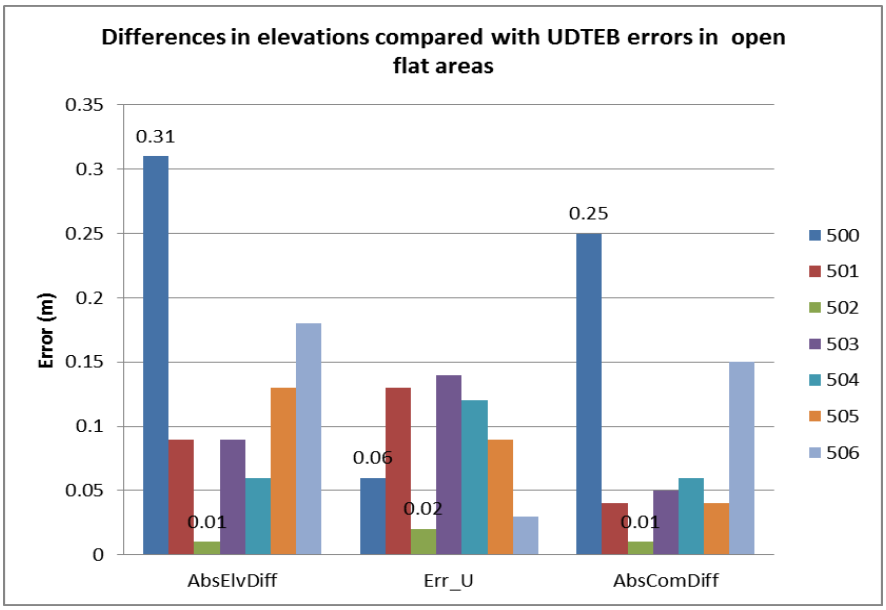

Figure 4.5. Differences in elevation compared with UDTEB errors in open flat areas

The areas of dense obstruction due to trees, an office building and a wire fence in the tennis court area yielded elevation differences up to 37 cm. In areas clear of obstructions, limitations to the UDTEB model are not an issue as further correction for obstructions due to vegetation cover, building and slope is not required. These results points to the effects of obstructions due to vegetative cover, multipath and incomplete slope on the error estimates of the model. Any error observed in this case could be due to inaccurate LiDAR elevation and/or inaccurate GNSS elevations in these areas resulting in these obstructions. Without the densely obstructed points in the open flat areas, the RMSE of the difference between the LiDAR and QCCs (elvdiff) will be 0.08 m and the RMSE of the error estimates from UDTEB will be 0.13 m. The will yield a RMSE difference of 0.05 m between *Err_U* and *AbsElvDiff* for the open flat areas clear of obstructions.

4.1.1.4 Steep Slope – Windsor Street, Fredericton

In order to investigate the effects of slope on elevation errors the Windsor Street at UNB Fredericton was considered for this analysis. Conditions and properties of the Street that make it ideal for this study are discussed in Section 1.1.2. There are no obstructions to ground hits on the Windsor Street. However, the street had a steep slope angle of 5 degrees which had an effect on the error estimates as shown in Table 4.5.

Table 4.5. Comparison of elevations in steep slope area

Ground				**LiDAR**	**Lelv-Celv**	**Obstn.**	**Abs Elv Diff**	**UDTUB error**	**Err_U - elvdiff**
Point	Easting	Northing	Celv	Lelv	ElvDiff			Err_U	ComDiff
200	682515.73	5090865.23	59.09	59.09	0.00	clear	0.00	0.05	0.05
201	682522.43	5090879.60	57.50	57.54	0.04	clear	0.04	0.12	0.08
202	682529.52	5090894.20	55.77	55.78	0.01	clear	0.01	0.15	0.14
203	682536.27	5090908.54	54.12	54.13	0.02	clear	0.02	0.13	0.11
204	682543.71	5090923.50	52.34	52.36	0.02	clear	0.02	0.11	0.09
205	682551.17	5090938.14	50.61	50.60	-0.01	clear	0.01	0.05	0.04
206	682558.16	5090952.68	48.93	48.94	0.01	clear	0.01	0.12	0.11
207	682564.21	5090966.17	47.36	47.38	0.02	clear	0.02	0.14	0.12
208	682571.89	5090979.89	45.67	45.75	0.07	clear	0.07	0.13	0.06
209	682579.29	5090993.91	43.94	43.92	-0.03	clear	0.03	0.11	0.08
210	682586.84	5091008.18	42.11	42.09	-0.02	clear	0.02	0.11	0.09
211	682594.17	5091021.95	40.27	40.29	0.01	clear	0.01	0.11	0.10
212	682601.14	5091035.36	38.68	38.67	-0.01	clear	0.01	0.09	0.08
213	682607.93	5091048.52	37.21	37.23	0.02	clear	0.02	0.15	0.13
214	682615.07	5091062.00	35.81	35.83	0.01	clear	0.01	0.12	0.11
215	682622.11	5091075.31	34.49	34.51	0.01	clear	0.01	0.11	0.10
216	682629.06	5091088.57	33.35	33.34	-0.01	clear	0.01	0.12	0.11
217	682636.23	5091102.31	32.30	32.34	0.05	clear	0.05	0.10	0.05
218	682643.22	5091115.62	31.39	31.39	0.01	clear	0.01	0.15	0.14
219	682650.43	5091129.17	30.56	30.66	0.11	clear	0.11	0.13	0.02
220	682657.48	5091142.07	29.82	29.86	0.03	clear	0.03	0.12	0.09
221	682664.46	5091154.71	29.13	29.18	0.05	clear	0.05	0.12	0.07
222	682671.41	5091167.30	28.42	28.51	0.09	clear	0.09	0.12	0.03
223	682678.68	5091180.56	27.70	27.71	0.01	clear	0.01	0.13	0.12
224	682685.77	5091193.35	27.02	27.10	0.08	clear	0.08	0.13	0.05
225	682692.85	5091206.30	26.32	26.37	0.05	clear	0.05	0.09	0.04
226	682700.18	5091219.62	25.61	25.65	0.04	clear	0.04	0.07	0.03
227	682707.36	5091232.58	24.82	24.83	0.02	clear	0.02	0.11	0.09
					RMSE		***0.04***	***0.12***	
							Diff	***0.08***	

The minimum difference in errors between the field observations and UDTEB estimates was 0.02 m occurring at checkpoint 219; the maximum difference was 0.14 m occurring

at checkpoints 202 and 218. The RMSE of the difference between the ground controlled checkpoints and the LiDAR elevations (ElvDiff) was 0.04 m. The RMSE of the corresponding estimated errors from UDTEB model was 0.12, yielding a difference of 0.08 m between the two RMSE, representing the biggest difference in RMSE between the estimated and field observed values. A further explanation for the highest difference in RMSE in slope areas is explained in 4.1.2 where the contribution of the direction of flight on error is discussed. The mean difference between the UDTEB errors and the field measurements was 0.08 cm while the minimum error was 0.02 cm occurring at the checkpoint 219 which was located in an area around a parking lot.

4.1.1.5 Sparsely Built-up Areas – Avondale Court, Fredericton

Avondale Court in Fredericton was employed to investigate the effects of errors in sparsely built-up areas as shown in Figure 4.6.

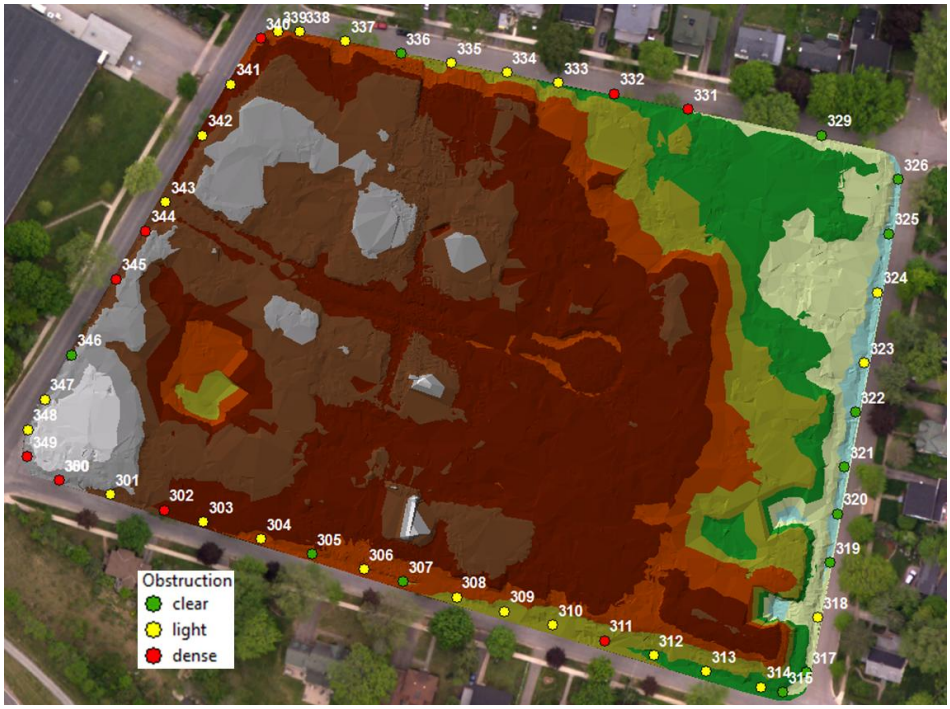

Figure 4.6 Obstruction and TIN of ground Hits.

It was found at point differencing between the GPS points and the ground hits at the sparsely dense area that the classification accuracy of points at this area was high compared to the downtown and Odell Park areas. When the $2m^2$ square window was applied around the checkpoints at this location, LiDAR ground hits were recorded for all the checkpoints. Obviously, the best classification accuracy was recorded in the open flat terrain area of the survey. The comparatively good classification at this location could be linked to the lower density of developments or the smaller canopy that could have affected the LiDAR or GNSS observation in the areas.

Given the easy access to the observation of checkpoints in this area, 51 QCCs were surveyed. Most of the checkpoints were clear with few being densely obstructed by tree cover in the project area as shown by the red dots in Figure 4.6. After the collection of QCCs for the area, TIN differencing, as done for the previous project sites, was employed to determine the differences between the checkpoints and corresponding LiDAR points was made.

Table 4.6 shows the comparison of the errors of the UDTEB and LiDAR data is made for the area. A difference of 0.02 m in RMSE was observed between the difference in elevation for the field measurements and the errors from UDTEB. Figure 4.6 shows the comparison of these errors values in the sparely dense area. The checkpoints 300, 302, 311, 331, 332, 340, 344, 345, 349 and 350 were observed during the survey to have high obstructions due vegetation. These points were located under some big trees in the project area. Sky obstruction from the points was estimated to be over 65% [Martin et al. 2001, p.7].

Table 4.6.Comparison of errors between, UDTEB and LiDAR with respect to Checkpoints in sparsely dense areas

Ground				LiDAR	Lelv-Celv	Obstn.	Abs Elv Diff	UDTUB error	Err_U - elvdiff	Abs Com Diff
Point	Easting	Northing	Celv	Lelv	ElvDiff			Err_U	ComDiff	
300	683009.01	5091177.76	9.41	9.53	0.12	dense	0.12	0.09	-0.03	0.03
301	683025.08	5091173.82	9.19	9.26	0.07	light	0.07	0.11	0.04	0.04
302	683042.17	5091169.39	8.84	9.03	0.19	dense	0.19	0.04	-0.15	0.15
303	683054.74	5091166.00	8.66	8.76	0.10	light	0.10	0.14	0.04	0.04
304	683072.91	5091161.25	8.51	8.60	0.09	light	0.09	0.05	-0.04	0.04
305	683089.02	5091156.97	8.47	8.52	0.05	clear	0.05	0.12	0.07	0.07
306	683105.52	5091152.67	8.38	8.45	0.07	light	0.07	0.12	0.05	0.05
307	683117.98	5091149.20	8.32	8.37	0.05	clear	0.05	0.11	0.06	0.06
308	683135.03	5091144.87	8.23	8.30	0.07	light	0.07	0.12	0.05	0.05
309	683150.14	5091140.92	8.15	8.21	0.06	light	0.06	0.07	0.01	0.01
310	683165.41	5091136.97	8.05	8.12	0.07	light	0.07	0.15	0.08	0.08
311	683181.97	5091132.65	8.02	8.13	0.11	dense	0.11	0.07	-0.04	0.04
312	683197.45	5091128.44	7.90	8.00	0.10	light	0.10	0.08	-0.02	0.02
313	683214.10	5091123.98	7.84	7.90	0.06	light	0.06	0.13	0.07	0.07
314	683231.49	5091119.61	7.75	7.83	0.09	light	0.09	0.09	0.00	0
315	683238.45	5091118.19	7.64	7.69	0.05	clear	0.05	0.15	0.10	0.1
317	683245.70	5091124.72	7.62	7.64	0.02	clear	0.02	0.15	0.13	0.13
318	683248.66	5091142.05	7.45	7.52	0.07	light	0.07	0.15	0.08	0.08
319	683251.98	5091159.50	7.36	7.35	-0.01	clear	0.01	0.14	0.15	0.15
320	683253.85	5091174.83	7.30	7.28	-0.02	clear	0.02	0.15	0.17	0.17
321	683255.54	5091189.63	7.21	7.26	0.05	clear	0.05	0.15	0.10	0.1
322	683258.43	5091206.95	7.11	7.10	-0.01	clear	0.01	0.15	0.16	0.16
323	683260.78	5091222.60	7.03	7.10	0.07	light	0.07	0.13	0.06	0.06
324	683264.21	5091244.83	7.12	7.18	0.06	light	0.06	0.15	0.09	0.09
325	683267.18	5091263.39	7.20	7.24	0.04	clear	0.04	0.12	0.08	0.08
326	683269.58	5091280.63	7.28	7.33	0.05	clear	0.05	0.09	0.04	0.04
329	683245.16	5091293.67	7.43	7.45	0.01	clear	0.01	0.07	0.06	0.06
331	683202.89	5091300.59	7.69	7.59	-0.10	dense	0.10	0.13	0.23	0.23
332	683179.62	5091304.67	7.82	7.57	-0.25	dense	0.25	0.14	0.39	0.39
333	683161.97	5091307.53	7.94	8.03	0.09	light	0.09	0.09	0.00	0
334	683145.59	5091310.23	8.08	8.15	0.08	light	0.08	0.06	-0.02	0.02
335	683128.02	5091312.78	8.21	8.27	0.06	light	0.06	0.06	0.00	0
336	683112.04	5091315.19	8.31	8.35	0.04	clear	0.04	0.12	0.08	0.08
337	683094.53	5091318.55	8.39	8.46	0.07	light	0.07	0.15	0.08	0.08
338	683080.20	5091321.09	8.46	8.45	-0.01	light	0.01	0.07	0.08	0.08
339	683073.20	5091320.91	8.49	8.53	0.05	light	0.05	0.04	-0.01	0.01
340	683067.87	5091318.55	8.48	8.64	0.16	dense	0.16	0.11	-0.05	0.05
341	683059.05	5091303.87	8.72	8.78	0.06	light	0.06	0.15	0.09	0.09
342	683050.46	5091287.55	8.85	8.93	0.08	light	0.08	0.11	0.03	0.03
343	683039.57	5091266.23	9.01	9.09	0.08	light	0.08	0.12	0.04	0.04
344	683033.73	5091256.95	9.03	9.15	0.11	dense	0.11	0.07	-0.04	0.04
345	683024.96	5091241.43	9.13	9.27	0.14	dense	0.14	0.07	-0.07	0.07
346	683011.65	5091217.28	9.29	9.34	0.05	clear	0.05	0.06	0.01	0.01
347	683003.62	5091202.95	9.42	9.48	0.07	light	0.07	0.05	-0.02	0.02
348	682998.59	5091193.31	9.48	9.54	0.06	light	0.06	0.04	-0.02	0.02
349	682998.77	5091184.81	9.53	9.63	0.10	dense	0.10	0.07	-0.03	0.03
350	683008.94	5091177.78	9.41	9.53	0.12	dense	0.12	0.09	-0.03	0.03
					RMSE		***0.09***	***0.11***		
							Diff	***0.02***		

During the field validation survey, for the area with dense obstructions a RMSE of 0.16m was found for the sparsely dense area. For the same area, a RMSE of 0.07m was found for areas with light obstructions while areas clear of obstructions recorded 0.04m in RMSE. In some places clear of obstructions or with light obstructions, UDTEB errors were higher due to the position of those points on SBET as explained in Section 4.1.2.

4.1.1.6 Ground Checkpoints Randomly Set Across the Project Area

Table 4.7 compares the UDTEB errors with the difference in elevation between existing checkpoints and the LiDAR elevations in the study area.

Table 4.7. Comparing overall elevation differences in the project area

Ground Truth							**UDTUB error =**	**Err_U - elvdiff**
Ground					LiDAR Z	Lelv-Celv=		
Point	Obst.	Easting	Northing	Celv	Lelv	elvdiff	**Err_U**	**ComDiff**
400	clear	682340.82	5091879.47	10.20	10.26	0.06	0.14	0.08
401	light	682524.45	5092845.87	13.95	13.97	0.02	0.14	0.12
402	clear	683045.73	5092560.13	6.54	6.67	0.13	0.15	0.02
403	clear	681755.94	5092791.87	9.91	10.01	0.10	0.11	0.01
404	light	682297.82	5092504.55	9.69	9.82	0.13	0.14	0.01
405	clear	682672.04	5092314.66	7.67	7.82	0.15	0.15	0.00
406	clear	683359.91	5091412.21	7.94	8.05	0.11	0.13	0.02
407	light	682955.69	5091610.16	8.70	8.77	0.07	0.15	0.08
408	light	682259.22	5091987.71	9.84	9.93	0.09	0.13	0.04
409	light	681901.99	5092216.40	10.10	10.12	0.02	0.13	0.11
410	light	681370.97	5092518.68	10.66	10.77	0.11	0.15	0.04
411	light	681117.47	5092734.35	10.58	10.64	0.06	0.15	0.09
412	clear	681149.87	5092101.32	13.16	13.21	0.05	0.09	0.04
413	clear	681692.28	5091774.00	15.22	15.25	0.03	0.06	0.03
414	light	682090.36	5091541.80	23.21	23.27	0.06	0.12	0.06
415	clear	682771.88	5091331.53	14.40	14.46	0.06	0.11	0.05
416	light	683240.34	5090780.19	11.13	11.18	0.05	0.10	0.05
417	clear	682340.81	5091879.46	10.19	10.26	0.07	0.11	0.04
418	light	683463.94	5090022.46	46.85	46.84	-0.01	0.07	0.08
419	clear	684395.20	5090998.44	7.58	7.62	0.04	0.06	0.02
420	clear	684613.87	5091573.19	9.19	9.19	0.00	0.04	0.04
421	light	683584.22	5090244.38	11.81	11.82	0.01	0.10	0.09
422	light	682608.99	5090455.33	82.86	82.88	0.02	0.09	0.07
423	clear	682737.01	5089886.03	97.54	97.59	0.05	0.11	0.06
424	light	682690.59	5089580.68	102.60	102.70	0.10	0.13	0.03
425	clear	683463.95	5090022.46	46.86	46.84	-0.02	0.10	0.12
					RMSE	***0.08***	***0.12***	
						Diff	***0.04***	

Table 4.7 provides a means of analyzing the variations of RMSE for the entire project area by employing already existing checkpoints that were used by the vendor during the field calibration survey. These points are evenly spaced throughout the areas with varying morphological differences. Ideally, the user should have access to the points used by the vendor for the field calibration survey and should observe these points independently as part of the quality control process. However, such an independent check could not be done during the field survey of this research as the checkpoints were temporary points and could not be located. As a work around, a quick comparison of the LiDAR points were made with a previous TIN obtained from a LiDAR ground points from a survey in 2007 with a maximum elevation RMSE of 0.14 m. This RMSE was within the vertical accuracy budget of the research. However, the differences in the field observed RMSE for the various terrain morphologies are significant since they are distorted by more than 25 percent from the given elevation RMSE of ±0.068 m for the entire survey discussed in Section 3.4.5. As mentioned in Section 1.2.2 such a change in elevation RMSE is significant and requires further investigation (as discussed in Section 4.2).

4.1.2 Obstruction Analysis

In most places with defined topography, it was observed in section 4.1.1 that the UDTEB errors were more than the real calculated differences between interpolated LiDAR elevations and GNSS elevations. This is expected as the UDTEB errors do not only reflect systematic errors (as described in the LUM model in Section 3.4.3), but also

include random errors (PRUM, DIUM and PUM) as discussed in Section 3.4.4. Also, for most areas, the elevations from the LiDAR data (Lelv) were higher than the elevations from the GNSS or Total Station surveys (Celv). A possible explanation could be that the laser was not really returning ground hits but, due to low vegetation cover, was returning heights a little above ground from reflections of the low grass on the ground.

The lowest differences in errors were observed at the tennis field – which is expected for a flat open area. However, at the time of observation, there were obstructions observed around the tennis field. One of such obstruction that could influence both the GNSS and LiDAR observations in the tennis field area was wired fence constructed around the tennis field area to keep the tennis balls within the field of play. This fence can obstruct LiDAR ground hits resulting in the elevations of the LiDAR points being higher than elevations of the ground controlled checkpoints. Another factor that could affect the LiDAR and GNSS observations at the tennis field area were negatively influenced the presence of trees grown to provide some shade to players on the field. Table 4.8 summarizes the analysis of the five project areas in terms of RMSE with respect to the amount of obstructions at the ground controlled checkpoints.

Table 4.8. RMSE of surveyed and field elevations in areas clear of obstructions

	RMSE(m)		
Area	Field	UDTEB	UDTEB-Field
Steep Slope Area	0.04	0.12	0.08
Open Flat Area	0.01	0.02	0.01
Dense Vegetation Area	0.03	0.10	0.07
Sparsely Dense Area	0.04	0.13	0.09
Overall Project Area	0.08	0.11	0.03
		Mean	*0.06*

With respect to Windsor Street which was employed for the study of the case for steep slope errors, it was observed that the points were all clear of obstructions.

From Figure 3.13, the trajectory of the aircraft during the time of flight was along the direction of Windsor Street. In the data acquisition process, the Riegl Q680i system was used. The scanning method of this laser scanner employs a rotating multi-facet scanning mirror and from Figure 2.7, the vertical errors will increase with increase in slope

The following graph in Figure 4.7 provides visual analysis of the RMSE for the various study areas in this section of the survey. The table clarifies that, for areas clear of obstructions, the areas with steep slope recorded the most variations between the RMSE of the vendor provided LiDAR points and the UDTEB estimated errors.

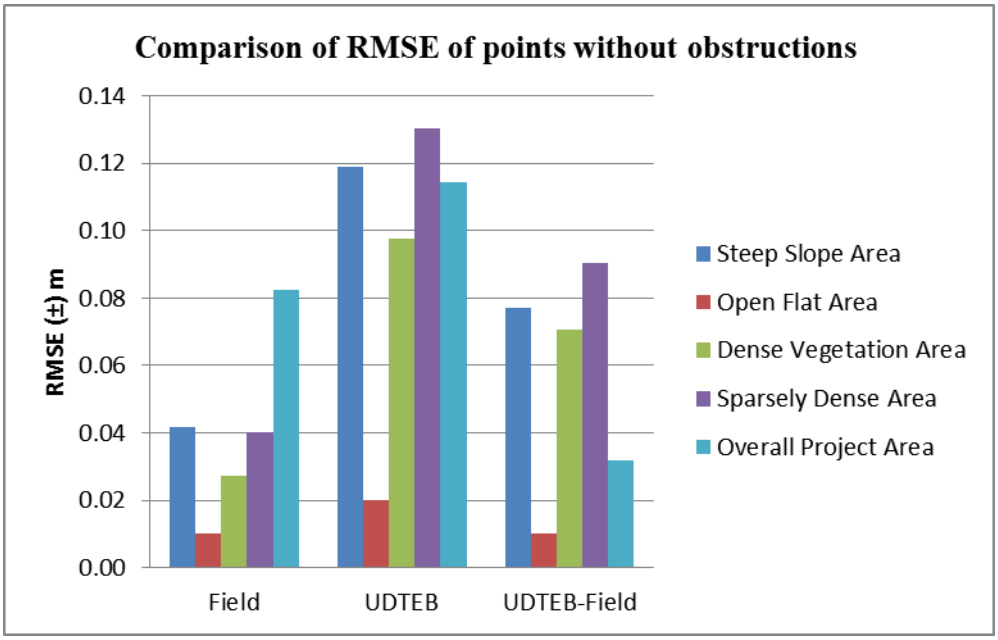

Figure 4.7. Graph of RMSE of surveyed and measured points in clear obstruction.

The least RMSE difference was recorded in the open flat areas. In this area, errors due to slope, vegetative cover and building obstructions causing multipath do not contribute

significantly to increase the overall error. Table 4.9 shows the RMSE of field measurements, UDTEB errors and their differences for areas with light obstructions.

Table 4.9. RMSE analysis between surveyed and measured points in places with light obstructions

	RMSE(m)		
Area	Field	UDTEB	UDTEB-Field
Open Flat Area	0.10	0.16	0.06
Dense Vegetation Area	0.07	0.10	0.03
Sparsely Dense Area	0.07	0.11	0.04
Built-up Area	0.09	0.17	0.08
Overall Project Area	0.07	0.13	0.06
		Mean	*0.05*

Figure 4.8 provides a graphical detail of the differences in errors in the areas with light obstruction.

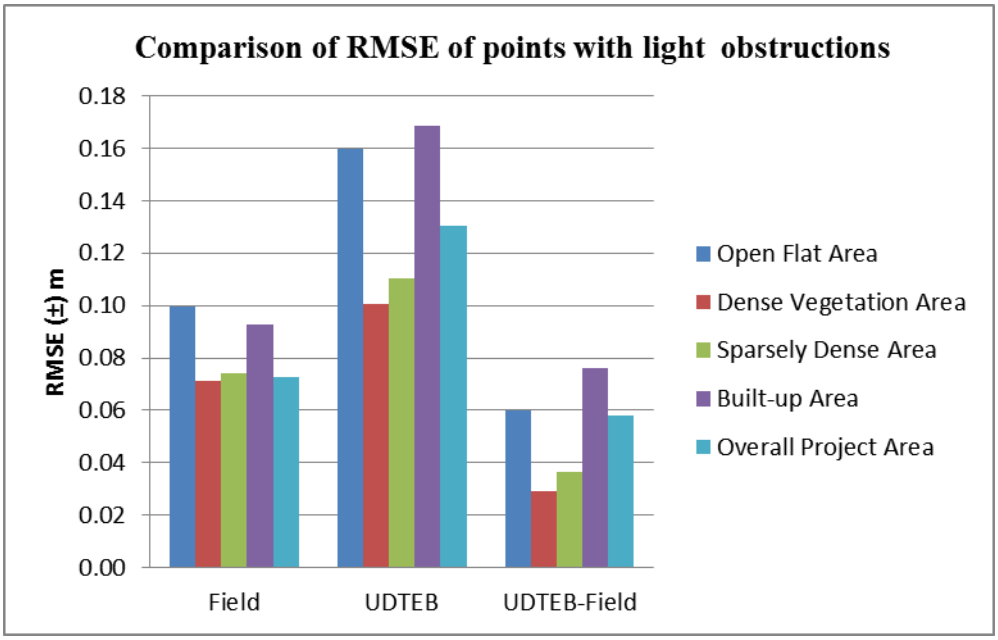

Figure 4.8. RMSE between surveyed and measured points in light obstruction areas.

From Figure 4.8, considering places with light obstruction, the built-up areas recorded the highest difference in RMSE (=0.08 m) between the UDTEB model and the field

measurements. The least difference in RMSE (=0.03 m) was recorded at the areas with dense vegetation. When the overall area is considered by employing the pre-existing QCCs across the project area, the difference between the RMSE of the UDTEB model and the field measurements was even less at ± 0.06 m. To determine the effects of dense obstructions on the UDTEB errors, all checkpoints and corresponding LiDAR points in areas with dense obstructions were investigated. Table 4.10 summarizes the RMSE obtained in areas with dense obstructions.

Table 4.10. RMSE of UDTEB compared to RMSE from field measurements in area with dense obstructions

	RMSE(m)		
Area	Field	UDTEB	UDTEB-Field
Open Flat Area	0.27	0.08	-0.19
Dense Vegetation Area	0.21	0.08	-0.13
Sparsely Dense Area	0.16	0.10	-0.06
Built-up Area	0.17	0.16	-0.02
		Mean	*-0.10*

It can be seen that the dense obstructions to ground cover due to vegetation, high rising buildings, wire fences and slope resulted in higher RMSE than what was estimate in the UDTEB model. Surprisingly, the built up areas had the least difference in RMSE (which is equal to 0.02) for dense obstructions while the open flat areas have the highest RMSE difference of 0.19 m. However, in areas with dense obstructions, the difference between the field observations and UDTEB RMSE followed a different trend than in the case of the areas with light and no obstructions. A possible reason was that the error effects from the amount of obstructions at these places were not estimated for in the model. Another reason could be errors in the GNSS and LiDAR measurements due to obstructions caused by the high-rising buildings within this particular area.

4.2 ERROR ANALYSIS OF PROJECT SPECIFIC APPLICATIONS

In order to clarify the comparison of user determined error budgets and manufacturer's uncertainty reports, an example in a flood modeling project is discussed from a project completed by the author in this research [Adda et al., 2011]. The purpose of the study was to advise the Department of Public Safety (DPS) on when it will be critical to intervene in an area likely to flood based in forecasted rainfall amounts. The decision to close an infrastructure or utility should be based on legitimate information that is not underestimated or overestimated. Some of the important questions to ask at the beginning of a flood model simulation are discussed as follows.

4.2.1 What are the User Requirements?

To achieve the set requirement for the flood mapping, the DPS will require dataset and processing methods capable of producing the dynamic maps at an elevation accuracy of ± 30 cm at 95 percent confidence interval. The coordinates of the data shall be referenced to the Canadian Spatial Reference System of 1998 of the North American Datum 1983 and employing the New Brunswick Double Stereographic Projection. Elevations shall be referenced to the geoid employing the H2_0 realization. Following the acquisition of the data, it shall be processed to DEM and water level polygons created from the hydrographic features. These hydrographic features which areas stored as polygons are modeled at 0.2m intervals and will be used to study flood effects at these intervals as no significant changes are observed beyond this interval [Adda et al., 2011].

4.2.2 What is the Error Budget for the Flood Inundation?

The following steps in Figure 4.9 summarize the flood inundation process.

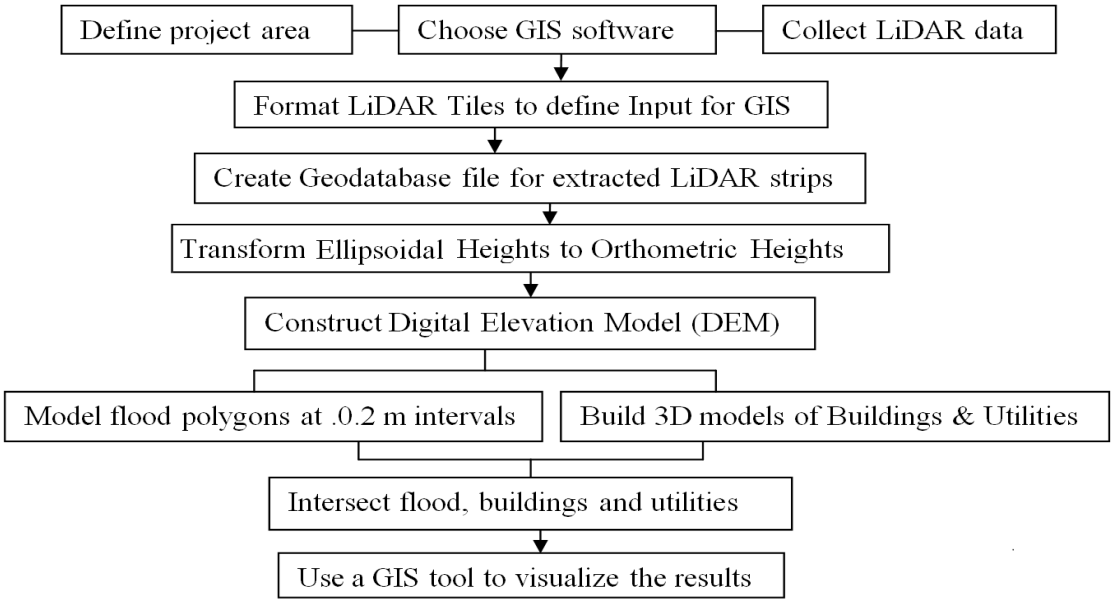

Figure 4.9. Proposed processing steps for the 3D flood models - from data acquisition to product creation.

The error contribution at each step is determined using the uncertainty identified in the UDTEB model. These errors are propagated to determine the total error budget.

How will the Accuracy of the Delivered Data be validated?

The LUM is used to simulate the mechanical uncertainties as shown in Figure 4.10.

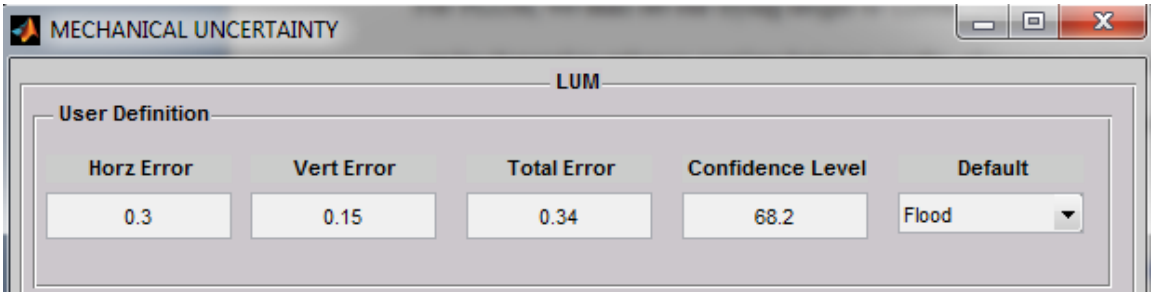

Figure 4.10. User defined directional accuracies in metres for an envisioned flood model.

The parameters required to estimate the uncertainties are system dependent, and are discussed in Section 3.4.5. To achieve an interpolation of 0.2m flood levels, DPS required at least a dataset with elevation information at every 1 point per square meter point density. By employing the square window approach the vendor reported along track point spacing of 0.72m and an across track point spacing 0.72 m was confirmed.

By engaging the LUM and employing the deterministic approach an estimate of the TPU for the LiDAR system is calculated as shown in Figure 4.11.

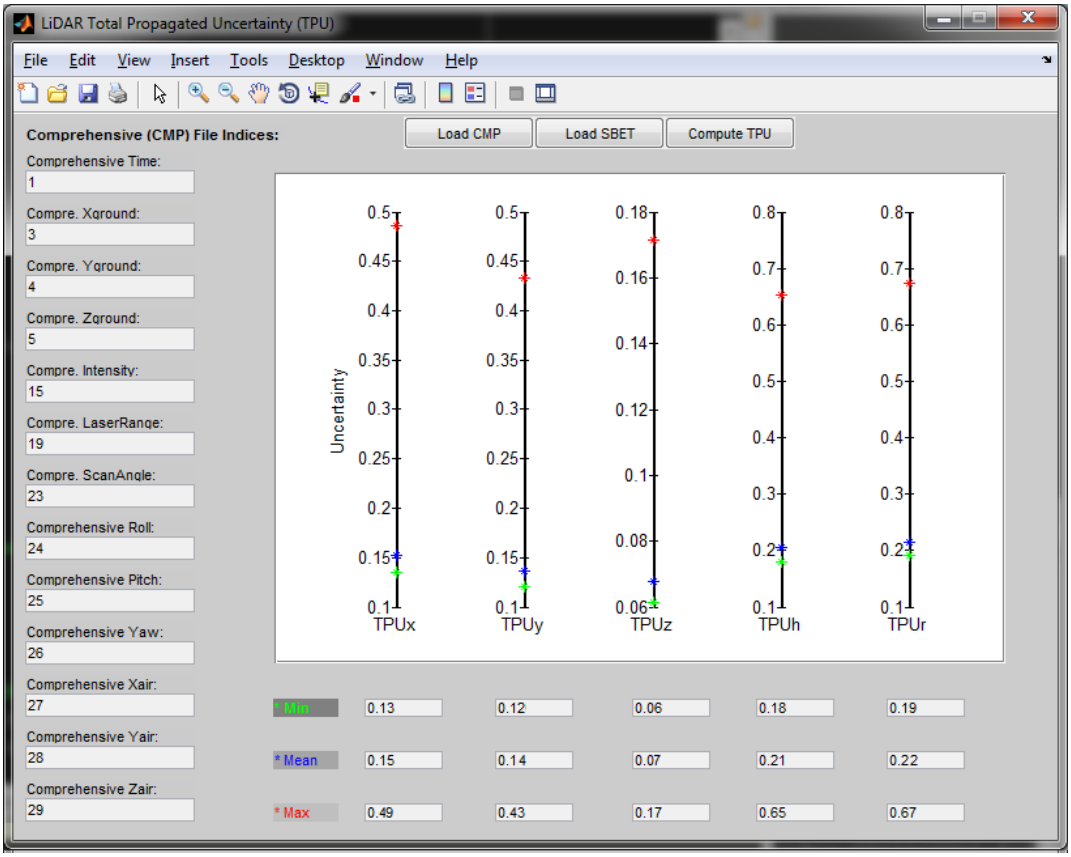

Figure 4.11. Summary of LUM TPUs based on system employed. All units in metres

A report is produced in the LUM graphic user interface summarizing the directional accuracy estimates of the area of survey. The TPU of each the point is stored in a file defined by the user on the user's computing system.

DPS can then engage the PLUM, to roughly estimate the range of uncertainties each of the components of the LiDAR system chosen could contribute to the overall error budget.

The next step is to engage the PRUM model. For our area parameters we shall select "rolling terrain" and estimate a data reduction of 20% of the original data (i.e. we could be working with 80% of the original data after filtering. For the study area a slope angle of 4 degrees will be employed [Aguilar et al., 2005, p.813] as shown in Figure 4.12. The user is then asked to confirm the average flying height above ground level (AGL) which was set to 1200 m.

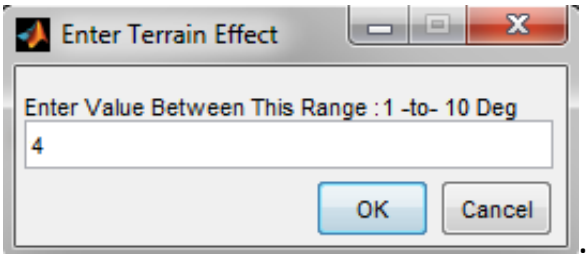

Figure 4.12. Estimating amount of slope change in area of Survey

If the calibration survey and checkpoints of the area are available to DPS project personnel, we shall define the checkpoints of the TPU estimates by loading these files. In that case it will not be necessary to estimate the terrain changes in slope as UDTEB calculates the average slope to employ in the calculation of the TPU by using the ground checkpoints to create the base surface that estimates the terrain of the areas under investigation.

From Section 3.4.4.3 we recall that for DIUM estimate to be considered in the TPU calculation, the condition of Eq.(3.52) will have to be met (i.e. the DIUM error has to be greater than the errors of both the LiDAR data and any post processing error of the data

where applicable). Once the DIUM is completed, the user will now estimate the PUM classification errors and confirmation of users reference systems and data integration intentions to be employed as shown in Figure 4.13.

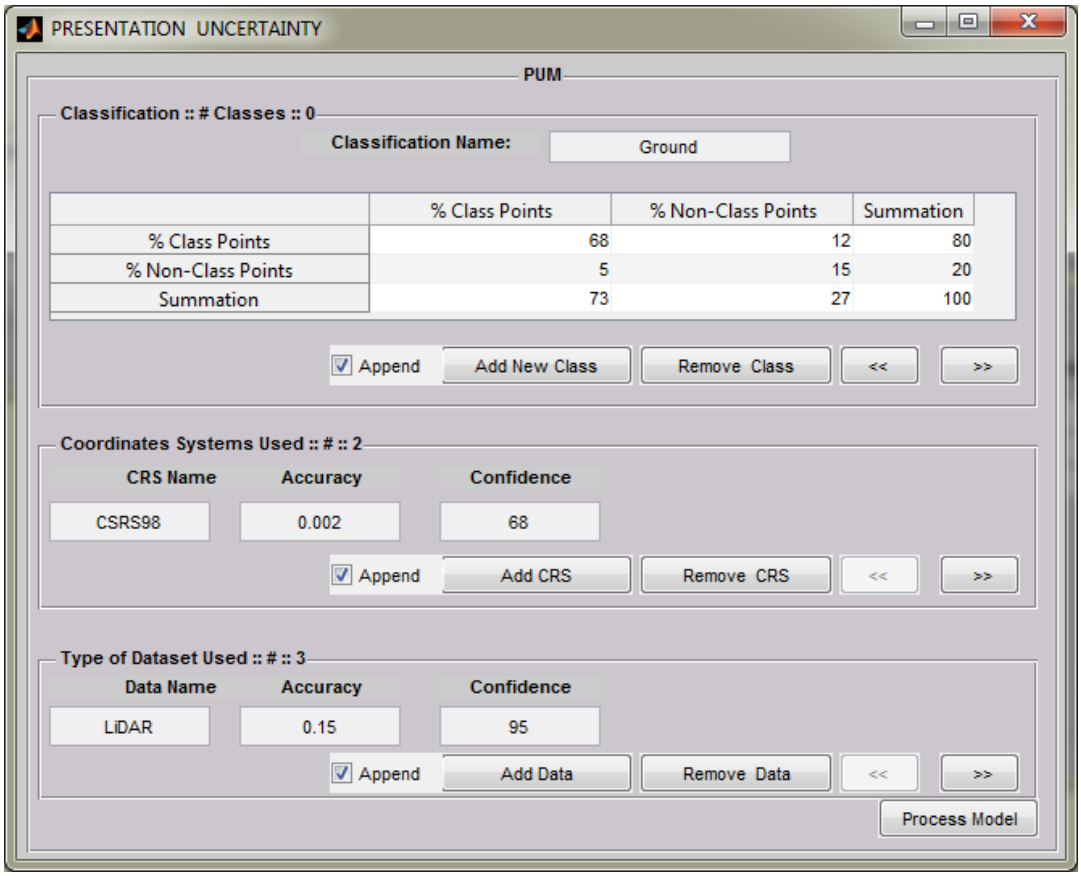

Figure 4.13. PRUM user interface

After PUM is calculated a report of the user defined error budget is now ready and a report is generated with the following results:

UDTEB REPORT
==========

Error Budget Summary (±m) Vertical accuracy CI% (vertical)
0.12 68.2
Horizontal Accuracy CI% (Horizontal)
0.30 68.2
Radial Accuracy CI% (Radial)

	0.29	68.2

User Accuracy Requirement (±m)	U (v)	U(h)	U(r)	U(CL) %
	0.14	0.3	0.34	68.2

Estimated LiDAR Accuracy (±m)	E (v)	E(h)	E (v,h)	CI
	0.07	0.21	0.22	68.2%

Reference System	Name	Accuracy (±m)	Conf. Interval (%)
	CSRS98	0.002	68
	CGVD28	0.005	95

Error Budgeting:

Will user specification for the project in mind using the systems defined be met?

Vertical: User Vertical Accuracy Requirements Met

Quality Control Vertical: User Vertical Requirements not over Specified

Horizontal: User Horizontal Accuracy Requirements have been met

Quality Control Horizontal: User Horizontal Requirements not over specified

Planning Uncertainty (±m) Vertical Precision of components (without correlated Errors)

range: Min Error (m)	Max Error (m)
0.10	0.335 ==> Range is within user requirements

LiDAR Uncertainty Deterministic / Non Deterministic

Deterministic: Same Values as "Estimated LiDAR Accuracy"

Processing Uncertainty (±m)

Reduction? Yes

%Point Reduction: 20

Uncertainty due to Interpolation and Morphology: 0.011 m at 95% CI

Consideration for PRUM at planning stage

Terrain Type	Slope Error Offset
Rolling	0.07

Consideration for Post Processing

Number of LiDAR points = 2530416

Number of Check points = 122

Standard deviation of Check points = 0.01

Estimated PRU 0.07

Data Integration Uncertainty (±m)

Number of data sets added: 3

Data	Accuracy	%Coverage	Combined Accuracy
CAD 2D	0.2	30	0.01
CAD 2.5D	0.15	70	0.02
Shape	0.15	70	0.02
Sum	0.5	170	0.05
	Total RMS	0.05	

Highest accuracy of integrated data = 0.20

Presentation Uncertainty (±m)

Class Accuracy

Class	Type I Error	Type II Error	%Agreement Rate	%Level of Agreement	Ω
Ground	0.02	0.013	86.01	92.71	0.83.

4.2.3 Users' Requirements Compared with Vendor Delivered Specifications

After users have estimated their error budget, the delivered data will now be validated through ground truthing surveys to ascertain the error of the data with respect to surveyed checkpoints (usually employ the same ground controlled checkpoints employed in the UDTEB PRUM model). From the RMSE values from a field validation a decision can me made whether or not initial the user defined error budget, which in this project was set to ±15 cm at 68% CI for the flood modeling was met. TIN to point differencing within ArcMap™ employing LAStools' *lascontrol* showed that that at 68% CI, the RMSE between the user determined error budget and the vendor reported uncertainty was ± 0.09 m which falls within the user requirements set initially at ± 0.15 m.

CHAPTER 5. SUMMARY, CONCLUSION AND RECOMMENDATION FOR FUTURE RESEARCH

CHAPTER 5.SUMMARY, CONCLUSION AND RECOMMENDATIONS
5.1 SUMMARY
5.2 . CONCLUSION
4.2.4 Accomplishments – Key Contributions
4.2.5 Limitations
5.3 RECOMMENDATION FOR FUTURE RESEARCH

Figure 5.1. Outline of Chapter 5.

5.1 SUMMARY

Rapid advancements in imaging and geospatial data capture technologies have led to major challenges in validating data quality. As the data and methods of acquisition become more complex, it is becoming increasingly difficult for end users to validate the data and processes for fitness for use. This is in contrast to what was done in traditional data capture techniques, for instance, surveying or aerial photogrammetry where photo identification is used to identify points on the ground which can easily be re-occupied to validate their spatial accuracies.

Based on experience in determining minimum specifications for LiDAR data collection and sharing among multiple organizations, solving this challenge can involve adopting flexible Quality Assurance and Quality Control specifications and metadata standards as suggested by Coleman and Adda [2010]. However, after the adoption of standards for data quality, there were still recurring limitations among LiDAR data users in this research to perform independent investigations to determine “false accuracies” and establish whether or not data accuracies are within tolerances for project-specific applications.

In summary the research aimed at designing LiDAR data error models that would allow for a user's side analysis of project deliverables of LiDAR data and derived products from LiDAR surveys. Table 5.1 provides a summary of RMSE among the various terrain morphologies.

Table 5.1. Summary of RMSE among the various areas with all obstructions

	Area	Morphology	RMSE (m)		
			Field	UDTEB	UDTUB-Field
1	Project Checkpoints	various	0.08	0.12	0.04
2	Odell Forest	vegetation	0.06	0.10	0.04
3	Wilmot Tennis Ct	open flat	0.17	0.10	-0.06
4	Windsor Street	steep slope	0.04	0.12	0.08
5	Avondale Court	sparsely dense	0.09	0.11	0.02
6	Downtown	dense	0.15	0.16	0.01

In both the UDTEB and field measurements, the steep slope area had the highest RMSE followed by the built-up areas.

The reporting of estimated errors and comparisons of vendor specifications and user-demanded specifications should be clear with respect to terminology, avoiding the confusion of terms in Table 3.3. In summary, an expression for error reports of LiDAR datasets, based on this research should have the following attributes:

1. There should be a users' requirement to be met;
2. There should be a standard for comparison, be it ground check points or estimates based on previous knowledge;
3. The uncertainty should be determined for the measured data based on a superior dataset, at least three times more accurate than the measured data;
4. The upper/lower limits of the error should be stated; and

5. The Confidence Interval for the measured quantities should be clearly determined and expressed – and where possible (optional) the Confidence Level can also be stated.

These should be clearly defined within the validation process of determining whether or not the data and processes involved satisfied the conditions for fitness for use. They should also be clearly stated so that the user can understand and interpret correctly what it means. A detailed discussion on the proposed best method for relaying uncertainty information of spatial datasets is discussed in Chapters 3 and 4.

5.2. CONCLUSION

The key objectives of the research (Section 3.3) were to:

1. critically compare user-demanded accuracy specifications for airborne LiDAR data with manufacturers' stated performance ;
2. determine the influence of varying topography and ground cover on the error;
3. analyze the respective influences of variations in user-demanded specifications, manufacturer's specifications, topography, and ground cover on the accuracy of information derived from Airborne LiDAR data
4. determine the reliability of products from LiDAR by determining the error at a given confidence interval; and
5. provide a deterministic or non-deterministic method to allow users independently quantify, validate or refute variations in user-demanded specifications and manufacturer's specifications.

4.2.4 Accomplishments – Key Contributions

Most of the objectives were met, while others could not be met.

Firstly, user's specifications were developed, considering the requirements of nine public organizations. A method for creating these user's specifications has been discussed in Section 3.4.2. Once user specifications have been clarified, a process to determine accuracy clarifying the strengths and limitations of the data at various terrain conditions at a given confidence is discussed. The accuracy and confidence of the data should be such that they are acceptable for a given project application within the life cycle of the said project. After the delivery of the data and or product, two methods were developed, namely the deterministic and non-deterministic methods, to allow the user to determine whether or not the LiDAR product was created according to specifications. The tasks to consider at this stage include field validation surveys to allow the user independently compare the users' requirements with the manufacturers' standards and determine whether or not the user's requirements have been met.

Secondly, the effects of variations of user demanded specifications with respect to manufacturers' specification for five areas of varying topographic attributes and land cover was critically investigated. The accuracy of information that can be derived from these areas was analyzed and the accuracy of information that can be derived from each set of data for given terrain morphology was discussed in Section 4.1.2. By employing ground truthing and point by point comparison of ground truth and LiDAR points for a

defined area, these uncertainty variations for varying topographic conditions were critically discussed.

Thirdly, the objective which was to provide a deterministic or non-deterministic method for estimating these errors to equip users to independently quantify, validate or refute variations in user-demanded specifications and manufacturer's specifications considering factors of terrain morphology on LiDAR products was also met. The deterministic approach, discussed in detail in Section 3.4.3.1 employed the CMP and SBET or their equivalent files obtained during the ALS survey, to determine LiDAR system errors (i.e., LUM errors). These files are used to extract the error of points with respect to the performances of the ALS system at the time of survey along a given trajectory. Where these files are not available, the non-deterministic method, discussed in 3.4.3.2 employs published LiDAR system parameters and performance reports to simulate the conditions of flight and estimate the errors of the point cloud. After determining the LiDAR system errors (LUM) other errors from random sources, namely, processing (PRUM), data integration (DIUM) and final presentation (PUM) are included. These error models are discussed in detail in Section 3.4.4. The overall effect of these errors is what defines the UDTEB model.

Fourthly, two methods were proposed for determining point by point comparisons between the LiDAR-derived elevations and corresponding ground checkpoints. Firstly, a novel approach of using square windows to determine the difference was proposed. This method intentionally deviated from conventional methods which employ a radius around the checkpoint to determine the height difference between the LiDAR points and

corresponding checkpoints. The advantages of using this method over the radius method are discussed in Section 3.4.8. The second method involved creating a TIN from the LiDAR ground points and intersecting the LiDAR-derived TIN with the checkpoints. The corresponding LiDAR derived elevation can then be deduced from the TIN for each ground checkpoint horizontal location.

Fifthly, by employing field surveys, the RMSE of elevations in the five study areas were discussed in Section 4.1. The error analysis in areas clear of obstructions, areas with light obstructions and areas with dense obstructions were discussed in Section 4.1.2.

Finally, a software prototype was created to provide a Graphic User Interface (GUI) towards helping simplify the estimation of errors. The software has been applied in Sections 3.4.6, 3.4.7, 3.4.8, and 4.2.2 to analyse error sources and their contributions to the total error budget. Appendix A gives details of the software code developed during a one year period (with a four months intensive mentoring on software development at CARIS Incorporated, Fredericton) to help calculate the total propagated errors in the UDTEB model.

4.2.5 Limitations

The field validation survey showed an influence on elevation errors with increase in ground cover. However, the model could not account for the influence of ground cover on predicted elevation errors.

The overall performance on specific terrain types show that there are systematic and random errors not accounted for in the UDTEB errors. As a result the modelled errors differ from those obtained from the physical measurements. It was clear from the large errors obtained in densely obstructed areas (e.g. the built-up area) compared to the smaller errors in areas clear of obstructions that obstructions play an important role in the total elevation error. However, there were not sufficient sampled ground checkpoints to arrive at a conclusive obstruction trend on the LiDAR-derived elevations. This is due to the limited topography around the project area. In other words, there were not enough different terrain morphologies in the research area to establish well-spaced checkpoints for the five topographies used in this research. An average of 100 checkpoints per area with specific terrain topography is required to arrive at a conclusive obstruction trend [Aguilar and Mills, 2008, p.163]. Also, the calibration file for the flight from which the CMP and SBET files are derived for the UDTUB model was only available for a limited area in Fredericton.

Areas with sharp slope showed created systematic bias that could not be accounted for in the UDTEB model. For instance in some areas in the Windsor Street where there were no obstructions, the difference between the modelled errors and the errors determined from physical measurements was 0.00 m at QCC 200. On the other hand, under the same conditions the difference reached 0.11 m for QCC 219 (Table 4.5). One reason identified was the position of these points within islands of the SBET data, meaning their errors had to be estimated with respect to the CMP file and the estimated terrain. There could be other factors not accounted for that have a bearing on this disparity and further research is

recommended. Although partly covered for in PUM (with respect to the quality of controls and references used), it can be seen in Section 4.1.2 (on obstruction analysis) that the total error increases when checkpoints are obstructed. To reduce this effect, only obstructions to bare ground points were employed in the elevation error analysis. Consequently, only ground classification of LiDAR points has been discussed.

5.3 RECOMMENDATIONS FOR FUTURE RESEARCH

It is recommended to have a further look at estimating the trend of errors in each of the five areas by employing a larger dataset that has defined trajectory parameters. Once the differences between the LiDAR elevations and GNSS elevations for the five test areas have been identified for a larger dataset than used in this research, the results can be used to further refine the UDTEB estimates by correcting for obstructions due to vegetation cover, multipath, flight direction with respect to a given slope.

Given a set of filtered points around the 2m window of controlled checkpoints, there were variable differences due to vegetative and ground cover obstruction of points within one meter radius from the checkpoints. Although the trend has been investigated for the project areas for the various terrain morphologies in Section 4.1.2, where a larger dataset is available, it will be interesting to further investigate this trend. A conclusive trend could not be arrived due to the limitations in size of the various terrain morphologies in the Fredericton area. The known trend could be used to refine the UDTEB model,

especially in densely obstructed areas where the RMSE of the field measurements were greater than the modelled RMSE.

The knowledge of the terrain type is essential in sharpening the ability of the UDTEB to estimate errors. Although this could not have been exactly known beforehand, the model only considered an estimate of terrain morphology by employing the measured QCCS and existing checkpoints. The UDTEB model also provides three morphological types, namely, flat, rolling and steep. These may be too generalized for certain applications. Further research to provide more terrain choices is recommended.

With respect to the classification of LiDAR points as discussed in Section 3.4.4, more research is required to statistically calculate correctly classified points from wrongly classified points. In the UDTEB model, manufacturers' classification specifications or an estimation of classification accuracy was made through visual inspection of random section of the LiDAR point cloud. However, a more empirical method could be developed and used for possible "fine-tuning" of the classification error estimation in the UDTEB model.

Finally, in order to validate LiDAR data classes other than bare earth points (e.g. vegetation and building points), a method to create checkpoints and checkpatches for these non ground points is recommended for future research.

REFERENCES

Adda P., A., Hoggarth (2011). "Simultaneous Processing of LiDAR for Effective Visualization and Analysis" Conference Presentation, *CIG 2011*. St. John's. Newfoundland & Labrador, Canada. October 5-7, 2011.

Adda P., Mioc D., Anton D., McGillivray F., E., A Morton, D Fraser (2011). "3D flood-risk models of government infrastructure". *ISPRS Commission VI, WG VI/4*. [Online] Last accessed online on January 2, 2012 at http://www.isprs.org/proceedings/XXXVIII/4-W13/ID_39.pdf.

Adda P., Tienaah T., Amer A., Moussadak M. (2009). "Flood Mapping for Downtown Fredericton Using LIDAR data and water gauges." Graduate Group Research Project Report –Unpublished. University of New Brunswick, Canada. pp. 1-26.

Aguilar F., J. P. Mills (2008). "Accuracy Assessment of LiDAR-Derived Digital Elevation Models". *The Remote Sensing and Photogrammetry Society* and Blackwell Publishing Ltd. *The Photogrammetric Record 23(122).* pp.148–169.

Aguilar F.J., J.P., Mills, J., Delgado, M.A.,Aguilar, J.G., Negreiros, J.L., Perez (2010). "Modeling vertical error in LiDAR-derived digital elevation models". *ISPRS Journal of Photogrammetry and Remote Sensing*, 65 (1), pp. 103-110.

Aguilar, F.J., F.Agüera, M.A. Aguilar, and F. Carvajal, (2005). "Effects of Terrain Morphology, Sampling Density and Interpolation Methods on Grid DEM Accuracy". *Photogrammetric Engineering and Remote Sensing*, 71(7), pp. 805-816.

Baltsavias, E.P. (1999). "Airborne Laser Scanning: Basic Relations and Formulas." *ISPRS Journal of Photogrammetry & Remote Sensing*, 54(2-3), pp. 199-214.

Bell, S. (1999). *Measurement Good Practice Guide. A beginner's Guide to Uncertainty of Measurement*. Issue 2: A report from the Centre for Basic, Thermal and Length Metrology National Physical Laboratory, Teddington, Middlesex, United Kingdom. pp., 1-33.

Bretar, F., M. Pierrot-Deseilligny, M. Roux (2004). "Solving the Strip Adjustment Problem of 3D Airborne LiDAR Data." *Proceedings of the IEEE IGARSS'04*, 20-24 September, Anchorage, Alaska.

Callow, J. N., K. P. van Niel, and G. S. Boggs (2007). "How does modifying a DEM to reflect known hydrology affect subsequent terrain analysis?" *Journal of Hydrology* 332(1-2), pp.30-39.

Carmel, Y., D.J. Dean, C.H. Flather (2001). Combining Location and Classification Error Sources for Estimating Multi-Temporal Database Accuracy. *Photogrammetric Engineering and Remote Sensing*, 67 (7): 865-872, 2001. [Online] July 12, 2012. http://www.asprs.org/a/publications/pers/2001journal/july/2001_jul_865-872.pdf.

CFLHD (2009). *Project study Application: Photogrammetric Airborne Positioning. Chapter 4. Technical Development papers*. [Online] September 3, 2009 from http://www.cflhd.gov/techDevelopment/completed_projects/survey/_documents/06_Chapter_4_Photogram_Airborne_Position.pdf

Chaplot, V., F. Darboux, H.Bourennane, S. Leguédois, N. Silvera, K. Phachomphon (2006). "Accuracy of interpolation techniques for the derivation of digital elevation models in relation to landform types and data density." *Geomorphology* 77(1-2), pp.126- 141.

Charaniya, A. P., R. Manduchi, and S. K. Lodha, (2004). "Supervised parametric classification of aerial LiDAR data." *Proceedings of 2004 Conference on Computer Vision and Pattern Recognition Workshop (CVPRW'04)*, Washington D.C, USA.

Charlton, M.E., A.R.G. Large, and I.C. Fuller (2003). Application of Airborne LIDAR in river environments: The River Coquet, Northumberland, UK, *Earth Surface Processes and Landforms* 28(3), pp. 299-306.

Chou, Y. H., Liu, P. S. and Dezzani, R. J. (1999). "Terrain complexity and reduction of topographic data."*Geographical Systems,* 1(2), pp. 179-197.

Chrzanowski, A. (1977). "Design and error analysis of surveying projects". Selected papers and lecture notes. Department of Surveying Engineering. University of New Brunswick, NB, Canada. Lecture Notes N. 47, pp. I-1-IV-13.

Cohen, J. (1960). A Measurement coefficient of agreement for nominal scales. *Education and Psychological Measurement* 20(1). pp.37-46.

Coleman D., P. Adda (2010). "LiDAR data acquisition and quality assurance specifications for New Brunswick." Draft II, June 28, 2010. pp 1-25. Project report delivered to SNB, Fredericton NB, Canada.

Crombaghs, M., E. De Min, and R. Bruegelmann, (2000). "On the Adjustment of Overlapping Strips of Laser Altimeter Height Data. International Archives of Photogrammetry and Remote Sensing." 33(B3/1), pp. 230-237.

Csanyi N., and Toth C. K (2007). "Improvement of Lidar Data Accuracy Using Lidar-Specific Ground Targets". *Photogrammetric Engineering and Remote Sensing*. [Online] http://www.asprs.org/a/publications/pers/2007journal/april/2007_apr_385-396.pdf on April 18, 2013. pp. 385-396.

Dare, P (2013). Personal interactions with the author.

Desmet, P. J. J. (1997). "Effects of interpolation errors on the analysis of DEMs." *Earth Surface Processes and Landforms* 22(6), pp.563-580.

El-Sheimy N. (2005) "Georeferencing Component of LiDAR Systems." Chapter 4, *Topographic Laser Ranging and Scanning: Principles and Processing*. Taylor & Francis Group, LLC., pp. 195-213.

El-Sheimy, N., Valeo, C., and Habib, A. (2005). *Digital Terrain Modeling: Acquisition, Manipulation, and Application* . Boston and London: Artech House Publication. pp. 1-15.

Federal Emergency Measures Agency (2003) Guidelines and Specifications for Flood Hazard Mapping Partner, Appendix A: Guidance for Aerial Mapping and Surveying. [Online] http://www.fema.gov/library/viewRecord.do?id=2206 on November, 2009.

Federal Geographic Data Committee (1998). Geospatial Positioning Accuracy Standards Part 3: National standard for Spatial Data Accuracy. Appendix 3-A (normative): Accuracy Statistics.

FEMA (2000). *Appendix 4B: Airborne Light Detection and Ranging Systems*. [Online] 3 April 2009. http://www.fema.gov/pdf/fhm/lidar_4b.pdf.

FEMA (2003). Federal Emergency Measures Agency. Guidelines and Specifications for Flood Hazard Mapping Partner, Appendix A: Guidance for Aerial Mapping and Surveying. [Online] http://www.fema.gov/library/viewRecord.do?id=2206 on November, 2009.

Fenstermaker, L. K. (1994) Remote Sensing Thematic Accuracy Assessment. A compendium. *American Society for Photogrametry and Remote Sensing* Bethesda Md, p.413.

Fisher, P. F. and Tate, N. J. (2006). "Causes and consequences of error in digital elevation models." *Progress in Physical Geography*, 30(4), pp. 467-489.

Flood, M. (Editor) (2004). ASPRS Guidelines Vertical Accuracy Reporting for Lidar Data V1.0. [On-line] Accessed on February 3, 2010 from http://www.asprs.org/society/committees/lidar/Downloads/Vertical_Accuracy_Reporting_for_Lidar_Data.pdf.

GIM (2010). "Comparison of products in the LiDAR market". *GIM international* magazine [Online] from http://www.gim-international.com/productsurvey/compare.php. Accessed on February 08, 2010.

Google maps, (2012). NB Canada maps. [Online] Accessed in January 2010 from www.google.com/maps.

Gonsalves, M., O (2010). "A comprehensive uncertainty analysis and method of geometric calibration for a circular scanning airborne LiDAR". PhD dissertation, the University of Southern Mississippi, pp.1- 417.

Goulden T., C. Hopkinson (2006a). "Error Sources in the LiDAR system". Applied Geomatics Research group. Project report on LiDAR error model report. Deliverable 3. Available on hard copy print at CARIS, Fredericton, NB. pp.1-28.

Goulden T., C. Hopkinson (2006b). "Creation of Error Models". Applied Geomatics Research group. Project report on LiDAR error model report. Deliverable 4. Available on hard copy print at CARIS, Fredericton, NB. pp.1-46.

Goulden T., C. Hopkinson (2006c). "Validation of error models". Applied Geomatics Research group. Project report on LiDAR error model report. Deliverable 5. Available on hard copy print at CARIS, Fredericton, NB. pp.1-37.

Goulden, T. (2009). "Prediction of Error Due to Terrain Slope in LiDAR Observations." M.Sc.E. thesis, Department of Geodesy and Geomatics Engineering Technical Report No. 265, University of New Brunswick, Fredericton, New Brunswick, Canada, pp.1-138.

Guo, Q., W. Li, H. Yu, O. Alvarez (2010). "Effects of topographic variability and LiDAR sampling density on several DEM interpolation methods". pp. 1-10.

Habib, A. F., M. Al-Durgham, A. P. Kersting, P. Quackenbush (2008). "Error Budget of LiDAR Systems and Quality Control of the Derived Point Cloud." *The International Archives of the Photogrammetry, Remote Sensing and Spatial Information Sciences*. Vol. XXXVII. Part B1. Beijing. pp. 203-210.

Habib, A., M. Ghanma, M. Morgan, and R. Al-Ruzouq (2005). "Photogrammetric and LiDAR data registration using linear features". *Photogrammetric Engineering and Remote Sensing*, 71 (6), pp. 699-707.

Hans K. H., J. Stoker, D. Brown, M. J. Olsen, R. Singh, K. Williams, A. Chin, A. Karlin, G. M., J. Janke, J. Shan, K. Kim, A. Sampath, S. Ural, C. E. Parrish, K. Waters, J. Wozencraft, C. L. Macon, J. Brock, C. W. Wright, C. Hopkinson, A. Pietroniro, I. Madin, J. Conner (2012). *Manual of Airborne Topographic LIDAR*, Applications. Subchapter (10), ASPRS, Renslow, M., editor, pp.238-427.

Hare, R. (2001). "Error Budget Analysis for US Naval Oceanographic Office (NAVOCEANO) Hydrographic Survey Systems" Final Report for the Naval Oceanographic Office. Prepared for the University of Southern Mississippi for Naval Oceanographic Office. pp.2ff.

Hodgson, M and P. Bresnahan (2004). "Accuracy of Airborne LiDAR-Derived Elevation: Empirical Assessment and Error Budget" *Photogrammetric Engineering and Remote Sensing*, 70(3), pp. 331- 339.

Hodgson, M. E., J. Jensen, G. Raber, J. Tullis, B. A. Davis, G. Thompson, and K. Schuckman (2005). "An evaluation of LiDAR-derived elevation and terrain slope in leaf-off conditions". *Photogrammetric Engineering and Remote Sensing*, 71(7), pp.817-823.

Hunter, G.J., M. Caetano, and M. F. Goodchild (1995) A methodology for reporting uncertainty in spatial database products. *Journal of the Urban and Regional Information Systems Association.* 7(2): pp. 11-21.

Isenburg, M. (2012). LAStools. [Online] from http://rapidlasso.com/lastools. Accessed on March 12, 2012.

JCGM 100 (2008). "Evaluation of measurement data-Guide to the expression of uncertainty in measurement". © JCGM member organizations (BIPM, IEC, IFCC, ILAC, ISO, IUPAC, IUPAP and OIML). Accessed [Online] on December 15, 2012 from http://www.bipm.org/utils/common/documents/jcgm/JCGM_100_2008_E.pdf. pp.1-120.

Jie, S., C. K. Toth (Editors) (2008). *Topographic Laser Ranging and Scanning Principles and Processing.* CRC Press. p.48, figure 2.17.

Junkins, D. (1991). The National Transformation for Converting Between NAD27 and NAD83 in Canada, in Moving to NAD83 (ed. D. C. Barnes), CISM, Ottawa, pp. 16 -40.

Katzenbeisser, R. (2003). "About the calculations of LiDAR sensors". *Proceedings ISPRS workshop on 3-D reconstruction from airborne laser-scanner and InSAR data*, 8-10 October 2003, Dresden, Germany.

Kerr, T. (1994). "Use of GPS/INS in the Design of Airborne Multisensor data collection missions (for tuning NN-based ATR algorithms)". In proceedings of *7th International Technical Meetings of Institute of Navigation (ION) GPS*, pp 1173-1188.

Kidman B. (2012). Leading Edge Geomatics (LEG). Personal correspondance on the specifications of the DPS 2012 LiDAR data.

Kilian, J., N. H., and M. Englich (1996). "Capture and evaluation of airborne laser scanner data." *International Archives of Photogrammetry, Remote Sensing and Spatial Information Sciences* 31(B3), pp 383-388.

Kothari, C. R. (1985). *Research Methodology, Methods & Techniques.* New Age International (P) Ltd. New Delhi, India. ISBN: 81-224-152-9, pp. 152-188, Figure 9.1.

Krakiwsky, E., J., D. J. Szabo, P. Vaníček, M. R. Craymer (1999). "Development and Testing Of In-Context Confidence Regions for Geodetic Survey Networks". 217(198). pp. 1-22.

Kraus, K. and Pfeifer N. (2001). "Advanced DTM Generation from LiDAR Data." Presented at ISPRS Workshop Land Surface Mapping and Characterization using Laser Altimetry, Annapolis, Maryland, USA. pp. 22-24.

Kutoglu, H.S., and P. Vaníček (2006). Effect of Common Point Selection on Coordinate Transformation Parameter Determination. Accessed August 03 [Online] from www.springerlink.com/content/l34406731155h7q6/fulltext.pdf.

Latypov, D. (2005). Effects of Laser Beam Alignment Tolerance on LiDAR Accuracy, *ISPRS Journal of Photogrammetry and Remote Sensing* 59. pp.361-368.

Leading Edge Geomatics, (2013). Interactions with the owner and Survey staff on validating LiDAR elevation accuracies under heavy vegetative conditions. January, 2013.

Li, Z., Q. Zhu, C. Gold (2005). *Digital Terrain Modeling: Principles and Methodology*. Boca Raton, London, New York, and Washington, D.C.: CRC Press.

Lim, K., P. Treitz, M. Wulder, and M. Flood,. (2003). "LiDAR remote sensing of forest structure." *Progress in Physical Geography* 27(1), pp 88-106.

Lipman, J. S. (1992). "Trade-offs in the implementation of Integrated GPS Inertia systems". ION GPS-92, *Fifth International Technical Meeting of the satellite division of the institute of navigation*, New Mexico, pp 1125-1133.

Liu X, (2008). "Airborne LiDAR for DEM generation: some critical issues." *Progress in Physical Geography,* 32 (1), pp. 31-49.

Liu X. and Z. Zhang (2008). LiDAR Data Reduction For Efficient and High Quality DEM Generation. The International Archives of the Photogrammetry, Remote Sensing and Spatial Information Sciences. 37 (B3b). Beijing 2008. pp.172-128.

Lloyd, C. D. and Atkinson, P. M. (2002). "Deriving DSMs from LiDAR data with Kriging." *International Journal of Remote Sensing,* 23(12), pp. 2519-2524.

Lloyd, C. D. and Atkinson, P. M. (2006). "Deriving ground surface digital elevation models from LiDAR data with geosatistics. *International Journal of Geographical Information Science,* 20(5), pp. 535-563.

Maas, H. G. (2000). "Least-Squares Matching with Airborne Laserscanning Data in a TIN Structure". *International Archives of Photogrammetry and Remote Sensing,* 33(B3/1), pp. 548-555.

Martin A. A., N. M. Holden, P. M. Owende, S. M. Ward (2001). "The Effects of Peripheral Canopy on DGPS Performance on Forest Roads". *International Journal of Forest Engineering*. 12(1). pp.1-9.

Merrett, 2008. Personal interactions with Peter Merrett, owner of Merrett Survey Partnership, UK/USA on June, 2008.

Mohammed, A. H., (1999). "Optimizing the estimation in INS/GPS Integration for Kinematic application". PhD Thesis, University of Calgary. Canada. pp 1-160.

NAP (2007). North American Profile of Geographic Information – Metadata, version 1.0.1. USA/Canada working group. [Online] Accessed on March 2010 from *http://www.fgdc.gov/standards/projects/incits-l1-standards-projects/NAP-Metadata.*

Nayegandhi A. (2007). Lidar Technology Overview. ETI – US Geological Survey, Florida Integrated Science Center, St. Petersburg, FL 33701. Presentation on Airborne Lidar Technology and Applications. Baton Rouge, LA. June 20-21, pp 1-66.

Oxford Dictionaries (2012a). The world's most trusted dictionaries. Definition of terms. 'budget'. [Online] http://oxforddictionaries.com/definition/english/budget.

Oxford Dictionaries (2012b). The world's most trusted dictionaries. Definition of terms. *[technical]* 'error'. [Online] http://oxforddictionaries.com/definition/english/error

Parrish, C. E., G. H., Tuell, W. E Carter, and R. L. Shrestha (2005). "Configuring an airborne laser scanner for detecting airport obstructions." *Photogrammetric Engineering and Remote Sensing* 71(1), pp 37-46.

Petrie, G., and C.K. Toth (2008). Introduction to Laser Ranging, Profiling, and Scanning. Chapter 1 in *Topographic laser ranging and scanning: principles and processing*, Published by Taylor & Francis Group, LLC. pp 80.

Pfeifer, N. and Briese, C. (2007). "Geometrical aspects of airborne laser scanning and terrestrial laser scanning." *International Archives of Photogrammetry, Remote Sensing and Spatial Information Sciences*, 36(part 3/W52), pp. 311-319.

Poole, D., E. A. Raftery (2000). "Inference for Deterministic Simulation Models: The Bayesian Melding Approach". *Journal of the American Statistical Association, Vol. 95, No. 452*. [Online] from http://www.jstor.org/stable/10.2307/2669764. Accessed on July 10, 2012 pp. 1244-1255.

Renslow, M. (2010). Lidar Workshop Presentation. Utilization/Integration of LiDAR for Mapping and GIS. Renslow Mapping Services in Eugene, OR on June 10, p. 251.

Reutebuch, S. E., H.-E. Andersen, and R. J. McGaughey (2005). "Light detection and ranging (LIDAR): an emerging tool for multiple resource inventory." *Journal of Forestry 103(6)*, pp 286-292.

Samberg, A. (2005). ASPRS LIDAR GUIDELINES: Horizontal Accuracy Reporting. Federal Geographic Data Committee FGDC-STD-007.3-1998. Geospatial

Positioning Accuracy Standards. Part 3: National Standard for Spatial Data Accuracy, pp. 1-36.

Samuels, B. M., & D.R. Sanders (2007). Practical law of architecture, engineering and geoscience. Toronto: Pearson Prentice Hall. pp 76 and 79.

Sheng, Y., P. Gong, and G. S. Biging (2003). "Orthoimage production for forested areas from large-scale aerial photographs." *Photogrammetric Engineering and Remote Sensing* 69(3), pp 259-266.

Sithole, G. and Vosselman, G. (2003). "Report: ISPRS Comparison of Filters." The Netherlands: Department of geodesy, Faculty of Civil Engineering and Geosciences, Delft University of Technology. pp. 1-17.

Smith, S. L., D. A. Holland, and P. A Longley (2005). "Quantifying interpolation errors in urban airborne laser scanning models." *Geographical Analysis 37(2),* pp 200-224.

SNB (2002). "New Brunswick Control Monument Database Information. Explanation of fields and Glossary of terms. Published by Service New Brunswick [Online] https://www.pxw1.snb.ca/webnbcontrol/snbe/UserGuide.pdf.

TopNET live, (2012). GNSS RTK Reference Network. Real Time Kinematic Data Services for Eastern Canada. [Online] http://www.topconpositioning. com/products/networks/topnet-live-networks/topnet-live-eastern-canada.

United States Defence Mapping Agency (1987). Supplement to Department of Defence World Geodetic System 1984 technical report. Defence Mapping Agency Technical report No. 8350.2-A, Washington, D.C. [Online] http://www.asprs.org/ a/society/committees/standards/Horizontal_Accuracy_Reporting_for_Lidar_Data.p df. Accessed on August 18, 2012.

United States Geological Survey (2010) national geospatial program base LiDAR Specification Version 13. Was last accessed on March 10, 2010 from http://lidar.cr.usgs.gov/USGS-NGP%20Lidar%20Guidelines%20and%20Base%20 Specification%20v13%28ILMF%29.pdf.

Ussyshkin, R. V., M. Boba, M. Sitar (2008). "Performance characterization of an airborne LiDAR system: bridging system specifications and expected performance." *The International Archives of the Photogrammetry, Remote Sensing and Spatial Information Sciences*. 37(B1). pp. 177-181.

Ussyshkin, R. V., B. Smith (2006). "Performance analysis of ALTM 3100EA: Instrument specifications and accuracy of LiDAR data*." ISPRS Conference Proceedings (Part B), Paris, France. 1-4 July*. pp.1-7.

Ussyshkin, R. V., R. B Smith (2007). "A new approach for assessing LiDAR data accuracy for corridor mapping applications." Conference Proceedings, *The 5th International Symposium on Mobile Mapping Technology*, Padua, Italy. On CD-ROM.

Vaníček, P., E. J. Krakiwsky (1986). *Geodesy: The Concepts. 2nd rev. ed.*, North--Holland, Amsterdam, The Netherlands. pp. 25-44;175-287.

Vaníček, P., R. Steeves (1996). "Transformation of Coordinates between two Horizontal Geodetic Datums". *Journal of Geodesy* Springer-Verlag 70:740-745. [Online].http://www.springerlink.com/content/kjtr7113721703wh/fulltext.pdf Accessed August 03 2012.

Wagner, W., A. Ullrich, T. Melzer, C. Briese, and K. Kraus (2004). "From single-pulse to full-waveform airborne laser scanners: potential and practical challenges". *International Archives of the Photogrammetry, Remote Sensing and Spatial Information Sciences 35(B3).*

Wang, C.K., Y.W. Liu and T. Yi-Hsing (2010). "Quality Assessment and Control of DEM Generation from Airborne LiDAR Data". *AARS Proceedings*. [Online] July 11, 2012. http://www.a-a-r-s.org/acrs/proceeding/ACRS2010/Papers/Poster%20 Presentation/ Session % 202/ PS02-18.pdf.

Webster, T. L. and G. Dias (2006). "An automated GIS procedure for comparing GPS and proximal LiDAR elevations." *Computers & Geosciences 32(6)*, pp 713-726

Wehr, A. (2008). "LiDAR Systems and Calibration." Chapter 4 in *Topographic laser ranging and scanning: principles and processing.* Taylor & Francis Group, LLC. pp.129-171.

Wehr, A. and U. Lohr (1999). "Airborne laser scanning - an introduction and overview." *ISPRS Journal of Photogrammetry and Remote Sensing 54(4)*, pp 68-82.

Witte, C., P. Norman, R. Denham, D. Turton, D. Jonas, P. Tickle (2000). "*Airborne Laser Scanning: A Tool for Monitoring and Assessing the Forests and Woodlands of Australia, Laser Altimetry Report 1*". Forest Ecosystem Research and Assessment, Department of Natural Resources, Natural Sciences Precinct, Queensland, Australia. [Online] http://aamgroup.com/resources/pdf/publications/ technical_papers/DNR_Laser_Altimetry_Report_1.pdf, pp. 1-17.

APPENDIX

APPENDIX A. UDTEB Matlab™ code

The main function for the application is shown here. Contact author to discuss access to complete UDTEB models code. Parts of the over eight thousand lines of Code are copyright to CARIS Inc. Fredericton, CANADA and Michael Gonsalves of the National Oceanic and Atmospheric Administration (NOAA). Permission was granted to the author to use and modify these codes during the UDTEB application development.

```
function  main_app
%MAIN_APP Main Application Interface to all Models
%   DIUM, LUM, PRUM , PUM

   %globals
   iconsCollection = struct();
   main_gui_data = struct();

   %main App
   clear ; clc; close all;
   %bootstrap the application
   bootstrap %bootstrap: adding all folders to matlab path
   %initialise app.

    figHt       = 100;
   figWidth    = 700;
   UDTUB_GUI    = figure('Units','pixels','Visible','on','Position',[400,400,figWidth,figHt]);

   %   init gui util variables
      init()

   set(UDTUB_GUI,'Name','USER DETERMINED UNCERTAINTY BUDGETING')
   set(UDTUB_GUI,'MenuBar','None') % FIGURE or NONE -- file, edit, etc.
   %set(tibo_GUI,'Toolbar','figure') % AUTO, FIGURE or NONE
   set(UDTUB_GUI,'NumberTitle','Off')
   set(UDTUB_GUI,'Resize','Off')
   set(UDTUB_GUI,'ResizeFcn',{@UIResize,'figMain'})
   %%
   %==============UI Controls ========================================
   %% Declare UI-controls
     %toolbar end ***
   % Create the bottom uipanel
      main_panel = uipanel('Units','pixels','Parent',UDTUB_GUI,...
         'BorderType','etchedin','BackgroundColor',[0.8,0.78,0.8],'Position',...
         [0 0 690 70],'Title','UDTUB','FontWeight','bold','TitlePosition','centertop');

      main_panel_sub1 = uipanel('Units','pixels','Parent',main_panel,...
```

```
    'BorderType','etchedin','BackgroundColor',[0.8,0.78,0.8],'Position',...
    [0 0 670 50],'Title','','FontWeight','bold','TitlePosition','lefttop');
  %User Defined Edit Controls
  btn_LUM = uicontrol('Parent',main_panel_sub1,'Style','pushbutton',...
                      'String','LUM',....
                      'Value',0,...
                      'Position',[0 0 100 40],...
                      'Callback',{@btn_Callback,'lum'});
  btn_PLUM = uicontrol('Parent',main_panel_sub1,'Style','pushbutton',...
                      'String','PLUM',...
                      'Value',0,...
                      'Position',[0 0  100 40],...
                      'Callback',{@btn_Callback,'plum'});
  btn_PRUM = uicontrol('Parent',main_panel_sub1,'Style','pushbutton',...
                      'String','PRUM',...
                      'Value',0,...
                      'Position',[0 0 100 40],...
                      'Callback',{@btn_Callback,'prum'});
  btn_DIUM= uicontrol('Parent',main_panel_sub1,'Style','pushbutton',...
                      'String','DIUM',...
                      'Value',0,...
                      'Position',[0 0 100 40],...
                      'Callback',{@btn_Callback,'dium'});
  btn_PUM= uicontrol('Parent',main_panel_sub1,'Style','pushbutton',...
                      'String','PUM',...
                      'Value',0,...
                      'Position',[0 0 100 40],...
                      'Callback',{@btn_Callback,'pum'});
  btn_GenReport = uicontrol('Parent',UDTUB_GUI,'Style','pushbutton',...
                      'String','Generate UDTUB Report',...
                      'Value',0,...
                      'FontWeight','bold',...
                      'Position',[0 0 200 25],...
                      'Callback',{@btn_Callback,'genreport'});

  %toolbar ***
UDTUB_toolbar  = uitoolbar('Parent',UDTUB_GUI);
btnAbout = uipushtool(UDTUB_toolbar,'CData',iconsCollection.about_icon,...
'TooltipString','About UDTUB','HandleVisibility','off','ClickedCallback',...
@about_UDTUB);

function [childRelPos]  = getUICenterLocation(childPos,parentPos)
  if nargin <2
    err = MException('','Err: getUICenterLocation, nargin must be two params','');
    throw(err);
  end
  if isempty(parentPos) || isempty(childPos)
    err_2 = MException('', 'Err: getUICenterLocation,args cannot be empty','');
    throw(err_2);
  end
  parent_W = parentPos(3);
  parent_H = parentPos(4);

  child_W = childPos(3);
  child_H = childPos(4);
```

```
    childRelPos_X = (parent_W* 0.5) - (0.5 * child_W);
    childRelPos_Y = (parent_H* 0.5) - (0.5 * child_H);

    childRelPos = [childRelPos_X ,childRelPos_Y,child_W,child_H];
end
function [ui_pos]= getUIPosition(UIHandler)
    try
        uiObj    = get(UIHandler);
    catch err
        err_cause = MException('','Err: getUIPosition, Invalid Handler ','');
        err = addCause (err, err_cause);
        rethrow(err);
    end
    if isfield(uiObj,'Position')
        ui_pos = uiObj.Position;
    elseif (isfield(uiObj,'ScreenSize'))
        ui_pos = uiObj.ScreenSize;
    else
        err = MException('','Err: getUIPosition, child has no position field','');
        throw(err);
    end
end
function setUICenterScreen(childHanler,parentHandler)
    if nargin < 2
        err = MException('','Err: setUICenterScreen, nargin must be two params','');
        throw(err);
    end
     set(childHanler,'Position',...
        getUICenterLocation( ...
                        getUIPosition(childHanler),...
                        getUIPosition(parentHandler)...
                       )...
        );
end
function setUIPosition(childHanler,parentHandler,xPercent,yPercent)
    if nargin < 2
        err = MException('','Err: setUIPosition, nargin must be two params','');
        throw(err);
    end
    child_pos       = getUIPosition(childHanler);
    parent_pos      = getUIPosition(parentHandler);
    child_pos_x     = xPercent * parent_pos(3); %index 3 width
    %setting the position anchor from left,bottom to left,top: thus - child_pos(4)
    child_pos_y     = yPercent * parent_pos(4) - child_pos(4); %index 4 height
    set(childHanler,'Position',...
          [child_pos_x,child_pos_y,child_pos(3),child_pos(4)]..);
end
function UIResize (hObject,~,arg1)
    sysHandler = 0; %system handler
    if strcmpi('figmain',arg1)
      setUICenterScreen(hObject,sysHandler);
      setUIPosition(main_panel,           UDTUB_GUI,     0.01,   0.99); %main panel in gui
      setUIPosition(main_panel_sub1,       main_panel,    0.01,   0.8); %user_panel in main

      %Edit controls
       setUIPosition(btn_LUM,       main_panel_sub1,     0.01,   0.88);
```

```
        setUIPosition(btn_PLUM,      main_panel_sub1,     0.2,    0.88);
        setUIPosition(btn_PRUM,      main_panel_sub1,     0.4,    0.88);
        setUIPosition(btn_DIUM,      main_panel_sub1,     0.6,    0.88);
        setUIPosition(btn_PUM,       main_panel_sub1,     0.8,    0.88);

        %main gui button
        setUIPosition(btn_GenReport,       UDTUB_GUI,     0.712,    0.27);
      end
    end
    %==============UI Calback Functions================================
    function btn_Callback(~,~,arg1)
      if strcmpi('lum',arg1)
        main_lum(UDTUB_GUI); % execute lum application
      elseif strcmpi('plum',arg1)
        main_plum(UDTUB_GUI); % execute plum application
      elseif strcmpi('prum',arg1)
        main_prum(UDTUB_GUI); % execute prum application
      elseif strcmpi('pum',arg1)
        main_pum(UDTUB_GUI); % execute pum application
      elseif strcmpi('dium',arg1)
        main_dium(UDTUB_GUI); % execute dium application
      elseif strcmpi('genreport',arg1)
        %generate report
        udap_report_gen(UDTUB_GUI);
      end
    end
    function about_UDTUB(~,~)
      about_fig=  figure('Units','pixels','Visible','on','Position',[550,350,378,449]);
      set(about_fig,'Name','ABOUT UDTUB')
      set(about_fig,'MenuBar','None') % FIGURE or NONE -- file, edit, etc.
      %set(tibo_GUI,'Toolbar','figure') % AUTO, FIGURE or NONE
      set(about_fig,'NumberTitle','Off')
      set(about_fig,'Resize','Off')
      axes('Parent',about_fig,'Units','pixels','Position',[0,0,378,449]);
      imshow(iconsCollection.about_image);
    end
    %==============UI Calback Functions============UTILITY FUNCTIONS=====
    function init
      %toolbar icons
      iconsCollection.('about_icon')    = imread ('misc/imgs/icons/gge.png');
      %image paths
      iconsCollection.('about_image')  = imread ('misc/imgs/icons/about.png');

      %set main handler 0 as udab_gui handler
      setappdata(0,'udab_gui',UDTUB_GUI)

      %set app data variables
      main_gui_data.('lum')   =struct();
      main_gui_data.('dium')  =struct();
      main_gui_data.('plum')  =struct();
      main_gui_data.('prum')  =struct();
      main_gui_data.('pum')   =struct();
      setappdata(UDTUB_GUI,'model',main_gui_data);
    end
  end
```

APPENDIX B. Matlab™ code to perform square window differencing

```
function  main
%main App
clear ; clc; close all;
%globals
contTitle   ='Select Control Points ';
control_shp = getShpData(contTitle);
lasTitle    ='Select LAS Shapefile : LiDAR Data ';
las_shp     = getShpData(lasTitle);
%        las_shp_zField  = 'Z';
%        cont_shp_zField = 'Elevation';
%        rect_length     = 5;
if isempty(las_shp) || isempty(control_shp)
   return ; %exit if any is empty
end
[control_fnames ,control_cell_data] = convertShpToCell (control_shp);
[las_fnames ,las_cell_data] = convertShpToCell (las_shp);

LASContDiff_Struct = struct();
%globals
LASContDiff_Struct.('cont_z_name')=control_fnames;
LASContDiff_Struct.('las_z_name') =las_fnames;
LASContDiff_Struct.('cont_zf') ='';
LASContDiff_Struct.('las_zf') ='';

figHt=130;figWidth=610;
LASCont_GUI  = figure('Units','pixels','Visible','on','Position',[400,400,figWidth,figHt]);

setappdata(0,'mainGui_Handler',LASCont_GUI); %setting the main gui handler  to the root app data

set(LASCont_GUI, 'Name','Compute LAS Diff From Control [Rect]')
set(LASCont_GUI, 'MenuBar','None') % FIGURE or NONE -- file, edit, etc.
set(LASCont_GUI, 'NumberTitle','Off')
set(LASCont_GUI, 'Resize','On')
set(LASCont_GUI, 'ResizeFcn',{@UIResize,'figMain'})

%==============UI Controls ========================================
%Declare UI-controls



%toolbar end ***
% Create the bottom uipanel
main_panel = uipanel('Units','pixels','Parent',LASCont_GUI,...
   'BorderType','etchedin','BackgroundColor',[0.8,0.78,0.8],'Position',...
   [0 0 600 120],'Title','Controls & LAS','FontWeight','bold','TitlePosition','centertop');


user_def_panel = uipanel('Units','pixels','Parent',main_panel,...
   'BorderType','etchedin','BackgroundColor',[0.8,0.78,0.8],'Position',...
   [0 0 580 100],'Title','-|-','FontWeight','bold','TitlePosition','lefttop');
```

```
%Buttons
%=======
btn_user_load_file = uicontrol('Parent',user_def_panel,'Style','pushbutton',...
   'String','Compute Diff',...
   'Value',0,...
   'Position',[0 0 100 25],...
   'Callback',{@btn_Callback,'comp_diff'}...
   );


%Labels
%=======
label_user_algo = uicontrol('Parent',user_def_panel,'Style','text',...
   'String','Control_____________________________LAS','Position',[0 0 400 20],...
   'HorizontalAlignment','center','BackgroundColor',[.797 .8 .797],...
   'FontWeight','bold');

%popups
algo_requirements = uicontrol('Parent',user_def_panel,'units','pixels','position',[0 0 200 50 ],...
   'style','popup','string',LASContDiff_Struct.('cont_z_name'),...
   'value',1,'callback',{@popup_callback,'cont_z_name'});

type_requirements = uicontrol('Parent',user_def_panel,'units','pixels','position',[0 0 200 50 ],...
   'style','popup','string',LASContDiff_Struct.('las_z_name'),...
   'value',1,'callback',{@popup_callback,'las_z_name'});



%==============UI Calback Functions===================================
   function btn_Callback(~,~,arg1)
      if strcmpi('comp_diff',arg1)
         if isempty(LASContDiff_Struct.cont_zf)
            errordlg('Control Z Field not Selected','Field Error');
            return ;
         end
         if isempty(LASContDiff_Struct.las_z_name)
            errordlg('LAZ Z Field not Selected','Field Error');
            return ;
         end
         prompt = {'Enter Rectangular Buffer Width:',};
         dlg_title = 'Rect Window Width';
         num_lines = 1;def = {'5'};
         rect_width = inputdlg(prompt,dlg_title,num_lines,def);
         if isempty(rect_width)
            errordlg('Rectangular Window Not Provided','Width Error');
            return ;
         end
         %compute and save diff
         main_calc(LASContDiff_Struct.cont_zf,...
            LASContDiff_Struct.las_zf,...
            str2double(rect_width{1}))
      end
   end

   function popup_callback(hObject,~,arg1)
      sel_index = get(hObject,'value');
```

```
        if strcmpi(arg1,'cont_z_name')
            ref_sample =LASContDiff_Struct.cont_z_name{sel_index};
            LASContDiff_Struct.('cont_zf')=ref_sample;
        elseif strcmpi(arg1,'las_z_name')
            aux_sample =LASContDiff_Struct.las_z_name{sel_index};
            LASContDiff_Struct.('las_zf')=aux_sample;
        end
    end
% UI control positioning Utility Functions
    function [childRelPos]  = getUICenterLocation(childPos,parentPos)
        if nargin <2
            err = MException('','Err: getUICenterLocation, nargin must be two params','');
            throw(err);
        end
        if isempty(parentPos) || isempty(childPos)
            err_2 = MException('', 'Err: getUICenterLocation,args cannot be empty','');
            throw(err_2);

        end
        parent_W = parentPos(3);
        parent_H = parentPos(4);

        child_W = childPos(3);
        child_H = childPos(4);

        childRelPos_X = (parent_W* 0.5) - (0.5 * child_W);
        childRelPos_Y = (parent_H* 0.5) - (0.5 * child_H);

        childRelPos = [childRelPos_X ,childRelPos_Y,child_W,child_H];
    end
    function [ui_pos]= getUIPosition(UIHandler)
        try
            uiObj    = get(UIHandler);
        catch err
            err_cause = MException('','Err: getUIPosition, Invalid Handler ','');
            err = addCause (err, err_cause);
            rethrow(err);
        end
        if isfield(uiObj,'Position')
            ui_pos = uiObj.Position;
        elseif (isfield(uiObj,'ScreenSize'))
            ui_pos = uiObj.ScreenSize;
        else
            err = MException('','Err: getUIPosition, child has no position field','');
            throw(err);
        end
    end
    function setUICenterScreen(childHanler,parentHandler)
        if nargin < 2
            err = MException('','Err: setUICenterScreen, nargin must be two params','');
            throw(err);
        end
        set(childHanler,'Position',...
            getUICenterLocation( ...
            getUIPosition(childHanler),...
            getUIPosition(parentHandler)...
```

```
        )...
        );
    end
    function setUIPosition(childHanler,parentHandler,xPercent,yPercent)
        if nargin < 2
            err = MException('','Err: setUIPosition, nargin must be two params','');
            throw(err);
        end
        child_pos       = getUIPosition(childHanler);
        parent_pos      = getUIPosition(parentHandler);
        child_pos_x     = xPercent * parent_pos(3); %index 3 width
        %setting the position anchor from left,bottom to left,top: thus - child_pos(4)
        child_pos_y     = yPercent * parent_pos(4) - child_pos(4); %index 4 height
        set(childHanler,'Position',...
            [child_pos_x,child_pos_y,child_pos(3),child_pos(4)]...
            );
    end
    function UIResize (hObject,~,arg1)
        sysHandler = 0; %system handler
        if strcmpi('figmain',arg1)
            setUICenterScreen(hObject,sysHandler);
            setUIPosition(main_panel,LASCont_GUI,   0.01, 0.99); %main panel in gui
            setUIPosition(user_def_panel,main_panel,  0.01, 0.9); %user_panel in main
            %labels
            setUIPosition(label_user_algo, user_def_panel,   0.1, 0.8);
            %popups
            setUIPosition(algo_requirements,user_def_panel,  0.1, 0.5); %popups algo
            setUIPosition(type_requirements,user_def_panel,  0.5, 0.5); %popups type
            %button
            setUIPosition(btn_user_load_file,user_def_panel, 0.82,0.25); %popups type

        end
    end


%==============UI Calback Functions=================================
%==============UTILS ================================================
%%
    function xy_data = getXYData(refFieldName,varFieldName)
        temp_x = LASContDiff_Struct.('data_struct').(refFieldName);
        temp_y = LASContDiff_Struct.('data_struct').(varFieldName);
        if size(temp_x,1)<size(temp_y,1)
            d_len = size(temp_x,1);
        else
            d_len = size(temp_y,1);
        end
        xy_data = [];
        for i = 1: d_len
            iX = temp_x{i};
            iY = temp_y{i};
            if isnumeric(iX) && isnumeric(iY)
                if ~isnan(iX) && ~isnan(iY)
                    xy_data = [xy_data;[iX, iY]];
                end
            end
        end
```

```
    end
    function [field_list,structCollection] = getFieldDataStruct()
        %take care of heading
        dataFields = LASContDiff_Struct.raw_Data(1,:);
        %get data fields
        structCollection = struct();
        field_list = cell(size(dataFields));
        for i = 1: size(dataFields,2)
            f_name = num2str(dataFields{i});
            if ~isempty(f_name) && ~strcmp(f_name,'NaN')
                f_name = strrep(f_name,'+','');
                f_name = strrep(f_name,'/','_');
                f_name = strrep(f_name,' ','');
            else
                f_name = ['col_',num2str(i)];
            end
            field_list{i} = f_name;
            structCollection.(f_name) = LASContDiff_Struct.raw_Data(:,i);
        end

    end

%%
    function [FileName,PathName] = getFilePath(ext, dialogTitle,mode)
        if strcmpi(mode , 'save')
            [FileName,PathName] = uiputfile(ext,dialogTitle);
        else
            [FileName,PathName] = uigetfile(ext,dialogTitle);
        end
        if ischar(FileName) && ischar(PathName) % if file selected
            return;
        else
            FileName = ''; PathName= '';
        end
    end
%%

    function main_calc(cont_shp_zField,las_shp_zField,rect_length)

        cont_index_X  = getnameidx(control_fnames,'X');
        cont_index_Y  = getnameidx(control_fnames,'Y');
        cont_index_Z  = getnameidx(control_fnames,cont_shp_zField);

        las_index_X = getnameidx(las_fnames,'X');
        las_index_Y = getnameidx(las_fnames,'Y');
        las_index_Z = getnameidx(las_fnames,las_shp_zField);

        control_cell_data{1,end+1} = {}; %allocate another column: BBox
        control_fnames{end+1,1} = 'bbox'; %add one field name
        cont_index_bbox = size(control_fnames,1);

        control_cell_data{1,end+1} = {}; %allocate another column: Las in BBox
        control_fnames{end+1,1} = 'lasInBBox'; %add one field name
        cont_index_lasinbbox = size(control_fnames,1);

        for b = 1: size(control_cell_data,1)
```

```
    cont_X = control_cell_data{b,cont_index_X};
    cont_Y = control_cell_data{b,cont_index_Y};
    cont_bbox = getBBox([cont_X,cont_Y],rect_length*0.5);
    control_cell_data{b,cont_index_bbox} = cont_bbox;
end

fetchDataInBBOX()
saveToFile()
disp('complete ....');
%UTIL

function saveToFile()
    dialogTitle = 'Save Las and Control Diff';
    [fileName,pathName] = uiputfile({'*.csv'},dialogTitle);
    if ischar(fileName) && ischar(pathName) % if file selected
        out_f   = fullfile(pathName,fileName);
        fout    = fopen(out_f,'w');
        pnt_count = 0;
        for i = 1:size(control_cell_data,1)
            cur_control_Z = control_cell_data{i,cont_index_Z};
            las_inR = control_cell_data{i,cont_index_lasinbbox};
            for j = 1: size(las_inR,1)
                las_x = las_inR(j,1);
                las_y = las_inR(j,2);
                las_z = las_inR(j,3);
                if pnt_count == 0
                    fprintf(fout,'%s,%s,%s,%s\n','X', 'Y', 'Z','Diff');
                end
                fprintf(fout,'%f,%f,%f,%f\n',...
                    las_x,las_y,las_z,...
                    round((cur_control_Z-las_z)*1000)/1000 ...
                    );
                pnt_count = 2;%any number from 0
            end
        end
        fclose(fout);
    end

end

function fetchDataInBBOX()
    x = cell2mat(las_cell_data(:,las_index_X));
    y = cell2mat(las_cell_data(:,las_index_Y));
    z = cell2mat(las_cell_data(:,las_index_Z));
    for i = 1: size(control_cell_data,1)
        cur_bbox = control_cell_data{i,cont_index_bbox};
        xv = cur_bbox(:,1);
        yv = cur_bbox(:,2);
        in = inpolygon(x,y,xv,yv);
        if i == 1
            figure('Name','LAS In Rectangular Window Plot','NumberTitle','off');
            plot(x,y,'bo');
            hold on;
            plot(xv,yv,x(in),y(in),'r+') ;
        else
            hold on;
```

```
            plot(xv,yv,x(in),y(in),'r+') ;
        end
        control_cell_data{i,cont_index_lasinbbox} = [x(in),y(in),z(in)];
      end

    end

    function bbox = getBBox(pnt,offsetXY)
      x = pnt(1);  y = pnt(2);
      x_ll = x - offsetXY;
      y_ll = y - offsetXY;
      x_ur = x + offsetXY;
      y_ur = y + offsetXY;
      bbox =  [x_ll,y_ll;x_ur,y_ll;x_ur,y_ur;x_ll,y_ur;x_ll,y_ll];
    end


  end
  function shp =  getShape(fileName,pathName)
    shp = [];
    if ischar(fileName) && ischar(pathName) % if file selected
      shp = shaperead(fullfile(pathName,fileName));
    end
  end
  function data_shp =  getShpData(dialogTitle)
    [fileName,pathName] = uigetfile({'*.shp'},dialogTitle);
    data_shp = getShape(fileName,pathName);
  end
  function [fnames,shp_cell]=  convertShpToCell(shpObj)
    fnames = {};
    if size(shpObj,1) > 0
      shp_struct = shpObj(1,1);
      fnames = fieldnames(shp_struct);
    end
    if ~isempty (fnames)
      shp_cell = cell(size(shpObj,1),size(fnames,1));
      for i = 1 : size(shpObj,1)
        temp_cell = cell(1,size(fnames,1));
        cur_obj = shpObj(i,1);
        for j = 1:size(fnames,1)
          temp_cell{1,j} = cur_obj.(fnames{j,1});
        end
        shp_cell(i,:) = temp_cell;
      end
    end
  end

%==============UTILS=================================================
disp('gui initialized...');
end
```

APPENDIX C. Example of point differencing between LiDAR and checkpoints

NB: 2 metre by 2 metre window around the controlled checkpoints was used to select LiDAR ground points around the checkpoints.

A sample of QCC points and their attributes for downtown Fredericton

QCC_100	Cont_X	Cont_Y	Cont_Z	Obstruction		
	682843.666	5092437.609	9.22	light		
LiDAR	LiD_X	LiD_Y	LiD_Z	Diff	RMSE	SD
	682844.199	5092437.304	9.27	0.05		
	682842.92	5092437.224	9.27	0.05		
	682844.388	5092438.227	9.33	0.11	0.09	0.03
QCC_101	Cont_X	Cont_Y	Cont_Z	Obstruction		
	682825.814	5092450.414	9.25	light		
LiDAR	LiD_X	LiD_Y	LiD_Z	Diff	RMSE	SD
	682826.138	5092450.99	9.38	0.13		
	682825.644	5092451.168	9.33	0.08		
	682825.733	5092449.501	9.33	0.08		
	682825.484	5092450.803	9.34	0.1		
	682826.71	5092450.395	9.31	0.06	0.10	0.03
QCC_102	Cont_X	Cont_Y	Cont_Z	Obstruction		
	682868.463	5092427.174	8.97	light		
LiDAR	LiD_X	LiD_Y	LiD_Z	Diff	RMSE	SD
	682869.041	5092427.608	9.03	0.06		
	682869.141	5092426.212	9.08	0.11		
	682868.293	5092427.238	9.02	0.05		

Curriculum Vitae

Candidate's full name:

Patrick Wetarni Adda

Universities attended:

March 2010: University of New Brunswick, Fredericton, Canada. CETL (Centre for Extended Teaching and Learning) Diploma in University Teaching.

2005-2007: Stuttgart University of Applied Science, Germany. MSc. Photogrammetry and Geo-Informatics (GIS).

1998-2002: Kwame Nkrumah University of Science and Technology, Ghana. B.Sc. Geodetic Engineering.

Publications:

Adda P., Coleman D., and Dare P. (2013). "Empirical Validation of Large Datasets– Experience using Airborne LiDAR data in New Brunswick, Canada –" GIM International magazine – *under editorial review.*

Adda P., Coleman D., and Masry M. (2012). "A User Determined Total Uncertainty Budget Model for Client side Control and Analysis of Laser Sensed Data" Conference Proceedings. ASPRS 2012 Annual Conference Sacramento, California March 19-23. Available in CD ROM.

Adda P and Coleman D (2012). "Scalable integration of multiple datasets towards meeting scalable user requirements" Poster prepared for the MAPPS/ASPRS 2012 Specialty Conference. Tampa, Florida USA October 29 - November 1, 2012 Tampa.

Adda P (2012) CARIS report CARIS LIDAR INITIATIVES for LiDAR and Laser scanning analysis. Contract Technical Report Submitted to R&D Manager, CARIS, 115 Waggoner's Lane, Fredericton, New Brunswick. June 13.

Adda P., Mioc D., Anton F., McGillivray E., Morton A., Fraser D.,(2011). "3D Flood-Risk Models of Government Infrastructure". ISPRS Commission VI, WG VI/4. [Online] http://www.isprs.org/proceedings/XXXVIII/4-W13/ID_39.pdf.

Adda P., W. (2011). “Open Source GIS and Cloud Computing – A Chance for Nations in Transition”? Proceedings of the 2010 Conference on Applied Geoinformatics for Society and Environment (AGSE 2011), Nairobi, Kenya. pp 124-130.

Adda, P. and Coleman, D. [2010]. "Developing LiDAR Data Acquisition and Quality Assurance Specifications for the Province of New Brunswick" Contract Report to Service New Brunswick, Fredericton, N.B. March.

Adda P (2010) CARIS-MITACS research grant. Development of software to clean LiDAR data by employing uncertainty values. Contracted research and development, CARIS, Fredericton, NB. June-December.

Adda, P., Coleman, D. and D. Finley [2010]. “Designing LiDAR Data Acquisition and Quality Assurance specifications for multiple organizations - Canada's first experience in New Brunswick”. Proceedings of the 2010 Conference on Applied Geoinformatics for Society and Environment (AGSE 2010), pp. 43-48. ISBN 978-3-940670-19-9. [Online] http://www.applied-geoinformatics.org/downloads/AGSE_2010_ Proceedings_2010_11_01.pdf.

Mioc D., Anton F., Nickerson B., M. Santos, Adda P., Tienaah T., Ahmad A., Mezouagh M., MacGillivray E., Morton A., Tang P.(2011). “Flood Progression Modeling and Impact Analysis”. [Online] http://www.isprs.org/proceedings/XXXVIII/ Gi4DM/PDF/OP53.pdf.

Conference Presentations:

Adda P. (2013). “Effects of LiDAR mapping errors - user-side analysis -” Presented at the Alberta LiDAR stakeholders’ workshop at the University of Lethbridge, Alberta, July 8-12, 2013.

Adda P., Coleman D., and Masry M. (2012). “A User Determined Total Uncertainty Budget Model for Client side Control and Analysis of Laser Sensed Data” Presented at the ASPRS 2012 Annual Conference Sacramento, California March 19-23, 2012.

Adda P., Coleman, D., Amolins, K. (2012) “Exploring LiDAR data as basis for validating Volunteered Geographic Information” Global Geospatial Conference presentation 2012. Spatially Enabling Government, Industry and Citizens. Québec City, Canada, 14-17 May 2012 GSDI conference. [Online abstract] http://www.geoide.ulaval.ca/news-detail.aspx?i=284.

Adda P W (2012) Developing LiDAR Data Acquisition and Quality Assurance Specification for New Brunswick. Semi-annual graduate seminars. Geodesy and Geomatics Engineering, University of New Brunswick.

Adda P. (2012). “LiDAR for C-Change”. LiDAR Workshop for Coastal Climate adaptation strategies. Canadian Caribbean collaboration, C-Change ACURA project. University of New Brunswick, Fredericton.

Adda P., Hoggarth, A., (2011) “Simultaneous Processing of LiDAR for Effective Visualization and Analysis”. Presented at the Geomatics Atlantic Conference. Newfoundland and Labrador Branch -Canadian Institute of Geomatics October 5-7, 2011

Adda P., Mioc D., Anton F., McGillivray E., Morton A., Fraser D.,(2011). “3D Flood-Risk Models of Government Infrastructure”. Presented to managers and officials of the Department of Public Safety, NB, Canada.

Adda P (2011) Developing LiDAR Data Acquisition and Quality Assurance Specification for New Brunswick. Semi-annual graduate seminars. Geodesy and Geomatics Engineering, University of New Brunswick.

Adda P., W. (2011) Open Source GIS and Cloud Computing – A Chance for Nations in Transition? Keynote Presentation at the 2010 Conference on Applied Geoinformatics for Society and Environment (AGSE 2011), Nairobi, Kenya.

Adda P (2010) CARIS-MITACS “Development of software to clean LiDAR data by employing uncertainty values” Presented at CARIS, Fredericton, NB. December 2010.

Adda P. (2010). LiDAR Workshop presentation to provincial and federal organizations from a funded research on determining Specifications for use by multiple organizations in New Brunswick. UNB-SNB collaboration, 2010.

Adda, P. and Coleman, D. [2010]. "Developing LiDAR Data Acquisition and Quality Assurance Specifications for the Province of New Brunswick" Presented to Service New Brunswick, Fredericton, N.B. March.

Adda, P., [2010]. “OGC Standards and their application for disseminating geodata”. Workshop Presentation. Applied Geoinformatics for Society and Environment (AGSE 2010), Arequipa, Peru. [Online] http://applied-geoinformatics.org/agse2010.html.

Adda, P., Coleman, D. and D. Finley [2010]. “Designing LiDAR Data Acquisition and Quality Assurance specifications for multiple organizations - Canada's first experience in New Brunswick”. Presented at the 2010 Conference on Applied Geoinformatics for Society and Environment (AGSE 2010) [Online] http://www.applied-geoinformatics.org/downloads/AGSE_2010_Proceedings_2010_11 _01.pdf.